Investigating the mechanism of action of USP19, a deubiquitinating enzyme, in glucocorticoid-induced muscle wasting

Julie Huynh

Department of Biochemistry

Faculty of Medicine and Health Sciences

McGill University

Montreal, Quebec, Canada

August 2022

A thesis submitted to McGill University in partial fulfillment of the requirements of the degree of Master of Science

© Julie Huynh 2022

Table of Contents

Abstract i					
Résumé			iii		
Acknowle	edgements		V		
Preface a	nd Contrib	ution of Authors	vi		
List of Fig	gures and T	Tables	vii		
List of Ab	breviation	s	viii		
Chapter 1	: Introdu	ction and Literature Review			
1.	Muscle		1		
	1.1. Comp	osition of Skeletal Muscle	1		
	1.2. Musc	le Atrophy	2		
	1.2.1.	Cellular Signaling Pathways Related to Muscle Atrophy	2		
	1.2.2.	The Ubiquitin Proteasome System in Muscle Atrophy	3		
2.	Ubiquitin	Proteasome System (UPS)	3		
	2.1. Ubiqu	uitination	3		
	2.1.1.	Ubiquitin Activating Enzymes (E1)	4		
	2.1.2.	Ubiquitin Conjugating Enzymes (E2)	4		
	2.1.3.	Ubiquitin Ligase Enzymes (E3)	4		
	2.1.4.	26S Proteasome	5		
	2.2. Deub	iquitination	7		
	2.2.1.	Ubiquitin C-Terminal Hydrolases (UCHs)	8		
	2.2.2.	Ubiquitin Specific Proteases (USPs)	8		
	2.2.3.	Ovarian Tumour Proteases (OTUs)	9		
	2.2.4.	Machado-Josephin Domain-Containing Proteases (MJDs)	9		
	2.2.5.	MIU-Containing Novel DUBs (MINDYs)	9		
	2.2.6.	Zinc-Finger Containing Ubiquitin Peptidase 1 (ZUP1)	10		
	2.2.7.	Jab1/MPN Domain-Associated Metallopeptidases (JAMM/MPN+)	10		
	2.2.8.	Regulation of DUBs	10		
	2.2.9.	Relation of DUBs to Muscle Atrophy	10		

	3.	Ubiquitin Specific Protease 19 (USP19)					
		3.1. The Structure of USP19					
		3.1.1.	CS Do	mains	. 12		
		3.1.2.	USP D	Oomain	. 13		
		3.1	.2.1.	UbL Domain	. 13		
		3.1	.2.2.	MYND Zn Domain	. 13		
		3.1.3.	SIAH	Domain	. 13		
		3.2. The F	unction	of USP19	. 14		
		3.2.1.	Role in	n Muscle Atrophy	. 15		
		3.2.2.	Role in	n Cell Cycle Regulation and DNA Damage Repair	. 16		
		3.2.3.	Role in	n Endoplasmic Reticulum Associated Degradation (ERAD) and			
			Unfold	ded Protein Response (UPR)	. 16		
		3.2.4.	Role in	n Misfolded-Associated Protein Secretion (MAPS)	. 17		
		3.2.5.	Role in	Neurodegenerative Diseases	. 18		
		3.2.6.	Role in	ı Hypoxia	. 18		
		3.2.7.	Role in	the Immune System	. 19		
		3.2.8.	Role in	n Carcinomas	. 20		
		3.2.9.	Role in	n the Heart	. 21		
		3.2.10.	Role in	n Autophagy	. 21		
		3.2.11.	Role in	n Nuclear Receptor Signaling	. 22		
	4.	Glucocorti	coid Re	eceptor	. 24		
		4.1. Cellul	ar Sign	aling Pathway	. 24		
		4.2. Key P	rocesse	s Regulated by Glucocorticoids in Skeletal Muscle	. 25		
		4.3. Struct	ure, Fui	nction and Regulation of GR	. 25		
		4.4. GC-In	duced 1	Muscle Wasting	. 28		
	5.	Objectives	s of this	Thesis	. 28		
		5.1. Hypot	hesis		. 28		
		5.2. The A	ims of 1	this Thesis	. 29		
Chapt	er 2	2: Methods					
	2.1	. Biolumine	escence	Resonance Energy Transfer (BRET) Assay	. 30		
		2.1.1.	Plasmi	ds and Site-Directed Mutagenesis	. 31		

2.1.2.	Cell Culture and Transfection	32
2.1.3.	BRET Assay	33
2.2. HA-tagge	d GR Overexpression	33
2.2.1.	Plasmids and Site-Directed Mutagenesis	33
2.2.2.	Cell Culture and Transfection	34
2.2.3.	Western Blotting	34
2.3. Nuclear T	ranslocation Assay	35
2.3.1.	Plasmids	35
2.3.2.	Cell Culture and Transfection	36
2.3.3.	Image Acquisition and Analysis	36
2.3.4.	Western Blotting	37
2.4. Statistical	Analysis	37
Chapter 3: Results		
3.1. USP19 in	teracts indirectly with GR via HSP90	38
3.1.1.	USP19 interacts with HSP90 and GR	38
3.1.2.	USP19 binds to the same region on HSP90 as p23	40
3.2. USP19 C	S2 domain is required but insufficient for GR stabilization	42
3.2.1.	CS2 binds to HSP90	42
3.2.2.	CS2 mutants and deletion fail to abolish HSP90 binding	44
3.2.3.	The CS2 domain is required for GR stabilization	47
3.2.4.	The CS2 domain is required for GR translocation	49
3.3. USP19 ca	talytic domain contains a nuclear receptor box (NR box) motif	53
3.3.1.	Identification of Nuclear Receptor Box (NR box) motif in USP19	53
3.3.2.	Mutating the NR box in USP19 reduces GR stability with and witho	ut the
(CS2 domain	55
3.3.3.	Mutating the NR box in USP19 reduces GR nuclear translocation	57
Chapter 4: Discussion	on	60
Chanton 5. Canalysis	on	66
Chapter 5: Conclusi	on	00
References		67

Abstract

Muscle wasting is a complication of many common conditions such as aging, prolonged inactivity or hypercortisolemia due to illness or glucocorticoid treatment. Previous work in our laboratory identified USP19 as a deubiquitinating enzyme induced in muscle in response to many catabolic stimuli including glucocorticoids⁹³. Inactivation of USP19 in mice protected against muscle wasting confirming its importance in the atrophic process¹¹⁷. Our recent work has revealed that this loss of USP19 enhances insulin signaling and decreases glucocorticoid signaling. The latter appears to be due to reduced glucocorticoid receptor (GR) protein levels in KO tissue¹⁸⁴. GR mRNA levels remain unchanged suggesting post-translational regulation of GR by USP19. Interestingly, the catalytic activity of USP19 is not required, suggesting a non-catalytic role for USP19 in GR regulation (Coyne et al., *manuscript in preparation*). However, the specific mechanism of action remains to be defined.

Interestingly, USP19 has two CS/p23-like domains homologous to p23, a co-chaperone of HSP90. HSP90 and p23 are involved in the maturation of GR and USP19 has been shown to interact with HSP90. So, we hypothesized that USP19 interacts indirectly with GR via HSP90. We used a bioluminescence resonance energy transfer (BRET) assay in cells that detect protein-protein interactions of less than 10 nm and showed that USP19 directly interacts with HSP90 through its CS2 domain. The co-expression of p23 disrupts the interaction of USP19 with HSP90, suggesting that USP19 binds to the same site on HSP90 as p23. Testing USP19 and GR in a similar assay generated a much weaker signal similar to that of a negative control, suggesting that USP19 indirectly interacts with GR through binding to HSP90.

We also observed that overexpressing USP19 increases levels of GR and its nuclear translocation, suggesting that USP19 promotes proper GR folding and function. Deletion of the CS2 domain abolishes these effects, supporting the intermediary function of HSP90 in this regulation of GR. Interestingly, overexpressing the CS2 domain itself is insufficient at mimicking the effect of USP19, suggesting that other domain(s) are also involved. We identified an α-helix in the catalytic domain of USP19 with a nuclear receptor box (NR box) motif, commonly found in co-activators of GR and are required for binding to GR. Mutating the NR box motif also abolished USP19's ability to increase GR levels and nuclear translocation. Therefore, we suggest the CS2 domain and the NR box are required for the full effect of USP19 on the stabilization of GR and its

subsequent function. Targeting the CS2 domain or the NR box with a small molecule may reduce GR levels and signaling and thereby represent a novel approach to prevent or treat muscle wasting.

Résumé

La fonte musculaire est une complication grave de plusieurs conditions telles que le vieillissement, l'inactivité prolongée ou l'hypercortisolémie causée par la maladie ou les traitements aux glucocorticoïdes. Nous avons précédemment identifié USP19, une enzyme de déubiquitination, induite dans les muscles en réponse à plusieurs stimuli cataboliques incluant les traitements aux glucocorticoïdes⁹³. L'inactivation de USP19 dans les souris mène à une protection musculaire, confirmant ainsi son importance dans le processus d'atrophie musculaire¹¹⁷. Nos récents travaux ont aussi révélé que l'inactivation de USP19 augmente la signalisation de l'insuline et diminue la signalisation des glucocorticoïdes. Ce dernier semble être causé par la diminution des niveaux protéiques du récepteur de glucocorticoïde (GR) dans les tissus KO¹⁸⁴. Les niveaux d'ARN messager de GR sont cependant inchangés suggérant que GR est régulé par USP19 de façon post-traductionnelle. Par ailleurs, nous savons aussi que l'activité catalytique de USP19 n'est pas requis, suggérant un rôle non-catalytique de USP19 dans la régulation de GR (Coyne et al., manuscript in preparation). Par contre, les mécanismes spécifiques d'action de USP19 sont encore incompris.

Il est intéressant de noter que USP19 contient deux domaines CS/p23, homologue à p23, une protéine co-chaperon de HSP90. HSP90 et p23 sont impliqués dans la maturation de GR et il a été démontré que USP19 interagit avec HSP90. Donc, nous avons avancé l'hypothèse que USP19 interagit indirectement avec GR via HSP90. Nous avons utilisé des essais BRET (Bioluminescence Resonance Energy Transfer) dans des cellules pour détecter des interactions de moins de 10nm entre deux protéines et avons démontré que USP19 interagit directement avec HSP19 via son domaine CS2. La co-expression de p23 détruit l'interaction entre USP19 et HSP90, ce qui nous indique que USP19 et p23 partagent le même site sur HSP90. Nous avons ensuite testé l'interaction entre USP19 et GR en utilisant les mêmes essais et avons observé un signal beaucoup plus faible, comparable au contrôle négatif, suggérant que USP19 et GR interagissent indirectement via HSP90.

Nous avons de plus observé que la surexpression de USP19 augmente les niveaux de GR ainsi que sa translocation nucléaire, indiquant que USP19 pourrait aider GR à adopter une structure et une activité complète. La délétion du domaine CS2 de USP19 abolit ces effets, soutenant la fonction intermédiaire de HSP90 dans la régulation de GR. Curieusement, la surexpression du

domaine CS2 seul est insuffisant pour imiter les effets de USP19, suggérant que un ou d'autres domaines sont aussi impliqués. Nous avons alors identifié une hélice-α dans le domaine catalytique de USP19 contenant un motif de récepteur nucléaire NR box, souvent observé dans les coactivateurs de GR et étant nécessaire pour se lier à GR. En introduisant des mutations dans le motif du NR box, la capacité de USP19 à augmenter les niveaux de GR ainsi que sa translocation nucléaire est abolie. Par conséquent, nous suggérons que le domaine CS2 et le motif NR box de USP19 sont requis pour la stabilisation et la fonction complète de GR.

En ciblant le domaine CS2 ou le motif NR box avec des molécules synthétiques, nous pourrions réduire les niveaux ainsi que la signalisation de GR et potentiellement prévenir ou traiter la perte musculaire.

Acknowledgements

First, I would like to sincerely thank my supervisor Dr. Simon Wing for his supervision and confidence in my scientific abilities. Thank you for taking me on as a MSc student and seeing my potential as a scientist. Thank you for your unlimited patience when walking me through to the answer so that I learn instead of just giving the answer. Thank you for your wisdom and curiosity that has allowed me to learn many new techniques and conduct some very interesting experiments throughout these past two years. Next, I would like to thank Ms. Nathalie Bedard for teaching me all the techniques I used in this thesis and answering my many questions even if they were very silly. Thank you to all my lab members, Ms. Marie Plourde, Dr. Lenka Schorova, Dr. Joao Pedroso and Hung-Hsiang Ho for making my time in the lab very memorable and fun! I am very lucky to have found such a great lab environment and supervisor!

I would also like to thank my Research Advisory Committee (RAC) members, Dr. Stephane Laporte and Dr. Jason Young for their support and guidance throughout my MSc. Thank you to Ms. Christine Laberge for ensuring I stay on track with my degree and for always answering my many administrative questions. Special thanks to Dr. Yoon Namkung from Dr. Stephane Laporte lab for helping us to set up the BRET assay and troubleshoot. Additionally, thank you to all the members of the Metabolic Diseases and Complications (MeDiC) program, especially Ms. Mary Lapenna, Ms. Kim Gardner and Dr. Rachel Massicotte.

I am extremely thankful to my family, my parents, Hai and Mai, for their never-ending love and support while I am on this journey living alone in a new city six-hours away from home during a pandemic. I am grateful that there is FaceTime so I can video call my parents daily and learn how to cook to survive. Thank you to all my close friends, you know who you are, for their support and coming up to visit me in Montreal. I am very grateful and appreciative of everyone in my life who has helped me to become the person I am today, both personally and academically.

Finally, I would like to thank the Research Institute of the McGill University Health Center, Healthy Brain Health Lives (HBHL) and the Canadian Institute of Health Research (CIHR) for their financial support over the past two years.

Preface and Contribution of Authors

This thesis was written based on the traditional style guidelines provided by the Graduate and Postdoctoral Studies (GPS) at McGill University. This thesis consists of an up-to-date literature review chapter, materials and methodology, results, general discussion, and conclusion. The entirety of this thesis was written by the author and thoroughly reviewed by Dr. Simon S. Wing. The author performed the majority of the experiments (Figures 3.1, 3.2, 3.4, 3.5, 3.7-3.10) included in this thesis with technical assistance from Nathalie Bedard and all the statistical analysis under the supervision and guidance of Dr. Simon S. Wing. Nathalie Bedard performed the experiment in Figures 3.3 and 3.6. Dr. Lenka Schorova acquired the GR nuclear translocation images (Figures 3.7 and 3.10) and the author performed the data analysis.

Figure 3.2D and 3.3D are included in the following publication:

Erin S. Coyne, Nathalie Bédard, <u>Julie Huynh</u>, Lenka Schorova, Yoon Namkung, Stéphane A. Laporte, Ewelina Rozycka, Xavier Jacq, Jason C. Young, and Simon S. Wing. Non-catalytic role of USP19 in the regulation of glucocorticoid receptor function. *Manuscript in preparation*.

<u>Involvement/publications in other projects:</u>

Project with Institute for Research in Immunology and Cancer (IRIC) at the University of Montreal. Characterization of a potential small molecule inhibitor of USP19. *Unpublished Data*.

Lenka Schorova, Nathalie Bedard, Joao Bolivar-Pedroso, Hung-Hsiang Ho, <u>Julie Huynh</u>, Mikaela Piccirelli, Yifei Wang, Anouar Khayachi, Maria LaCalle, Anita Kriz, Marie Plourde, Wen Luo, Esther Del Cid, Yihong Ye, Thomas Durcan, Simon S. Wing. Genetic inactivation of the USP19 deubiquitinase in mice inhibits α -synuclein aggregation and propagation in the brain. *Manuscript in preparation*.

List of Figures and Tables

Figure 1.1: Composition of Skeletal Muscle
Figure 1.2: The Ubiquitin Proteasome System
Figure 1.3: Structural and functional domains in USP19
Figure 1.4: Comparison of CS1 and CS2 solution structures to p23
Figure 1.5: Comparison of Ub with USP19 UbL domain and SIAH domain
Figure 1.6: The function of USP19
Figure 1.7: HPA Axis
Figure 1.8: Structure and functional domains of GR
Figure 1.9: GR translocation from cytoplasm to nucleus
Figure 2.1: BRET Assay
Figure 3.1: USP19 interacts directly with HSP90 and indirectly with GR
Figure 3.2: p23 competes the interaction of rLuc-USP19Cyt with hrGFP-HSP90
Figure 3.3: USP19 CS2 domain competes interaction of USP19 with HSP90 and with GR 43
Figure 3.4 USP19 CS2 mutants still compete the interaction of USP19 with HSP90
Figure 3.5: USP19ΔCS2 still competes interaction of USP19 with HSP90
Figure 3.6: The CS1 domain is not required for USP19 stimulated increases in GR protein
levels
Figure 3.7: The CS1 domain is not required for USP19 stimulation of GFP-GR nuclear
translocation
Figure 3.8: Identification of a nuclear receptor box motif in the catalytic domain of USP19 54
Figure 3.9: CS2 domain or intact NR box is required for USP19 stabilization of overexpressed
HA-GR
Figure 3.10: The NR box is required for USP19 stimulation of GFP-GR nuclear translocation 57
Table 1: List of plasmids co-transfected in the BRET assay
Table 2: List of primers used for site-directed mutagenesis of p23 and CS2 with the residues
mutated underlined and coloured in red
Table 3: List of plasmids co-transfected in COS7 overexpression
Table 4: List of Primers used for site-directed mutagenesis of the nuclear receptor box (NR box)
motif with the residues mutated underlines and coloured in red
Table 5: List of plasmids co-transfected in COS7 cells for the nuclear translocation assay 35

List of Abbreviations

ACTH = Adrenocorticotropic Hormone

ADP = Adenosine Diphosphate

Arp = Aspartic Acid

ATG7 = Autophagy Related 7

ATP = Adenosine Triphosphate

Atx-3 = Ataxin-3

BAP1 = Breast Cancer Type 1 (BRCA1) Associated Protein-1

BRET = Bioluminescence Resonance Energy Transfer

Cdc34 = Cell division cycle 34

CDK = Cyclin-Dependent Kinases

CHOP = C/EBP homologous protein

CHORD = Cysteine and Histidine Rich Domain

cIAP = Cellular Inhibitors of Apoptosis

COS-7 = CV-1 in Origin with SV40 genes

CRFR1 = CRH type 1 receptor

CRH = Corticotropin-Releasing Hormone

CS = CHORD-containing proteins and SGT1

Ctl = Control

Cyp40/PPID = Cyclophilin-40/Peptidyl-Prolyl Cis-Trans Isomerase D

Cys = Cysteine

DBD = DNA Binding Domain

DUB = Deubiquitinating enzyme

E1 = Ubiquitin-activating enzymes

E2 = Ubiquitin conjugating enzymes

E3 = Ubiquitin ligase enzymes

ERK = Extracellular Signal-Regulated Kinase

FAM63A = Family with Sequence Similarity 63 Member A

FBox32 = F-box only protein 32

FKBP = FK506-Binding Protein

FoxO = Forkhead box Class O transcription factors

GC = Glucocorticoid

GLUT4 = Glucose Transporter Type 4, Insulin-Responsive

GR = Glucocorticoid Receptor

GRE = Glucocorticoid Response Element

GRIP = Glucocorticoid Receptor Interacting Protein 1

 $GSK3\beta = Glycogen Synthase Kinase 3-\beta$

HECT = Homologous to E6AP C-terminus

HEK = Human Embryonic Kidney

His = Histidine

HPA = Hypothalamic-pituitary-adrenal axis

hrGFP = humanized *Renilla Renformis* green fluorescent protein

IGF1 = Insulin-like growth factor 1

Il- 1β = Interlukin- 1β

IL-6 = Interleukin-6

IRS-1 = Insulin Receptor Substrate-1

JAK = Janus Kinase

JAMM/MPN+ = Jab1/MPN domain-Associated Metallopeptidases

kDa = kilodalton

KLF15 = Kruppe-like factor 15

LAMP2A = Lysosome-associated membrane protein 2

LBD = Ligand Binding Domain

MAFbx/Atrogin-1 = Muscle Atrophy F-box/Atrogin-1

MC2-R = Melanocortin type 2 receptor

MHC = Myosin Heavy Chain

MINDY = Motif Interacting with Ubiquitin (MIU)-Containing Novel DUB

MJD = Machado-Josephin Domain-Containing Proteases (MJDs)

Mstn = Myostatin

mTOR = mammalian Target of Rapamycin

MuRF1 = Muscle RING Finger 1

MUSA1 = Muscle Ubiquitin Ligase of SCF Complex in Atrophy-1 (Fbox30)

MYND = myeloid translocation protein 8, Nervy and Deaf1 zinc finger domain

 $NF-\kappa B = Nuclear$ factor kappa-light-chain-enhancer of activated B cells

NR Box = Nuclear Receptor Box Motif

OTU = Ovarian Tumour Proteases

Pi = Inorganic phosphate

PI3K = Phosphoinositide 3-kinase

RBR = RING-between-RING

REDD1/DDIT4 = Protein Regulated in Development and DNA Damage Response 1/DDIT4

RING = Really Interesting New Gene

rLuc = *Renilla Renformis* luciferase

Rpn1/10/13 = Regulatory Particle Non-ATPase 1/10/13

SCF = Skp-Cullin-F-box protein

Sgt1 = Suppressor Of G2 Allele Of SKP1

SIAH = Seven in absentia homolog

SMART = Specific of Muscle Atrophy and Regulated by Transcription

SRC = Steroid Receptor Co-Activator

Stat3 = Signal Transducer and Activator of Transcription 3

TAK1 = Tumor Growth Factor- β (TGF β)-Activated Kinase 1

 $TGF-\beta = Transforming Growth Factor-\beta$

TIF2/NCoA2 = Transcriptional Intermediary Factor 2/Nuclear Receptor Coactivator 2

TNF = Tumor Necrosis Factor

TRAF6 = Tumor Necrosis Factor (TNF) Receptor Associated Factor 6

TRIM63 = Tripartite Motif Containing 63

Ub = Ubiquitin

UBC = Ubiquitin conjugating domain

UbL = Ubiquitin Like Domain

UCH = Ubiquitin C-Terminal Hydrolases

UFD = Ubiquitin Fold Domain

UIM = Ubiquitin Interacting Motif

UPS = Ubiquitin Proteasome System

USP = Ubiquitin Specific Proteases

ZUP = Zinc-Finger Containing Ubiquitin Peptidase 1

Chapter 1: Introduction and Literature Review

1. Muscle

Approximately half of the human body mass consists of skeletal muscle^{1,2}. The main roles of skeletal muscle are to facilitate locomotion as well as be involved in energy metabolism as a reservoir of essential and non-essential amino acids^{1,3}.

1.1 Composition of Skeletal Muscle

Skeletal muscle is highly organized with the fundamental unit being the sarcomere which consists of a precise arrangement of myofilaments^{1,4}. There are two main groups of myofilaments, thin and thick. Thin myofilaments consist of actin, troponin and tropomyosin and thick myofilaments consist of myosin II^{1,5}. The alignment of thousands of sarcomeres form myofibrils, which assemble together to form muscle fibers or myofibers⁵. The process of generating skeletal muscle fibers is known as myogenesis and is regulated by a number of transcription factors and myogenic regulatory factors^{5,6}. Myofibrils are the contractile organelle of the muscle. Muscle contraction is stimulated by calcium influx into the cytoplasm or sarcoplasm. The calcium interacts with troponin C on a thin actin myofilament to induce the interaction of actin and myosin head to form a crossbridge^{1,5,7}. The ATPase in myosin is in the head, where the release of ADP and Pi after ATP hydrolysis results in the bending of myosin that pulls actin towards the middle of the sarcomere⁸. The binding of a new ATP molecule dissociates myosin from actin. Repetition of the cycle generates the force of muscle contraction⁵. Since ATP is fundamental to muscle contraction, skeletal muscle is dependent on optimal mitochondrial function and dysfunction can lead to detrimental consequences⁹.

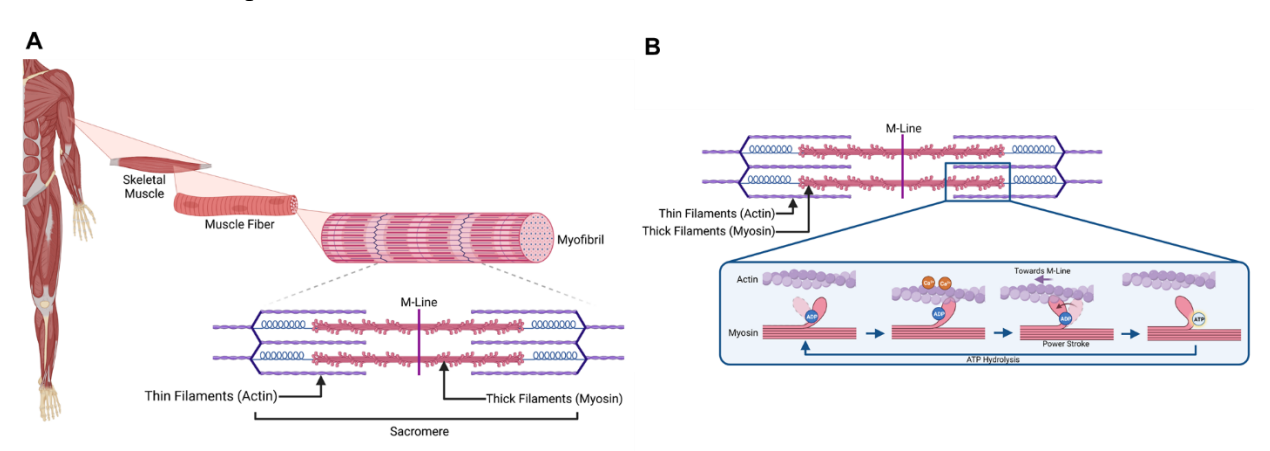


Figure 1.1: Composition of Skeletal Muscle. (A) The fundamental unit of skeletal muscle is the sarcomere, consisting of thin actin and thick myosin filaments. Thousands of sarcomeres form myofibers or muscle fibers that then assemble to form skeletal muscle. (B) Skeletal muscle contraction is stimulated by calcium influx that results in a crossbridge formation between actin and myosin. ATP hydrolysis pulls actin towards the middle of the sarcomere (M-line) and binding of a new ATP molecule dissociates myosin from actin. Repetition of this cycle generates the force of muscle contraction. Created on BioRender.com.

1.2 Muscle Atrophy

Dysregulation of the fine balance of muscle protein synthesis and breakdown is implicated in many catabolic conditions including cancer, inactivity and increased glucocorticoid action due to endogenous production in response to stress or illness or exogenous therapeutic administration¹⁰. In these catabolic conditions, there is typically increased muscle protein breakdown and decreased protein synthesis leading to decreased muscle mass and muscle weakness, which is highly detrimental to the quality of life and when severe, can result in death.

1.2.1 Cellular Signaling Pathways Related to Muscle Atrophy

In catabolic conditions, increased muscle protein breakdown occurs through the combined activation of the ubiquitin proteasome system and autophagy². Upregulation of ubiquitin ligase enzymes (E3) such as muscle atrophy F-box (MAFbx)/Atrogin-1/Fbox32 and muscle-specific RING finger 1 (MuRF1)/TRIM63 is observed in muscle atrophy, which leads to increased ubiquitination of muscle proteins and subsequent degradation¹¹. Inactivation of these ubiquitin ligases can be beneficial in some models of muscle atrophy but not in all, suggesting there are other mechanisms involved. Additionally, sarcopenia is defined as the loss of muscle mass due to aging. The mitochondria gradually become dysfunctional, which triggers the activation of autophagy⁴. Silencing ATG7 inhibits autophagy and prevented muscle degradation in aging¹².

Inflammatory signaling often plays an important role in muscle wasting. An important mediator is nuclear factor κB (NF- κB) signaling, which itself increases cytokine production and this has been observed in muscle atrophy. Inhibition of a component of NF- κB signaling is able to reduce the severity of muscle atrophy². In addition to NF- κB signaling, IL6-JAK-Stat3 is also involved in the muscle atrophy induced by cancer, or cancer cachexia. In these conditions, Stat3 phosphorylation and activation leads to muscle atrophy^{2,13}. Catabolic conditions such as diabetes

and glucocorticoid (GC) treatment, breakdown muscle to provide substrates for metabolic pathways such as gluconeogenesis^{4,14}. The insulin signaling pathway is upstream of and activates mechanistic target of rapamycin (mTOR), a master regulator of protein synthesis. It is also upstream and a negative regulator of FoxO transcription factors which activate ubiquitin ligases, Fbox32 and Trim63, as well as a number of autophagy genes¹⁵. This signaling pathway is modulated in diabetes and GC treatment. GCs inhibit protein synthesis through inhibition of insulin signaling, leading to the unbalanced proteostasis¹⁶.

1.2.2 The Ubiquitin Proteasome System in Muscle Atrophy

Since muscle atrophy arises from altered proteostasis, the ubiquitin proteasome system (UPS) was speculated to be involved. Components of the UPS were found to be upregulated in parallel with the increased rates of proteolysis^{11,17–19}. In catabolic conditions, the upregulation of two ubiquitin ligases, muscle atrophy F-box (MAFbx)/Atrogin-1/Fbox32 and muscle-specific RING finger 1 (MuRF1)/TRIM63 have been frequently observed and appear to play important roles in muscle atrophy^{11,15}. Specifically, MuRF1 was found to degrade troponin in thin myofilaments and the myosin heavy chain leading to breakdown of the highly organized sarcomere²⁰. There are additional ubiquitin ligases that have been found induced in muscle atrophy such as TRIM32, TRAF6, MUSA1 and SMART^{21–23}. This suggests that the UPS plays an important mechanistic role in muscle atrophy and modulation of these UPS components may be potential therapeutic approaches against muscle atrophy.

2. Ubiquitin Proteasome System (UPS)

The ubiquitin proteasome system (UPS) is one of the protein quality control systems in place to maintain protein homeostasis within the cell through protein degradation^{24,25}. The key seminal findings on the UPS were obtained by Aaron Ciechanover, Avram Hershko and Irwin Rose, who won the 2004 Nobel Prize in Chemistry for identification of ubiquitin, its conjugation to proteins and the demonstration that such ubiquitination can lead to the degradation of the modified protein. This post translational modification is reversible and such deubiquitination by deubiquitinating enzymes can protect the target protein from being degraded²⁶.

2.1. Ubiquitination

Ubiquitination involves the covalent attachment of ubiquitin (Ub), a 76 amino acid protein, to a lysine residue on the target protein. Ub itself contains 7 lysine residues which along with its

N-terminal methionine can be sites of attachment of additional Ub moieties to generate polyubiquitin (polyUb) chains of various structures. PolyUb on Lys48 (K48) residue of Ub can mark the protein for degradation by the 26S proteasome. An enzymatic cascade is responsible for ubiquitination and there are three main enzymes involved, the ubiquitin activating (E1), the ubiquitin conjugating (E2) and ubiquitin ligase (E3) enzymes^{26,27}.

2.1.1. Ubiquitin Activating Enzymes (E1)

The first step in ubiquitination is mediated by ubiquitin activating enzymes (E1s). The human genome only encodes two E1s and the mechanism is well-established^{28,29}. The activation mechanism requires ATP hydrolysis and results in the binding of the C-terminus of Ub through a high energy covalent thioester bond to the catalytic cysteine in the active site of E1^{29–31}. The structure of E1s consist of a complex arrangement of six domains, where Ub binding occurs near the ubiquitin fold domain (UFD)²⁸. Although there are two E1 genes, most cells express only one of them and loss of function of this E1 results in a critical defect in the cell cycle³².

2.1.2. Ubiquitin Conjugating Enzymes (E2)

The second step in ubiquitination is mediated by ubiquitin conjugating enzymes (E2s) that take the Ub from E1 and transfers it onto a substrate lysine residue through the binding of an ubiquitin ligase enzyme (E3)²⁶. The human genome encodes at least 38 E2s, which are classified into 17 phylogenetic sub-families³³. E2s have a core ubiquitin-conjugating (UBC) domain with a catalytic cysteine that accepts the Ub molecule from E1. UBC domains of many E2s share high sequence and structural homology^{34–36}. Since there are at least 38 E2s and hundreds of E3s, a single E2 can interact with several E3s. The binding of E3 to the E2 increases the rate of Ub transfer from the catalytic cysteine in E2 to the substrate and in absence of E3 binding, many E2s are loaded with Ub, ready for transfer^{34,37,38}. Mechanistically, the binding of E3 to E2 locks E2 into a committed state for transfer. After the initial Ub transfer onto the substrate, E2 may choose to elongate the Ub chain or not based on the initial lysine residue. One well-characterized E2-E3 pair is the yeast E2 cell division cycle 34 (Cdc34) and the E3 Skp-Cullin-F-box protein (SCF), which provided insight into the mechanism of E2-E3 interaction³⁴.

2.1.3. Ubiquitin Ligase Enzymes (E3)

The third step in ubiquitination is mediated by ubiquitin ligase enzymes (E3). E3s play a critical role in recognizing the substrate for ubiquitination³¹. There are between 600-1000 E3s

encoded by the human genome, which confers a high degree of substrate specificity^{34,38,39}. The many E3s are divided into three classes based on the mechanism of ubiquitin transfer onto the substrate. The largest class of E3s are the really interesting new gene (RING) E3s, which promote the transfer of Ub directly from the E2 to the substrate and require two zinc ions for proper folding of the RING domain⁴⁰. Mutation of the cysteine and histidine residues that coordinate the zinc ions results in a loss of E3 ligase activity, showing the importance of zinc ions to RING E3 Ub transfer mechanism. Interestingly, U-box proteins have the same Ub transfer mechanism and structure as RING E3s, but lack zinc ions⁴¹.

The other two classes of E3s promote the transfer of Ub from E3 to a cysteine residue in the E3 as an intermediate step before conjugation onto the substrate. The human genome encodes 28 homologous to E6AP C-terminus (HECT) E3s whose structure consists of a N-terminal lobe, flexible hinge and C-terminal lobe 42,43. E2-Ub binds to the N-terminal lobe and the flexible hinge brings the lobes closer together facilitating the Ub transfer onto the catalytic cysteine in the Cterminal lobe, which then is moved onto the substrate⁴³. The same Ub transfer mechanism is utilized by the 14 RING-between-RING (RBR) E3s; however, the structure is distinct making this a separate class from HECT E3s. One well-characterized RBR is PARKIN, whose structure resembles a hybrid of RING and HECT E3s. E2-Ub binds to PARKIN RING1 and the Ub is transferred to a catalytic cysteine in RING2, then transferred to the substrate⁴⁴. As mentioned earlier, Ub can be transferred onto an acceptor Ub on one of the seven lysines (lys6, lys11, lys27, lys29, lys33, lys48 and lys63) as well as the N-terminal methionine. The linkage type used appears to be influenced by both the E2 and the E3 involved. The chosen linkage dictates the fate of the substrate. Monoubiquitinated substrates are often involved in DNA repair and chromatin remodelling whereas Lys48-linked polyUb substrates are recognized by the 26S proteasome for degradation^{45–49}.

2.1.4. 26S Proteasome

The 26S proteasome is the enzyme responsible for the degradation of ubiquitinated substrates, hydrolyzing the substrate into short peptides varying between 5 to 30 amino acids in length⁵⁰. Structurally, the 26S proteasome consists of a 20S core particle and a 19S regulatory particle bound to one or both ends of the core particle. The 20S core is a cylindrical barrel with a hollow center formed from four stacked rings, of which the central two contain the protease active sites. The 19S regulatory particle consists of nineteen subunits of which six are distinct ATPases

and is responsible for recognition, Ub removal and unfolding of the ubiquitinated substrate⁵⁰. The recognition of the ubiquitinated substrate is mediated by ubiquitin receptors, Rpn1, Rpn10 and Rpn13, that contain ubiquitin binding sites and can interact with three deubiquitinating enzymes (DUBs), USP14, Rpn11 and UCHL5, respectively^{51,52}. These DUBs help the ubiquitin receptors remove Ub from the substrate and reduce the chances of substrate stalling, allowing for optimal degradation. The 20S core particle takes the unfolded polypeptide and cleaves it into short peptides using chymotrypsin- and trypsin-like sites, which are released and recycled^{50,53}.

There are four steps to the degradation cycle by the 26S proteasome, which is an ATP consuming process. The first step is substrate accepting, where the ubiquitin receptors are spaced apart and ready to bind ubiquitinated substrates. Upon substrate binding, a conformational change occurs that locks the substrate onto the proteasome. The ubiquitin receptors move closer together and start to disassemble the Ub chains with some help from the DUBs^{54,55}. The process of disassembling the Ub chains from the substrate continues in the substrate-engaged state, where the substrate is fully committed to degradation. Then the ATPase activity of the 19S regulatory particle starts to unfold the substrate and pulls the unfolded sections towards the 20S core particle. Once the unfolded polypeptide enters the 20S core particle, the polypeptide is cleaved into short peptides. It takes some time for the 26S proteasome to reset and prepare for another cycle of degradation of 50,53,56. Through protein degradation using the 26S proteasome, aggregated and misfolded proteins that are potentially cytotoxic can be removed which reduces some cellular stress and restores proteostasis.

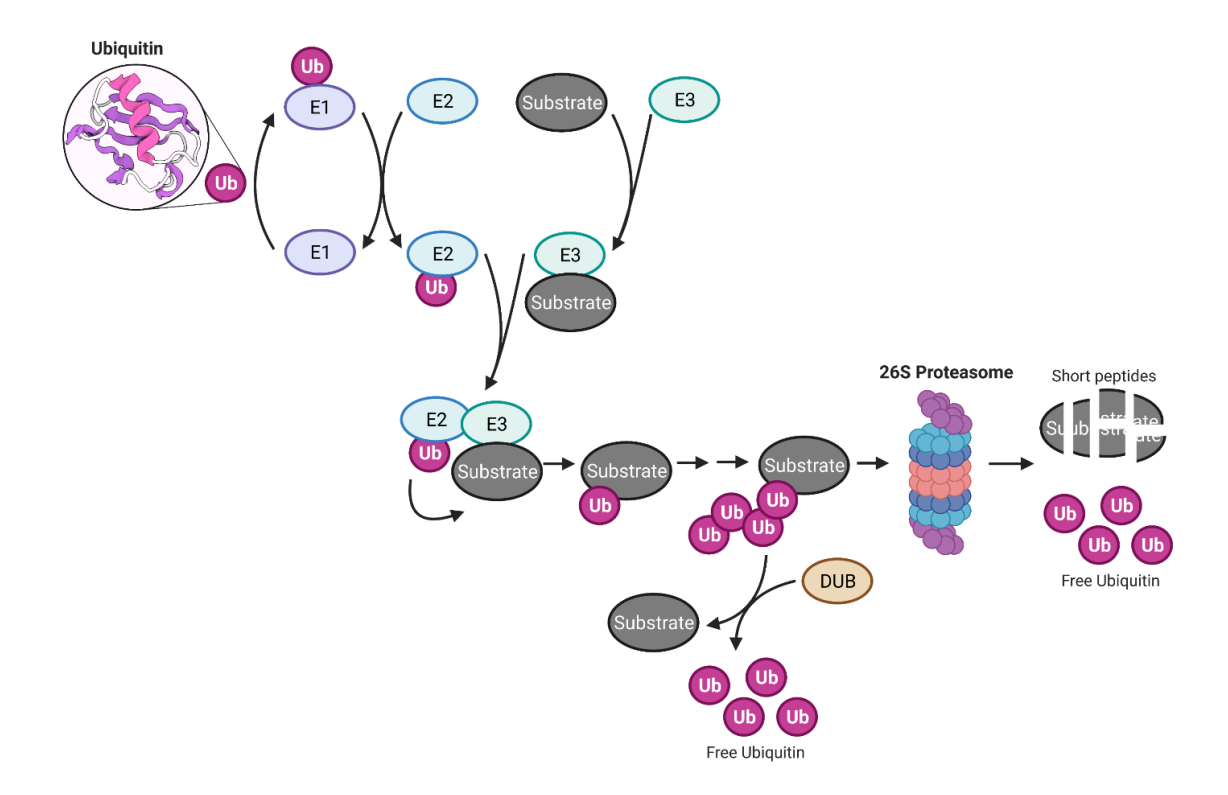


Figure 1.2: The Ubiquitin Proteasome System. Ubiquitination is mediated by ubiquitin activating enzyme (E1) that transfers ubiquitin (Ub) to ubiquitin conjugating enzymes (E2). Ubiquitin ligase enzymes (E3) recognize the substrate and bind to E2 allowing for the transfer of Ub from E2 to E3. This marks the substrate for degradation by the 26S proteasome whereby short peptides are formed. The reversal of ubiquitination is deubiquitination mediated by deubiquitinating enzymes (DUBs), protecting the substrate from degradation. Created on BioRender.com.

2.2. Deubiquitination

Deubiquitination involves deubiquitinating enzymes (DUBs) that remove ubiquitin from the target protein, negatively regulating degradation by the 26S proteasome or non-proteolytic functions of ubiquitination. There are approximately 99 human DUBs, which are classified into seven families based on the similarity of the structure and sequence of their catalytic domains^{27,57–59}. Of the seven classes of DUBs, six are cysteine-dependent proteases and the other are zinc-dependent metalloproteases reflecting the catalytic mechanism used to hydrolyze the isopeptide bond between ubiquitin and the targeted protein^{27,59}.

The six cysteine-dependent proteases families are Ubiquitin C-Terminal Hydrolases (UCHs), Ubiquitin Specific Proteases (USPs), Ovarian Tumour Proteases (OTUs), Machado-Josephin Domain-Containing Proteases (MJDs), MIU-Containing Novel DUB (MINDY) And Zinc-Finger Containing Ubiquitin Peptidase 1 (ZUP). The one zinc-dependent metalloprotease family are the Jab1/MPN domain-Associated Metallopeptidases (JAMM/MPN+).

2.2.1. Ubiquitin C-Terminal Hydrolases (UCHs)

The ubiquitin C-terminal hydrolases (UCHs) were the first DUBs identified and there are four members in humans. UCHs are around 20-40 kDa, with BAP1 exceptionally being approximately 80 kDa, and they preferentially cleave ubiquitin from small peptides. The crystal structure of UCH-L1 revealed a peptide segment over the active site, making it only accessible to smaller peptides^{60,61}. Despite low sequence similarity to papain-like cysteine proteases, the crystal structure showed high similarity to cysteine-proteases and their crucial catalytic triad⁶¹. In addition to the His and Asp residues that activate Cys to attack the scissile bond, there is a Gln residue that interacts with the Cys amide to form an oxyanion hole where the carbonyl oxygen of the substrate situates during catalysis⁶¹. Some notable members of the UCH family of DUBs are UCH-L1 which has been found mutated in some cases of Parkinson's Disease and BAP1 which is involved with BRCA1 in the development of breast cancer^{60,61}.

2.2.2. Ubiquitin Specific Proteases (USPs)

Ubiquitin specific proteases (USPs) are the largest family of deubiquitinating enzymes with 54 members, sharing strong homology in the catalytic domain. The crystal structure of USP7 was one of the first insights into the catalytic mechanism of the USP family and the catalytic domain interestingly resembles a right-hand^{62,63}. There are three main domains, the fingers, thumb, and palm. The crucial cysteine residue is in the thumb and the histidine and aspartate/asparagine residues are in the palm^{62,63}. This forms the catalytic triad in the hydrolytic cleft, which appears to be accessible to larger proteins and suggests the substrate differences between the UCH and USP families. This architecture of the catalytic domain was found to be highly conserved among the members of the USP family, therefore making it characteristic of this family of DUBs. The substrate specificity and localization of USPs is dependent on the additional domains found in the sequence, such as ubiquitin-like (UbL) domains, ubiquitin-interacting motif (UIM), etc^{58,63}.

2.2.3. Ovarian Tumour Proteases (OTUs)

The ovarian tumor (OTU) proteases were identified by Makarova et al. in *Drosophila Melanogaster*. The sequence of the ovarian tumor (OTU) gene bears similarity to cysteine proteases⁶⁴. There are 16 members of the OTU family of which OTU-domain Ubal-binding protein (Otubain)-1 and Otubain-2 were the first members shown to have *in vitro* deubiquitinase activity⁶⁵. Shortly after the identification of these two OTU members, a structure of Otubain-2 revealed an incomplete catalytic triad and stabilization using a hydrogen bond network⁶⁶. Another OTU member that has been studied is A20, which inhibits tumor necrosis factor (TNF) and NF-κB signaling^{65–67}. There are additional OTU members studied, but their function in health and disease are yet to be understood.

2.2.4. Machado-Josephin Domain-Containing Proteases (MJDs)

The Machado-Josephin domain containing proteases (MJDs) all have a N-terminal Josephin domain, and four members have been described. Ataxin-3 (Atx-3) is the most-studied MJD member. Mutations in Atx-3 have been implicated in a neurodegenerative polyglutamine (polyQ) expansion disease known as spinocerebellar ataxia type 3 (SCA3)^{68,69}. A crystal structure of Atx-3 revealed that the Josephin motif has a helical nature and interestingly, a distinct fold compared to papain-like cysteine proteases. The Josephin fold is more similar to bacterial *staphopain* and *pseudomonas* avirulence protein AvrPphB, although it still uses the conserved catalytic triad in the same manner as the other members of the cysteine protease DUBs^{70,71}.

2.2.5. MIU-Containing Novel DUB (MINDY)

In 2016, Rehman et al. discovered a new family of DUBs which they named motif interacting with ubiquitin (MIU)-containing novel DUB (MINDY)^{72,73}. There are four members of MINDY which have a distinct fold in the catalytic domain and bear no sequence homology to the other cysteine proteases. In their investigation, they identified an MIU in FAM63A that bound K48-specific poly-Ub chains. Sequence analysis revealed a putative cysteine protease active site and FAM63A was found to cleave K48-linked chains, and so FAM63A was renamed to MINDY-1⁷². A crystal structure of the catalytic domain of MINDY-1 revealed a novel folding variant with the same catalytic triad as other cysteine-dependent DUBs⁷².

2.2.6. Zinc-Finger Containing Ubiquitin Peptidase 1 (ZUP1)

In 2018, another new family of DUBs was identified and named zinc-finger containing Ub peptidase 1 (ZUP1)^{27,74–76}. ZUP1 is made up of 578 amino acids with two zinc fingers at the N-terminus and a MIU within the catalytic domain. The crystal structure bears no similarity to any structure in the protein data bank (PDB), but revealed the conserved catalytic triad of cysteine-dependent DUBs^{74,77}. ZUP1 selectively cleaves K63-linked polyUb chains and is involved in the regulation of DNA repair and replication as depletion of ZUP1 results in genomic instability^{27,59,74,76}.

2.2.7. Jab1/MPN Domain-Associated Metallopeptidases (JAMM/MPN+)

A JAMM motif binds metal and is found within a Jab1/MPN domain, a motif previously recognized in the COP9 signalosome (CSN) subunit 5 (CSN5)^{78,79}. CSN5 is a paralog of Rpn11, a subunit of the 19S proteasome lid with DUB activity^{78,80}. A crystal structure of *Archeaoglobus fulgidus* AfJAMM revealed distinct differences of the JAMM fold compared to cysteine proteases, suggesting it belongs to a novel family of metallopeptidases⁷⁸. There are currently 14 members of the JAMM metallopeptidases. Only 7 of the 14 are catalytically active and they are AMSH, AMSH-LP (AMSH-like protein), BRCC36, Rpn11 (POH1), MYSM1, CSN5 and MPND^{58,81–83}. The active JAMM metallopeptidases use a zinc molecule and water to coordinate a nucleophilic attack between ubiquitin and the target protein^{58,84}. In the crystal structure of AfJAMM, the stabilization of zinc was revealed to be due to an aspartate residue and two histidine residues, suggesting a mechanism likely similar to thermolysin, which contains a similar triad^{78–80}.

2.2.8. Regulation of DUBs

Deubiquitinating enzymes are regulated by multiple mechanisms including phosphorylation and ubiquitination²⁷. For example, USP4 is ubiquitinated by Ro52, which targets USP4 for degradation. However, USP4 has auto-deubiquitination mechanisms to prevent its degradation and there could be other post-translational modifications in place to ensure USP4 does eventually become degraded^{85–87}. In addition, DUBs can be transcriptionally regulated and regulated by substrate binding and subcellular localization.

2.2.9. Relation of DUBs to Muscle Atrophy

In addition to the upregulated ubiquitin ligases such as MAFbx/Atrogin-1 and MuRF-1, in muscle atrophy, four DUBs have been identified to have a role in skeletal muscle and they are

USP19, USP14, USP2 and A20⁸⁴. Of these four DUBs, USP19 is the best studied in muscle atrophy as explained in section 3.2.1. USP14 is induced in catabolic conditions, but the exact molecular mechanism and effect in muscle remain to be explored⁸⁸. USP2 was shown to have an effect in muscle cell differentiation but does not appear to be essential^{89,90}. A20 is a member of the OTU family, is highly expressed in muscle fibers and has an essential role in muscle cell differentiation through NF-κB signaling; however, its specific role in muscle atrophy remains unexplored^{91,92}.

3. Ubiquitin Specific Protease 19 (USP19)

USP19 is a 150 kDa deubiquitinating enzyme that was first identified in skeletal muscle and found to be upregulated under catabolic conditions such as glucocorticoid treatment, starvation and cancer⁹³. USP19 is highly expressed in the testis, brain, heart, kidney and skeletal muscle^{93,94}.

3.1 The Structure of USP19

The USP19 gene consists of 28 exons and alternative splicing produces multiple isoforms. The two major isoforms of USP19 differ in the identity of their last exon. Inclusion of exon 27 results in USP19 with a transmembrane domain, allowing for insertion into the endoplasmic reticulum (ER) and this isoform is referred to as USP19-ER. The replacement of exon 27 with exon 28 results in a cytoplasmic USP19, which is referred to as USP19-Cyt⁹⁵. The presence of a transmembrane domain in USP19 makes it unique among the DUBs. In addition, there are two CS (CHORD & Sgt1-like) domains in the N-terminal, a ubiquitin-like domain (Ubl) and a SIAH degron and within the catalytic domain, a myeloid translocation protein 8, Nervy and Deaf1 (MYND) zinc finger domain⁹⁶. Each of these domains has the potential to be involved in protein-protein interactions, a few of which have been studied as described in section 3.2.

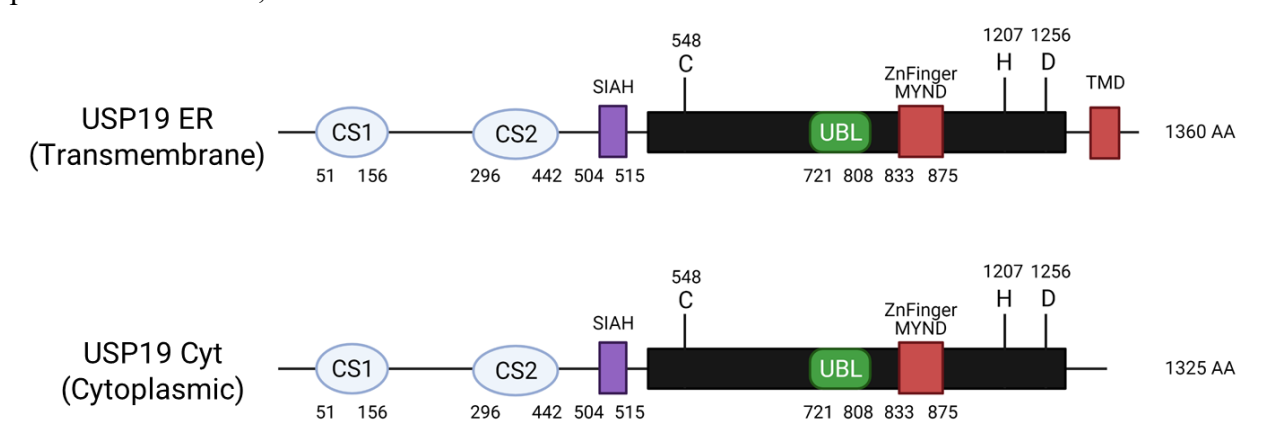


Figure 1.3: Structural and functional domains in USP19. Alternative splicing of the USP19 gene results in two isoforms, an endoplasmic reticulum (ER) and a cytoplasmic (Cyt) isoform that differ in the transmembrane domain (TMD), There are two CS (Chord-Sgt1) domains like the CS domains in p23, a SIAH degron and the catalytic domain that contains the catalytic triad (C,H,D), a UbL (ubiquitin-like) domain and a MYND (Myeloid-Nervy-DEAF1 domain). The amino acids numbering corresponds to mouse USP19.

3.1.1. CS domains

The CS (CHORD and Sgt1-like) domain was originally described in *C. elegans* through the identification of a common motif in CHORD (cysteine and histidine rich domain)-containing proteins and suppressor of G2 allele of skp1 (Sgt1)^{97–99}. There are several CS domain-containing proteins such as p23, a co-chaperone of HSP90, Sgt1, eukaryotic nuclear movement protein nudC and mammalian integrin beta-1-binding protein 2 (melusin)⁹⁹. In each of these proteins, the structure of the CS domain is an anti-parallel β -sandwich fold with seven β -strands, although Sgt1 only has six β -strands ^{99,100}.

Interestingly, the CS domains in USP19 are homologous to the CS domain in p23 and Sgt1. The solution structures of the CS domains in USP19 have been recently uncovered by Xue et al. showing the characteristic structural features seen in other CS domain-containing proteins¹⁰¹. In USP19, the CS domains are divided into the CS1 domain (residues 51-156) and the CS2 domain (residues 296-442). Since the CS domains in USP19 are like the CS domain in p23, it raised the question whether USP19 could interact with HSP90. This has been investigated by two reports where the CS domains, specifically the CS2 domain, do interact with HSP90¹⁰¹.

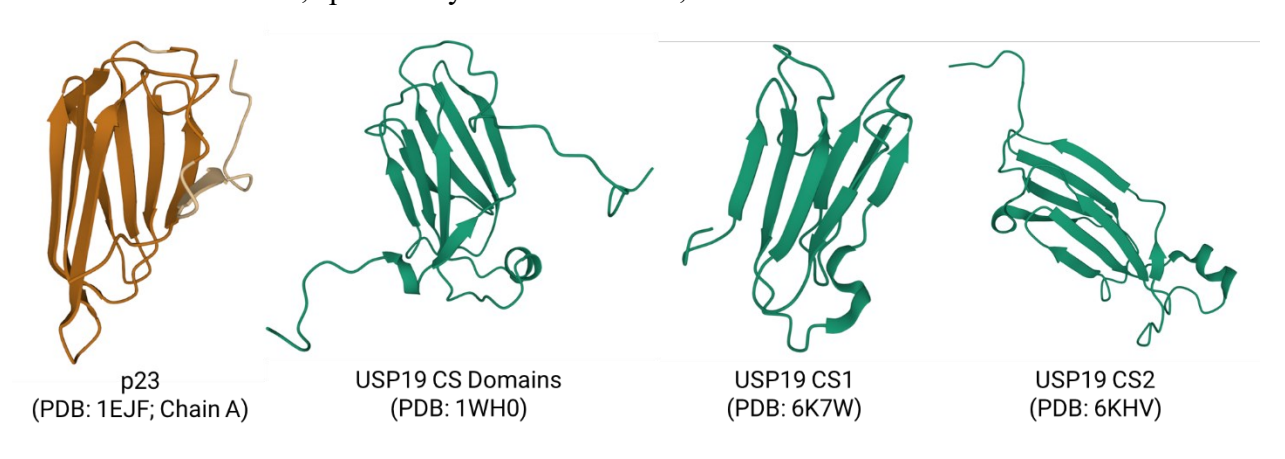


Figure 1.4: Comparison of CS1 and CS2 solution structures to p23. The CS domains in USP19 (PDB: 1WH0, 6K7W, 6KHV) are homologous with the CS domain of p23 (PBD: 13JF chain A). Side-by-side comparison of the structures show their high degree of similarity ^{101,102}.

3.1.2. USP domain

The ubiquitin specific protease (USP) or catalytic domain of USP19 is highly conserved, containing the catalytic triad of cysteine, histidine, and arginine residues. Within the USP domain is located the UbL domain and a MYND Zn domain, both are further explained below. Interestingly, the catalytic domain of USP19 has also been reported to interact with HSP90. The deletion of a region in the middle of the catalytic domain was able to abolish the interaction of USP19 and HSP90^{103,104}.

3.1.2.1. UbL domain

The ubiquitin-like or UbL domain is found in several members of the USP family, sharing a β-grasp fold with ubiquitin^{63,105}. The UbL domain lacks a terminal glycine residue that ubiquitin uses to form a covalent bond with lysine residues on the target protein. Interestingly, UbL domains are found in the catalytic domains of some other USPs¹⁰⁵. USP19 has one UbL domain whereas USP7 has five UbL domains. A regulatory role of the UbL domain in USP19 has recently been reported. It appears to interact intramolecularly with the CS1 domain to elicit an auto-inhibitory conformation of USP19 that is relieved upon binding of the CS2 domain to HSP90 binding¹⁰¹.

3.1.2.2. MYND Zn Domain

The MYND domain was initially described in *Drosophila* deformed epidermal autoregulatory factor 1 (DEAF-1) protein. It contains a highly conserved cysteine-rich region in the C-terminus that bears similarity to a domain in myeloid translocation protein 8 (MTG8) and *Drosophila* Nervy protein and so became known as the MYND domain 106. The composition of the MYND domain is two CXXC and two C/HXXXC motifs, which are similar to zinc fingers, and interacts with transcriptional co-repressor proteins 63,107. USP19 contains one MYND Zn domain in the catalytic region (833 CAACQRKQQSEEEKLKRCTRCYRVGYCNQFCQKTHWPDHK GLC 875). The function of this domain in USP19 remains unknown as it has not been reported whether USP19 interacts with transcriptional co-repressor proteins such as members of the nuclear receptor co-repressor family (NCoR).

3.1.3. SIAH Domain

Seven in absentia homologs or SIAHs are RING-type E3 ubiquitin ligases, involved in stress-related cellular pathways^{108,109}. SIAH recognizes its substrates through a consensus motif or degron PxxxVxP and it was identified that USP19 contains three SIAH-interacting consensus motifs, two in the N-terminus of the USP catalytic domain and one towards the C-terminal^{108,110,111}. Only one of the identified SIAH-interacting motifs (⁵⁰⁴PKPTCMVPPMPH⁵¹⁵) is crucial for the interaction of USP19 with SIAH1 and SIAH2 and this sequence is highly conserved. It was observed that co-expressing SIAH1 and SIAH2 with USP19 reduced the expression of USP19 suggesting SIAH1 and SIAH2 target USP19 for degradation^{108,110}. Deletion of the consensus motif abolished the interaction of either SIAH with USP19 and prevented its degradation, illustrating a means to negatively regulate USP19 expression. Recently, an x-ray crystal structure of SIAH1 in complex with a short peptide of USP19 was reported¹⁰⁸.

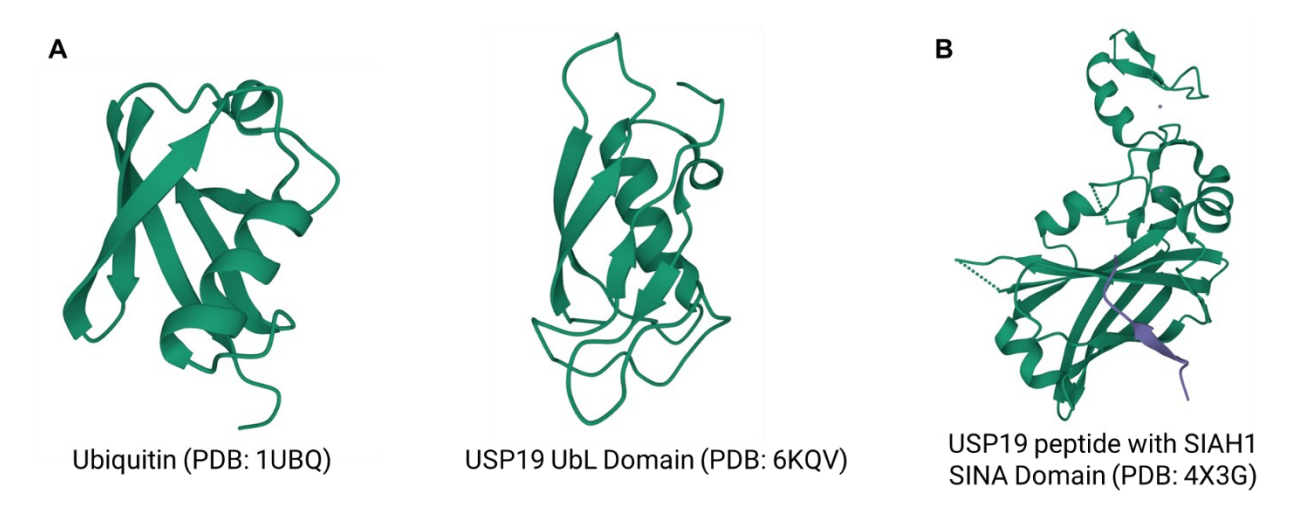


Figure 1.5: Comparison of Ub with USP19 UbL domain and SIAH domain. (A) Side-by-side comparison of the structure of ubiquitin (PDB: 1UBQ)¹¹² and the NMR solution structure of the UbL domain in USP19 (PDB: 6KQV)¹⁰¹ shows a high degree of similarity. (B) Structure of a peptide of USP19 in complex with SIAH1 showing their interaction (PDB: 4X3G)¹⁰⁸.

3.2 The Function of USP19

A first role of USP19 was proposed in 2005, when USP19 was observed to be upregulated in catabolic conditions that lead to muscle atrophy⁹³. Since then, USP19 has been found to be involved in numerous processes such as in cancer, hypoxia, cell cycle regulation, autophagy and endoplasmic reticulum associated degradation (ERAD).

3.2.1. Role in Muscle Atrophy

A negative balance between muscle protein synthesis and protein breakdown results in a loss of skeletal muscle mass or muscle atrophy. Both protein synthesis and degradation are precisely regulated by hormones. Insulin and glucocorticoids are classical anabolic and catabolic hormones respectively for muscle mass. Experimentally, treatment with streptozotocin which induces insulin deficiency or dexamethasone (Dex), a potent synthetic glucocorticoid, can induce muscle atrophy in animal models. Under these conditions, USP19 was found to be upregulated alongside two well-known muscle-specific E3 ligases, MuRF1 and MAFbx/Atrogin-193. To further investigate the role of USP19 within the muscle, L6 myotubes were studied. Silencing USP19 increased myogenin, a myogenic regulatory transcription factor, which plays a critical role in myogenesis to promote myoblast fusion to form myotubes¹¹³. Myosin heavy chain (MHC) and tropomyosin are two downstream targets of myogenin and indeed, silencing USP19 increased MHC and tropomyosin levels. Concomitant silencing of myogenin abolished this increase of MHC and tropomyosin confirming the key role of myogenin in mediating the effect of USP19¹¹³. The opposite effect on myogenin, MHC and tropomyosin were observed when USP19 was overexpressed and led to a delay in formation of myotubes¹¹⁴. This indicated that USP19 modulates the expression of myogenic and myofibrillar proteins and muscle cell fusion ^{113,114}.

The USP19 isoform responsible for the modulation of muscle cell fusion was identified to be USP19-ER, since the cytoplasmic isoform and the catalytic mutant had no effect on the expression of myogenic proteins and muscle fusion¹¹⁴. Interestingly, ER stress markers and unfolded protein response (UPR) activation have been studied in muscle atrophy inducing conditions¹¹⁵. One UPR target gene is a transcription factor, C/EBP homologous protein (CHOP). CHOP expression delays muscle differentiation and decreases expression of myogenin and MHC¹¹⁶. Overexpressing USP19-ER attenuates CHOP expression, suggesting USP19 suppresses the UPR induction during myogenesis to inhibit muscle cell differentiation¹¹⁴. Additionally, in mice, inactivation of USP19 reduced the extent of muscle atrophy and weakness when treated with dexamethasone and the increased the myofiber cross-sectional area (CSA)¹¹⁷. This suggests that inactivating USP19 protects against muscle atrophy by enhancing muscle cell differentiation and increasing myofiber growth under catabolic conditions¹¹⁴.

There is increased production of reactive oxygen species (ROS) during muscle atrophy induced by catabolic conditions. The use of β -carotene, a naturally-occurring anti-oxidant, was able to inhibit the upregulation of USP19, MuRF1 and MAFbx after denervation ¹¹⁸. This suggests that the use of antioxidants may delay the progression of muscle atrophy, although the specific mechanism of how β -carotene modulates the expression of USP19, MuRF1 and MAFbx is yet to be explored. In addition to USP19 upregulation under catabolic conditions, exposure of muscle cells to cigarette smoke exposure induces atrophy and upregulates USP19 expression, concomitant with activation of p38 and ERK1/2¹¹⁹. Treatment with a p38 kinase inhibitor blocked the upregulation of USP19 and atrophy. This suggests that cigarette smoke exposure may work in a USP19-dependent pathway to induce muscle atrophy.

3.2.2. Role in Cell Cycle Regulation and DNA Damage Repair

The regulation of the cell cycle is important to maintain genomic stability. Cell cycle progression is dependent on precisely timed activation and inhibition of cyclin-dependent kinases (CDK). One of the best studied CDK inhibitors is p27^{Kipl}, which inhibits entry into the S phase from G1. The degradation of p27^{Kipl} is mediated in part by KIP1 ubiquitination-promoting complex (KPC), an E3 ligase that ubiquitinates p27^{Kipl} and promotes its proteasomal degradation¹²⁰. KPC is made up of two subunits, KPC1 and KPC2. Overexpressing USP19 increased KPC1 expression and decreased KPC1 ubiquitination. This suggests that USP19 stabilizes KPC1 using its enzymatic activity and thus promotes p27^{Kipl} degradation and cell proliferation¹²⁰. However, the effect of USP19 on cell proliferation appears to be cell-dependent, since USP19 regulates KPC1 in FR3T3 cells but not in breast normal cells or prostate cancer cell lines¹²¹. Additionally, USP19 was found to be involved in regulating DNA damage repair process, where USP19 regulates histone deacetylases 1 and 2 (HDAC1/2) by translocating into the nucleus¹²². Silencing USP19 results in reduced DNA repair and accumulation of damaged DNA, which can lead to chromosome instability and tumorigenesis¹²². This suggests an essential role for USP19 in DNA damage repair.

3.2.3. Role in Endoplasmic-Reticulum Associated Degradation (ERAD) & Unfolded Protein Response (UPR)

The transmembrane domain in USP19-ER is inserted into the endoplasmic reticulum (ER) where the catalytic domain faces the cytoplasm^{95,96}. The presence of the CS domains in USP19 is

suggestive of chaperone activity, so Hassink et al., hypothesized that USP19 may have a role in regulating the response to ER stress through the unfolded protein response (UPR).

The endoplasmic reticulum (ER) is a hub for protein maturation where newly synthesized proteins enter the ER, undergo post-translational modifications and interact with molecular chaperones to ensure proper folding and functionality prior to being released^{123–125}. Proteins that do not pass the stringent ER quality-control tests are sent to be degraded through the endoplasmic reticulum associated degradation (ERAD) pathway. Briefly, there are four steps of ERAD, (1) recognition of the misfolded protein, (2) retro-translocation across the lipid bilayer to the cytoplasm, (3) ubiquitination and (4) degradation by the 26S proteasome^{124,125}. ERAD aims to prevent the accumulation of aberrant proteins to reduce cellular proteotoxicity, which maintains ER homeostasis. Dysregulation of ERAD leads to the accumulation of misfolded proteins in the ER lumen and triggers ER stress, activating the unfolded protein response (UPR)^{124–127}.

The unfolded protein response (UPR) coordinates multiple signaling pathways to attempt to restore ER homeostasis by reducing the rate of protein synthesis and subsequent influx into the ER as well as increasing protein folding, maturation and quality control^{126,128–130}. Upon induction of ER stress that triggers the activation of UPR, USP19 mRNA levels were found to be upregulated⁹⁶. To investigate the role of USP19 in regulating UPR, the effect of USP19 on the degradation of two ERAD substrates, cystic fibrosis transmembrane conductance receptor mutant (CFTR Δ 508) and T cell receptor α subunit (TCR α) were examined^{96,125}. CFTR Δ 508 and TCR α degradation are both rescued by co-expressing USP19-ER; however, only the rescue of CFTR Δ 508 requires USP19-ER catalytic activity and TCR α does not. This suggests that USP19 potentially rescues retro-translocated ERAD substrates, possibly through deubiquitination⁹⁶.

The ubiquitination of ERAD substrates is crucial for the degradation of aberrant proteins, and is mediated by several E3 ubiquitin ligases including HMG-CoA reductase degradation protein 1 (HRD1) and membrane-associated RING-CH6 (MARCH6)^{125,131}. As described earlier, USP19 can deubiquitinate and stabilize some E3s. Overexpressing USP19 can interact and stabilize MARCH6 and HRD1 and so play a role in ERAD in this indirect manner^{131,132}.

3.2.4. Role in Misfolded-Associated Protein Secretion (MAPS)

In contrast to ER associated proteins, misfolded proteins that accumulate in the cytoplasm can be degraded by the UPS or autophagy. Recently it has also been reported that misfolded

proteins can be secreted from the cell by an unconventional pathway called misfolded-associated protein secretion (MAPS)^{133,134}. The misfolded protein is recruited into a late endosome which fuses to the plasma membrane, resulting in the export of the misfolded protein, relieving some of the proteotoxic stress within the cell¹³³. Overexpressing or silencing USP19 promotes or inhibits MAPS activity respectively. The catalytic activity and ER-localization of USP19 are required¹³⁵. Current data are consistent with a model in which USP19 recruits misfolded cytosolic proteins to the ER, deubiquitinates them and then interact with Hsp70 and its co-chaperone DNAJC5 to load the misfolded protein into late endosomes^{104,133,135–137}.

3.2.5. Role in Neurodegenerative Diseases

USP19 has been identified to modulate the protein level and aggregation of polyglutamine (polyQ)-containing proteins that are associated with neurodegenerative diseases such as Huntingtin's Disease (HD)¹³⁸. Overexpressing the cytoplasmic USP19 isoform increased the levels and cytotoxicity of Ataxin3 (Atx3) and polyQ expanded huntingtin (Htt)¹³⁸. Interestingly, treatment with 17-AAG, a HSP90 inhibitor, reduced the protein levels of Atx3 and Htt, suggesting the involvement of HSP90 in USP19 regulation of polyQ-containing proteins. Specifically, the hydrophobic side of an amphipathic α -helix of HSP90 interacts with the N-termini of Htt and abolishment of this interaction prevents USP19 from regulating Htt protein levels and aggregation¹³⁹. As described earlier, USP19 interacts with HSP90 through its CS2 domain resulting in the release of CS1 domain autoinhibition of USP19 and activation of its catalytic activity^{101,138}. This results in polyQ-containing protein stabilization and promotes aggregation.

3.2.6. Role in Hypoxia

The cellular environment requires an adequate amount of oxygen for aerobic processes. A low oxygen or hypoxic environment induces a number of molecular changes to enhance oxygen delivery and ensure survival¹⁴⁰. Hypoxia-inducible factor 1 (HIF-1) is a transcription factor that accumulates in the cytoplasm and translocates into the nucleus to activate genes related to angiogenesis, erythropoiesis and energy metabolism^{140–142}. HIF-1 is made up of an α -subunit and a β -subunit and HIF-1 α is tightly regulated by the UPS¹⁴³. USP19 interacts with HIF-1 α and the overexpression of the cytoplasmic isoform of USP19 prevents its degradation under hypoxic conditions¹⁴³. Conversely, silencing USP19 abolished HIF-1 α accumulation, suggesting USP19 stabilizes HIF-1 α to ensure proper transcriptional response under hypoxic conditions. The

interaction of USP19 with HIF-1 α can be promoted by the expression of Prox1 (Prospero-related homeobox 1), a transcription factor associated with HIF-1 α protein stability. Overexpressing Prox1 enhanced USP19 and HIF-1 α interaction as well as decreased the levels of ubiquitinated HIF-1 α ¹⁴⁴.

Under hypoxic conditions, mitochondrial function is impaired, and the damaged mitochondria undergo a process of fission by recruiting dynamin-related protein 1 (Drp1) prior to clearance by mitophagy^{142,145}. FUNDC1 is a mitochondrial outer membrane protein that accumulates at the ER-mitochondria contact sites and is required for the oligomerization of Drp1 and downstream mitochondrial fragmentation. In hypoxia, USP19 accumulates at ER-mitochondria contact sites and promotes mitochondrial fission by deubiquitinating and stabilizing FUNDC1^{146,147}.

3.2.7. Role in the Immune System

Cells damaged beyond repair undergo programmed cell death or apoptosis and this can be prevented by inhibitors of apoptosis (IAPs)⁹⁴. Interestingly, IAPs contain a baculoviral IAP repeat (BIR) domain that facilitates its protein-protein interaction and a RING domain that contains E3 ubiquitin ligase activity⁹⁴. In mammalian cells, IAPs are called cellular IAPs (c-IAPs) and two have been well-studied, c-IAP1 and c-IAP2. Both interact with components of NF-κB signaling to attenuate its activation¹⁴⁸. Overexpressing USP19 can interact and stabilize c-IAP1 and c-IAP2, inhibiting tumor necrosis factor (TNF)-α induced apoptosis⁹⁴.

The activation of NF- κ B signaling occurs through a canonical or non-canonical manner. The canonical pathway is stimulated by the immune system using toll-like receptors (TLRs) or tumor necrosis factor receptors (TNFRs)^{149,150}. USP19 negatively regulates TLR3/4-mediated signaling by deubiquitinating a TIR domain containing adapter-inducing interferon β (IFN β) (TRIF). This prevents the interaction of TRIF with TLR3/4 and subsequent downstream immune response¹⁵¹. Similarly, USP19 interacts with and deubiquitinates tumor necrosis factor receptor-associated factor 3 (TRAF3), suppressing type I interferon signaling, which was suggested to help enterovirus 71 (EV71) evade host antiviral defenses¹⁵². Additionally, USP19 interacts and deubiquitinates tumor growth factor- β (TGF β)-activated kinase 1 (TAK1), inhibiting TNF α and interleukin-1 β (II-1 β)-mediated activation of NF- κ B^{149,153}. This suggests USP19 negatively

regulates TNF α and Il-1 β -mediated NF- κ B activation and it was shown that the CS domains of USP19 interact with TAK1¹⁵³.

3.2.8. Role in Carcinomas

Cell cycle regulation and DNA damage repair are often hijacked in cancer and USP19 has been shown to have a regulatory role in both processes¹⁵⁴. One of the signaling pathways implicated in cancer is the Wnt signal transduction cascade as it is involved in tissue development and function¹⁵⁵. A key component of Wnt signaling is the low-density lipoprotein receptor-related protein 6 (LRP6)^{156,157}. USP19-ER interacts with and deubiquitinates LRP6 preventing its degradation and resulting in LRP6 initiation of Wnt signaling¹⁵⁷. In a non-invasive breast cancer cell line (MCF7), silencing USP19 reduced LRP6 expression and increased cell migration, suggesting a role for USP19/LRP6 in the cellular migration of breast cancer¹⁵⁸. Additionally, USP19 positively correlates with BRCA1-associated protein-1 (BAP1), a commonly mutated protein found in many cancers such as clear cell renal cell carcinoma (ccRCC)¹⁵⁹. The specific interaction and mechanism of USP19 with BAP1 is yet to be explored¹⁵⁹. Interestingly, in ccRCC and high-grade serous carcinomas (HGSCs), reduced USP19 expression was observed in patients with poorer prognosis^{160,161}. Overexpressing USP19 reduced ccRCC cell proliferation and migration *in vitro*, suggesting USP19 may act as a tumor suppressor in ccRCC.

USP19 has also been reported in Ewing sarcoma, a rare childhood cancer of the bone and soft tissue¹⁶². In Ewing sarcoma, a chimeric transcription factor, EWS-FLI1 is continuously expressed and interacts with the N-terminal domain of USP19. Silencing USP19 reduced EWS-FLI1 protein levels and delayed tumor growth and proliferation¹⁶². Colorectal cancer (CRC) cells highly express cytoplasmic-localized malic enzyme 1 (ME1)¹⁶³. USP19 interacts with and stabilizes ME1, promoting its tumorigenic role. Depleting USP19 in a CRC mouse model prolonged survival and decreased tumor development, suggesting a pathogenic role of USP19 upregulation in CRC¹⁶³.

In hepatocellular carcinoma (HCC), a common liver cancer, high levels of sterol O-acyltransferase (SOAT) 1 and 2 are detected and SOAT1 protein levels increased upon the absence of p53, a tumor suppressor protein. Interestingly, USP19 interacts with and stabilizes SOAT1 and putative p53 binding sites were identified in both USP19 and SOAT1 Overexpressing USP19 accelerated hepatocarcinogenesis and high expression of USP19 and SOAT1 correlated with

diminished survival in patient samples. This suggests USP19 promotes HCC development through stabilizing SOAT1 and p53 represses USP19 to attenuate HCC development ¹⁶⁴.

An additional way cancer cells metastasize is through manipulation of the epithelial-mesenchymal transition (EMT)¹⁵⁴. Matrix metalloproteases (MMP) regulate the extracellular matrix and elevated MMP2 and MMP9 expression is observed in gastric cancer patients¹⁶⁵. Overexpressing USP19 enhances cell invasiveness and upregulates MMP2 and MMP9 expression. Silencing USP19 reduced tumor growth in gastric cancer cells, similar to the effect of USP19 in Ewing sarcoma^{162,165}. This suggests that the inhibition of USP19 may be beneficial in Ewing sarcoma, gastric cancer, CRC and HCC to delay tumor growth and metastasis.

3.2.9. Role in the Heart

USP19 is highly expressed in the heart. Miao et al. investigated the protective role of USP19 against cardiac hypertrophy, the enlargement of cardiac muscle 166. Under hypertrophic stimuli, USP19 was upregulated, SIAH2 decreased and reduced the inflammatory response, suggesting an anti-hypertrophic role for USP19. Previous reports showed USP19 inhibits TAK1 preventing the activation of downstream inflammatory genes and reduces cardiac hypertrophy 166. Treatments for ischemic injury, a reduction in blood flow that can induce cardiac hypertrophy, can also lead to myocardial ischemia/reperfusion (I/R) injury 167. I/R injury upregulated USP19 expression along with autophagy markers, Beclin-1 and LC3I/LC3II. Treatment with C3G, a naturally occurring flavonoid with anti-inflammatory properties, reversed the expression, suggesting C3G inhibits autophagy to have a beneficial effect in I/R injury 168,169. A similar observation was made using Reveratrol (Res), a naturally occurring polyphenol with anti-oxidant and anti-inflammatory activities 170,171. Both Res and C3G were observed to have protective effects against myocardial I/R injury through inhibiting ferroptosis, an iron-dependent non-apoptotic cell death mechanism 169,171. They suggest the inhibition of ferroptosis is through USP19/Beclin-1, although further investigation of the role of USP19 in ferroptosis is required.

3.2.10. Role in Autophagy

Autophagy is another protein-quality control system within the cell. Beclin-1 (BECN1) is an autophagy-related protein (ATG) important for the initiation and progression of autophagy to remove aggregated and misfolded proteins¹⁷². Briefly, in autophagy, autophagosomes form and engulf cellular debris and then fuse with lysosomes for degradation¹⁷³. USP19 interacts with and

stabilizes BECN1 leading to USP19-mediated autophagic flux^{174,175}. Additionally, USP19 suppresses type I IFN signaling through association with BECN1^{174,175}.

The crosstalk between USP19, autophagy and the immune system was recently investigated. USP19 inhibits a downstream component of NF-κB signaling, NOD-like receptor family, pyrin domain containing protein 3 (NLRP3)¹⁷⁶. NLRP3 inflammasome is activated by ROS production. Silencing USP19 increased ROS production and inflammasome activation. Additionally, USP19 interacts and stabilizes NLRP3, preventing NLRP3 from participating in the inflammasome and enhances ROS removal¹⁷⁶. USP19 is suggested to act as an anti-inflammatory switch by modulating NLRP3 from being pro-inflammatory to anti-inflammatory. Similarly, USP19 interacts with TANK-binding kinase 1 (TBK1), a serine/threonine kinase involved in both autophagy and the immune system¹⁷⁷. Overexpressing wild-type USP19 and its catalytic mutant both decreased TBK1, suggesting deubiquitination is not required. USP19 co-localizes with TBK1 along with LAMP2A, a component of the lysosome, suggesting TBK1 degradation is through autophagy, and impairs the TBK1-mediate immune response¹⁷⁷.

3.2.11. Role with Nuclear Receptors

Nuclear receptors (NRs) are ligand-activated transcription factors that modulate a variety of genes related to metabolism, cell proliferation, reproduction, etc¹⁷⁸. Interestingly, USP19 is involved with two NRs, estrogen receptors (ERα and ERβ) and glucocorticoid receptor (GR), both fall within the third NR subfamily. The endogenous ligand for ER is 17β-estradiol (E2) and E2 treatment inhibited myogenesis and upregulated USP19 expression¹⁷⁹. Silencing ERα reversed the upregulation of USP19 and inhibition of myogenesis although this was only observed in young female mice *in vivo*, suggesting USP19 has a sex-related effect on myogenesis¹⁸⁰. Unsurprisingly, ERβ inhibits ERα-regulated gene transcription since they both bind to the same estrogen-response element (ERE) on the DNA¹⁸¹. Overexpressing ERβ inhibited the upregulation of USP19 observed with E2 treatment and reversed the effects on myogenesis¹⁷⁹. Daidzein is a phytoestrogen and an ERβ agonist that downregulates USP19 expression only in female mice¹⁸². In addition, E2 also has non-genomic mechanisms. E2 acts on G-protein coupled estrogen receptor (GPER) to have an angiogenic effect and USP19 was found to be involved with a downstream effector, PKFKB¹⁸³. This suggests USP19 may have a role in endothelial cell angiogenesis.

Another important function of USP19 is in muscle atrophy and a specific signaling pathway was recently uncovered. In USP19 knockout (KO) mice, protection from muscle atrophy was observed concomitant with improved insulin sensitivity and glucose tolerance^{184,185}. Knockout of USP19 increased insulin stimulated Akt activation and decreased expression of GR target genes, suggesting USP19 may be modulating GC signaling. Interestingly, in the muscle of USP19 KO mice, GR protein levels were decreased by 50% with unchanged mRNA, suggesting a post-transcriptional effect of USP19. Restoration of GR expression resulted in GC-induced muscle atrophy¹⁸⁴. This study provided mechanistic insight on how USP19 may be regulating muscle mass and further investigation could provide a therapeutic target to alleviate GC-induced muscle atrophy.

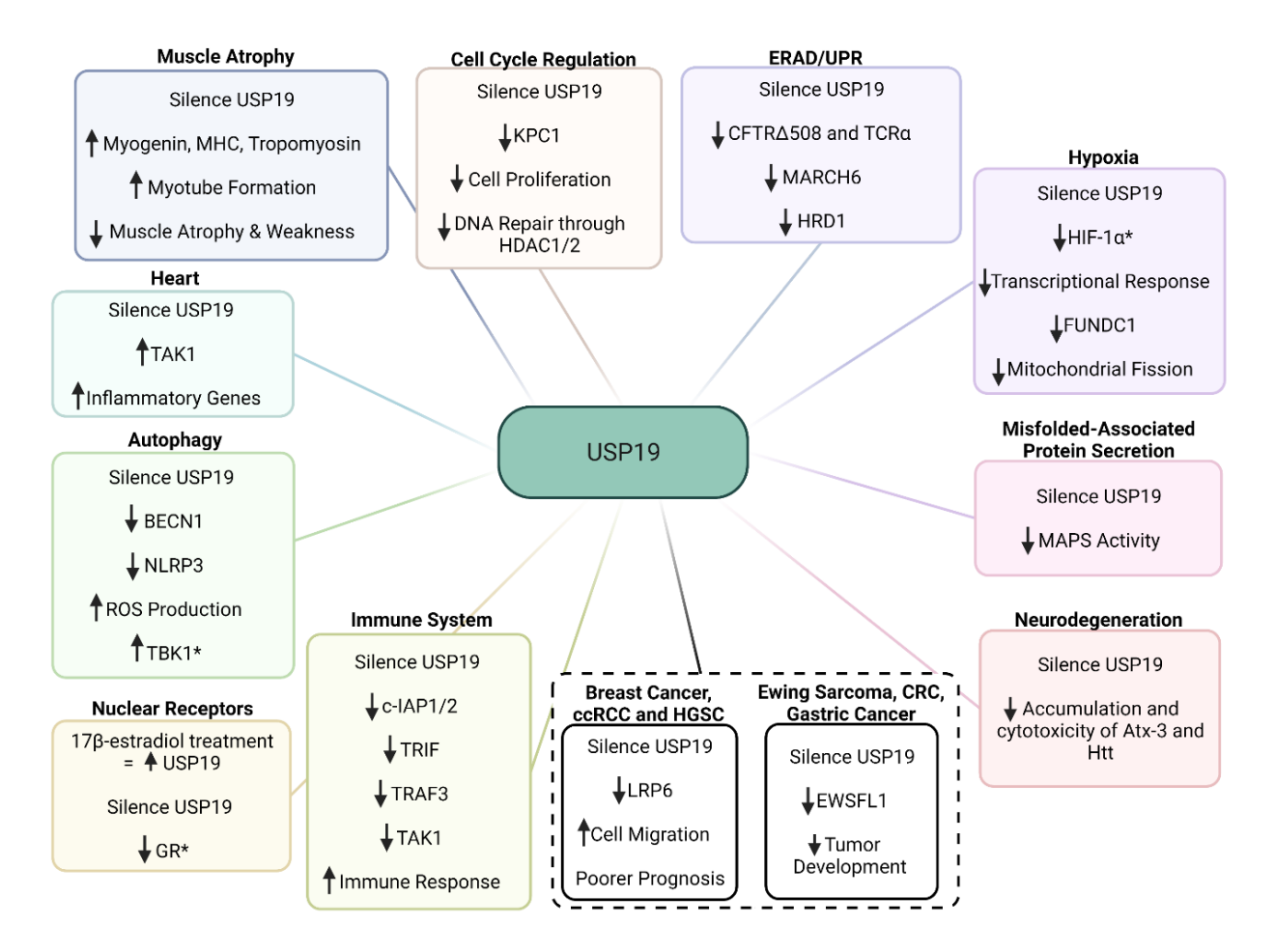


Figure 1.6: The function of USP19. Currently, USP19 has been shown to have a role in several diseases and conditions including muscle atrophy, cell cycle regulation, hypoxia, cancer, etc. The effect of inactivation of USP19 within each of these conditions are noted and an asterisk (*) designates the catalytic activity of USP19 is not needed. Created on BioRender.com.

4. Glucocorticoid Receptor

GR modulates the expression of genes involved in metabolism, stress response, cell proliferation and development^{178,186}. NRs are divided into seven subfamilies based on sequence alignment and phylogenetics¹⁸⁷. GR was one of the first NRs cloned in the late 1990s and has been extensively studied over the past two decades¹⁸⁸.

4.1. Cellular Signaling Pathway

The endogenous ligand for GR is glucocorticoids (GCs). In humans, the main glucocorticoid is cortisol and in rodents, corticosterone. Glucocorticoids secretion is regulated by the hypothalamic-pituitary-adrenal (HPA) axis¹⁸⁹. Briefly, the hypothalamus releases corticotropin-releasing hormone (CRH). In the pituitary gland, CRF binds to CRF type 1 receptor (CRFR1) which stimulates the release of adrenocorticotropic hormone (ACTH). In the adrenal gland, ACTH binds to melanocortin type 2 receptor (MC2-R), releasing GCs, that then inhibit the release of ACTH and CRF as part of a negative feedback loop^{14,189}. Stress stimulates the release of CRH and ultimately GCs. GCs bind to inactive GR in the cytoplasm, promoting nuclear translocation and binding to glucocorticoid response elements (GRE) on target genes, leading to their transactivation or repression^{14,189}. Some well-studied genes modulated by ligand-bound GR are phosphoenolpyruvate carboxykinase (PEPCK), glucose-6-phosphatase (G6Pc), pyruvate dehydrogenase kinase (Pdk4) and phosphoinositide-3-kinase regulatory subunit 1 (Pik3r1)^{14,190}. Under stress conditions, GCs increase blood glucose levels by inducing gluconeogenesis in the liver. GR also has effects in other key metabolic organs such as skeletal muscle and adipose tissue.

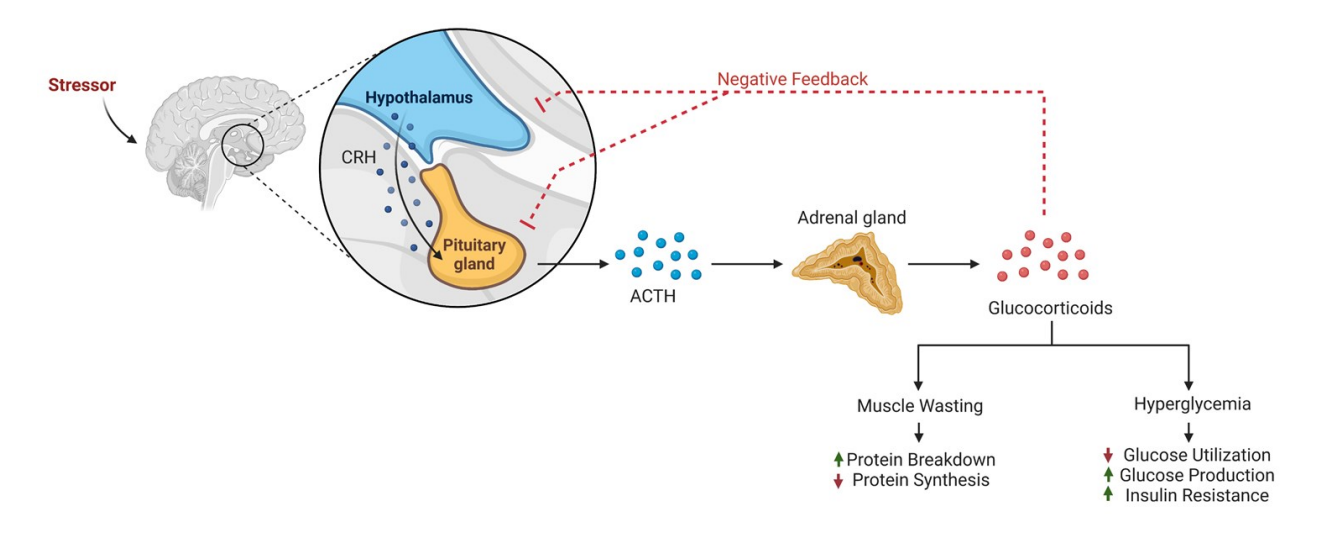


Figure 1.7: HPA Axis. Stress stimulates the hypothalamus to release CRH (corticotropin-releasing hormone), which binds to a receptor on the pituitary gland and stimulates the release of ACTH (adrenocorticotropic hormone). ACTH binds to the adrenal gland and releases glucocorticoids (GCs), that negatively regulate ACTH and CRH release. Excessive or prolonged usage of GCs results in muscle wasting and hyperglycemia. Created and modified an existing template on BioRender.com.

4.2. Key Processes Regulated by Glucocorticoids in Skeletal Muscle

Since skeletal muscle is a major reservoir of amino acids, GCs induce muscle catabolism to generate amino acids that can be used in gluconeogenesis¹⁹¹. One of the ways GCs decrease muscle anabolism is by inhibiting the insulin/insulin-like growth factor 1 (IGF-1)-phosphatidylinositol-3-kinase (PI3K)-Akt signaling pathway^{186,192}. In the muscle, IGF-1 promotes myogenesis and decreases muscle proteolysis resulting in muscle anabolism or muscle growth^{193,194}. Insulin or IGF-1 binds to membrane-bound insulin receptors (IR) or IGF-1 receptors that associate with insulin receptor substrates (IRS). GCs have been shown to inhibit the production of IGF-1 in the muscle and disrupt the association of IR with IRS^{195,196}. GCs also increase the transcription of REDD1 and KLF15 to inhibit mTOR, that is downstream of Akt¹⁹⁷. In addition to disrupting IGF-1/P13K/Akt signaling, GCs decrease the transport of amino acids into the muscle and promote the production of myostatin (Mstn) to inhibit myogenesis, resulting in decreased muscle protein synthesis¹⁹⁸. Conversely, GCs induce muscle catabolism through increasing FoxO transcription factors, which induce expression of ubiquitin ligases, MAFbx/Atrogin-1/Fbox32 and MuRF1/Trim63 that increases protein ubiquitination and subsequent proteolysis^{11,199}.

4.3. Structure, Function, and Regulation of GR

GR is 94 kDa and consists of three main domains, a disordered N-terminal domain (NTD), a structured DNA binding domain (DBD), a flexible hinge region and a structured C-terminal ligand binding domain (LBD)^{14,200}. The NTD contains a ligand-independent activation function 1 (AF-1) region that is crucial for transcriptional activity and deletion of AF-1 abolishes GR activity completely. The DBD consists of two zinc fingers (ZnF), where the four cysteine residues coordinate one zinc ion^{201,202}. GR can be found as a monomer or as a homodimer. The DBD is responsible for the dimerization in addition to binding to the GREs of target genes and nuclear

translocation. The LBD also participates in homodimerization, but its main function is to recognize and bind GCs using a combination of hydrophobic interactions and hydrogen bonding^{200,203}. The LBD also contains an activation function 2 (AF-2) helix that undergoes conformation change upon ligand binding to reveal a hydrophobic groove where co-regulators are able to bind²⁰⁴. One of the first structures of the LBD revealed the interface of the LBD and a co-activator fragment, Tif2²⁰⁴. Co-activators have a highly conserved sequence of LXXLL (where X designates any amino acids), required for binding to NR and this is called the nuclear receptor box (NR box) motif^{205,206}. There are several co-activators that enhance transcription and the best studied are the steroid receptor co-activator (SRC) family^{206–208}.

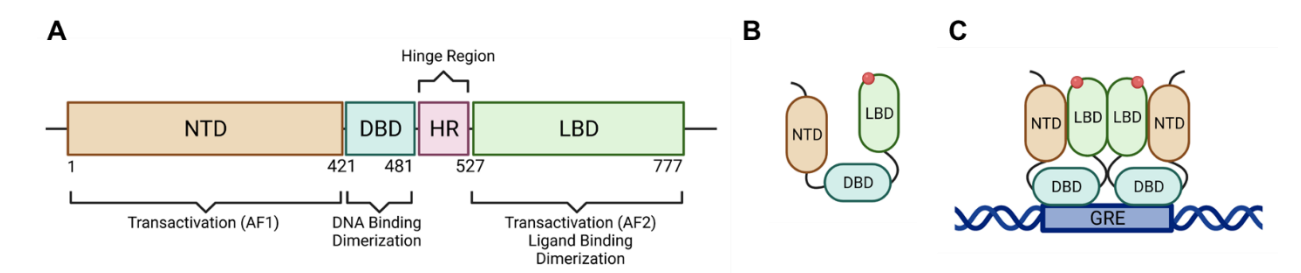


Figure 1.8: Structure and functional domains of GR. (A) The NTD (N-terminal domain) of GR contains a transactivation (AF1) helix that is involved in protein-protein interactions. The DBD (DNA-binding domain) is responsible for binding to glucocorticoid response elements (GREs) on the DNA and dimerization. The HR (hinge region) allows for flexibility and interaction of AF1 with the LBD. The LBD (ligand binding region) contains another transactivation helix (AF2) that interacts with co-regulators and is primarily responsible for ligand binding as well as dimerization. (B) Cartoon depiction of the structure of ligand-bound GR monomer. (C) Ligand-bound GR dimerization binds to GREs on the DNA resulting in transcriptional activation or repression. Created on BioRender.com.

In absence of a ligand, a multi-protein complex is found in association with GR in the cytoplasm to help GR mature and prevent its degradation²⁰⁹. The multi-protein complex consists of heat shock protein 90 (hsp90), hsp70, p23 and immunophilins such as FKBP51, FKBP52, Cyp44 and PP5^{209–211}. Recently, high-resolution structures of GR in association with the multi-protein complex has shed light into how hsp90, hsp70 and p23 specifically interact with GR. Briefly, GR is first in a loading complex with hsp90, hsp70 and hop, where hsp70 inhibits GR through interacting with GR pre-helix 1. ATP binding and hydrolysis by hsp90 releases hsp70 and

hop as well as recruits p23, a co-chaperone of hsp90, to now form the maturation complex. p23 binds to the N-terminal region of hsp90 through its CS domain and a motif distal to that domain in the C-terminal tail directly interacts with GR to enhance ligand binding^{212,213}. The binding of GC to GR leads to the dissociation of the multi-protein complex and ligand-bound GR undergoes nuclear translocation through the binding of importins to move through the nuclear pore complex (NPCs)²⁰⁹. In the nucleus, GR is normally a homodimer. The binding of co-regulatory proteins modulate GR transcriptional activity as well as generate post-translational modifications such as ubiquitination, SUMOylation, phosphorylation and acetylation²¹⁴.

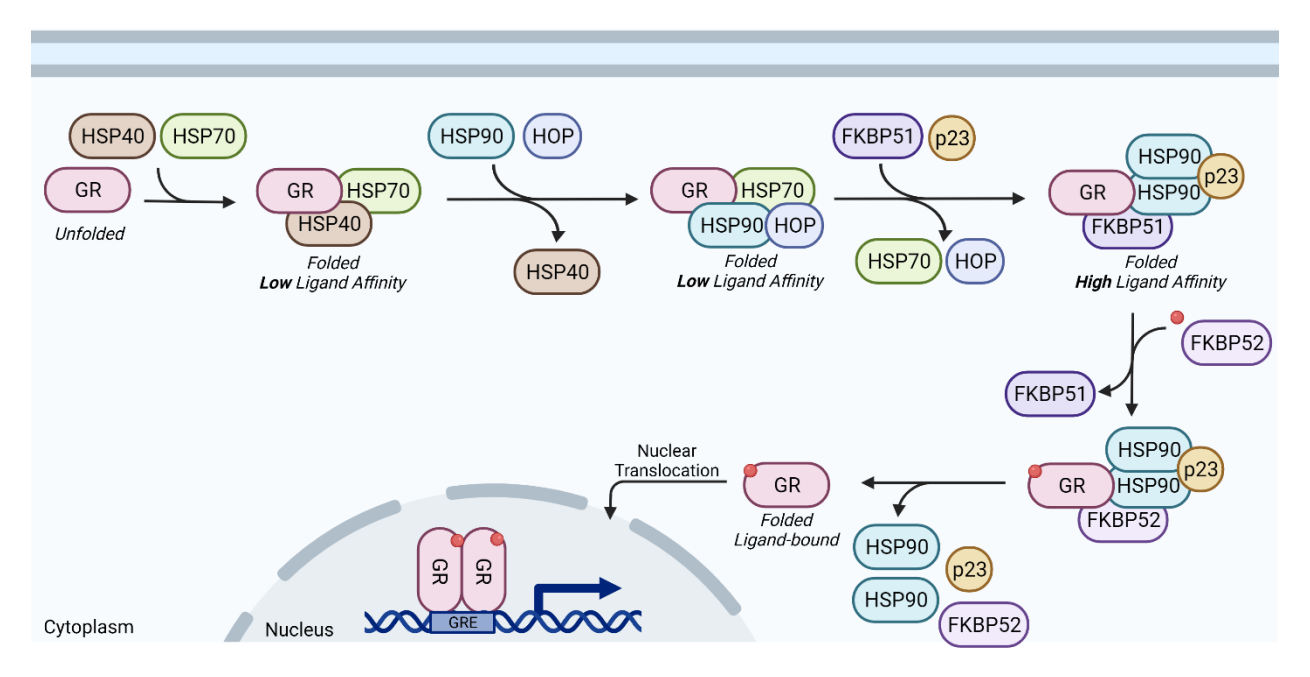


Figure 1.9: GR translocation from cytoplasm to nucleus. HSP40 and HSP70 binds to newly synthesized GR to assist with protein folding. Then HSP90 and HOP, a co-chaperone of HSP70, bind to GR to continue to mature GR and HSP40 dissociates. The binding of FKBP51, an immunophilin, and p23, a co-chaperone of HSP90, dissociates HSP70 and HOP, and results in a properly folded GR with high ligand affinity. The binding of GC to GR exchanges FKBP51 for FKBP52, another immunophilin. The components of the multi-protein complex dissociate, and ligand-bound GR undergoes nuclear translocation and homo-dimerizes to bind to the glucocorticoid response elements (GREs) on the DNA and leads to transcriptional activation or repression. Adapted from Figure 1 in Sinclair et al.²¹⁵, Figure 4 in Timmermans et al.²¹⁶ and Figure 3d in Noddings et al.²¹². Created with BioRender.com.

4.4. GC-Induced Muscle Wasting

Endogenous GCs are normally released under stress, but catabolic conditions such cachexia and starvation increase GC release through disabling the negative feedback loops^{217,218}. Synthetic GCs such as dexamethasone (Dex) have anti-inflammatory effects and are commonly used for arthritis, asthma and other allergic disorders²¹⁹. However, excessive, or prolonged usage of GCs can induce muscle atrophy, weight gain and osteoporosis. Mechanistically, in skeletal muscle, GCs increase muscle catabolism, decreases myogenesis through upregulating myostatin and decreases glucose uptake through inhibition of GLUT4^{14,220,221}. In addition, GCs upregulate MAFbx/Atrogin-1 and MuRF1, leading to increased muscle protein degradation¹¹. There is vast interest to reduce GC-induced muscle wasting, so patients taking GCs can benefit from the anti-inflammatory effects without suffering from the numerous adverse side effects.

5. Objective of this Thesis

5.1. Hypothesis

Our laboratory previously observed that USP19 knockout mice are protected against GC-induced muscle wasting¹¹⁷. USP19 knockout mice showed increase muscle strength and functionality as well as increased levels of muscle protein synthesis¹⁸⁴. USP19 knockout mice have enhanced insulin signaling, sensitivity and ability to maintain blood glucose levels. Gene analysis on muscle from USP19 knockout mice treated with dexamethasone, revealed downregulation of several GR target genes suggesting that USP19 modulates glucocorticoid signaling¹⁸⁴. The decreased glucocorticoid signaling appeared to be due to decreased GR protein levels in the muscle¹⁸⁴. Interestingly, GR mRNA levels were unchanged, suggesting that USP19 modulates GR in a post-translational manner¹⁸⁴. Additionally, silencing USP19 decreased GR protein levels and overexpressing it increased GR levels. The latter was observed with the overexpression of either wild-type USP19 or a catalytically inactive mutant, suggesting USP19 may modulate GR in a non-catalytic manner.

Ligand-free GR is associated in a multi-protein complex to assist with the maturation cycle and two key components are heat shock protein 90 (HSP90) and p23, a co-chaperone of HSP90. Previous studies have shown that USP19 interacts with HSP90 although the specific site of interaction remains controversial. One study suggests it is the catalytic domain of USP19 that interacts with HSP90, and another study suggests it is the CS domains ^{101,103}. The CS domains in

USP19 are homologous to those found in p23 and Sgt1, where the CS domain is responsible for their interaction with HSP90. Therefore, we hypothesize that USP19 binds to GR indirectly through HSP90 using the CS domain(s).

5.2. The Aims of this Thesis

Aim 1: To test whether the CS domains of USP19 binds to HSP90 similarly to that of the CS domain of p23, a co-chaperone of HSP90

Aim 2: To test whether one or both USP19 CS domains interact with HSP90 and are required for the stabilization and nuclear translocation of GR

Aim 3: To determine whether a nuclear receptor box (NR box) motif in USP19 is required for USP19's ability to stabilize GR and promote its nuclear translocation

Chapter 2: Methodology

2.1. Bioluminescence Resonance Energy Transfer (BRET) Assay

To investigate the interaction of USP19 with HSP90 and/or GR, one of the key methods used in this thesis is a bioluminescence resonance energy transfer (BRET) assay. In the BRET assay, non-radiative energy is transferred from a donor to an acceptor fluorophore²²². The fluorophores need to be within 10 nm of each other and the closer the donor and acceptor, the greater the energy transferred, making BRET a highly sensitive technique to detect and measure protein-protein interactions^{222–224}. The first generation of BRET assays (BRET1) utilizes renilla luciferase and yellow fluorescent protein (YFP)²²⁵. The second generation of BRET assays (BRET2) optimizes the signal-to-background ratio by using blue-shifted acceptor fluorophores, such as GFP₂ or GFP₁₀ and a blue-shifted luciferase substrate, coelentrazine-400a or deep blue C (DBC)^{222,226}. Additionally, there is a naturally occurring pair of *Renilla renformis* luciferase (rLuc) and Renilla renformis GFP (rGFP), that has improved signal and sensitivity. This combination has been used in bystander BRET assays, which looks at the inherent interaction between rLuc and rGFP²²³. Interestingly, rGFP appears to be the only GFP known to naturally exist as a globular dimer²²⁷. In our BRET assay, renilla luciferase is fused to the N-terminal of cytoplasmic USP19 (rLuc-USP19) and humanized renilla green fluorescent protein (hrGFP) is fused to the N-terminal of HSP90 or GR (hrGFP-HSP90/hrGFP-GR) (Figure 2.1). If these proteins are closely associated, luminescence from rLuc-USP19 excites hrGFP-HSP/GR, leading to fluorescence. The resulting BRET ratio is obtained by dividing the fluorescence by the luminescence.

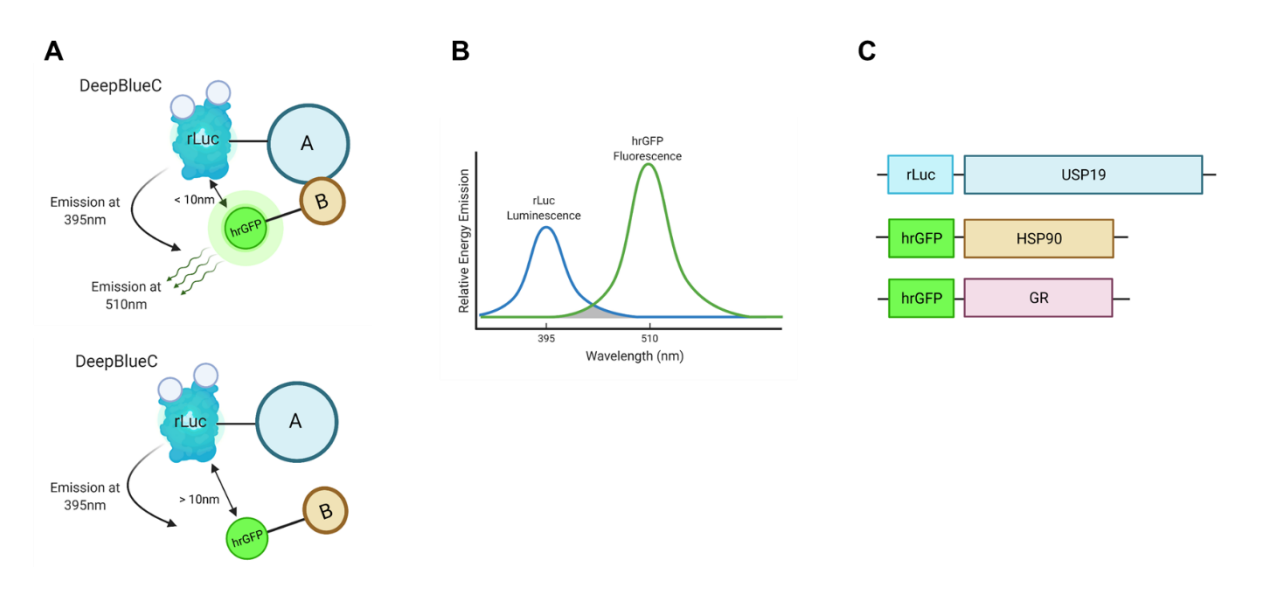


Figure 2.1: BRET Assay. (A) Illustration of the BRET assay showing that if protein A and B interact and are within 10 nm of each other, energy is efficiently transferred from rLuc (*renilla* luciferase) to hrGFP (humanized *renilla* green fluorescent protein), leading to its fluorescence at 510 nm. If the proteins do not interact, then energy is not efficiently transferred and very little or no fluorescence is observed. (B) The luminescence from rLuc is within the excitation spectrum of hrGFP, providing energy for hrGFP to fluoresce (C) Constructs used in our BRET assay with rLuc fused to the N-terminus of USP19 and hrGFP fused to HSP90 or GR. Created in BioRender.com.

2.1.1. Plasmids and Site-Directed Mutagenesis

To express the N-terminally tagged *Renilla renformis* luciferase (rLucII) fused to cytoplasmic *Rattus norvegicus* USP19 (rUSP19Cyt), we amplified by PCR the coding sequence of rUSP19Cyt with 5' and 3' primers containing XbaI and PmeI restriction sites respectively and digested with these restriction endonucleases. Dr. Stephane Laporte kindly provided a HA-rLucII-LC3b plasmid, which was double-digested with XbaI and PmeI to release the LC3b insert and then ligated with the above mentioned rUSP19Cyt and HSP90 PCR products. The ligated product was transformed into DH5α competent cells, screened using colony PCR and verified by sequencing (Genome Quebec).

To express the N-terminally tagged humanized *Renilla renformis* green fluorescent protein (hrGFP) fused to HSP90 or GR, we amplified HSP90 and GR with 5' and 3' primers containing XbaI and PmeI respectively. Dr. Stephane Laporte kindly provided the hrGFP-LC3b plasmid which was double-digested with XbaI and PmeI to release the LC3b insert and ligated with HSP90 and GR. The ligated product was transformed into DH5α competent cells, screened using colony PCR and verified by sequencing (Genome Quebec).

To generate p23 (PTGESD3) F103A and W106A single and double mutants, site-directed mutagenesis (Agilent QuikChange II Site-Directed Mutagenesis) was performed as directed by the manufacturer on Myc-DDK-tagged PTGES3 plasmid using the HPLC-purified mutagenic oligonucleotides listed in table 2. To generate CS2 Y330A and Y342A single and double mutants, site-directed mutagenesis on pcDNA3.1-6xHis-3xFlag-rUSP19CS2 was performed in the same manner as p23 mutagenesis.

Table 1: List of plasmids transfected in the BRET assay

Plasmid	Description	Amino Acid Residues
rLuc-USP19Cyt	N-terminally tagged rLuc fused to USP19Cyt	1-1281
hrGFP-HSP90β	N-terminally tagged hrGFP fused to HSP90β	1-724
hrGFP-GR	N-terminally tagged hrGFP fused to GR	1-777
Myc-DDK-tagged-PTGES3	Expressing human PTGES3 (p23; NM_006601) purchased from OriGene (Cat. #RC201254)	1-160
pcDNA3.1-6xHis-3xFlag- rUSP19Cyt	Expressing full-length cytoplasmic USP19 (On AddGene: Plasmid #155238)	1-1281
pcDNA3.1-6xHis-3xFlag- rUSP19CS1	Expressing USP19 CS1 domain only	51-156
pcDNA3.1-6xHis-3xFlag- rUSP19CS2	Expressing USP19 CS2 domain only	296-442

Table 2: List of oligonucleotides used for site-directed mutagenesis of p23 and CS2 with the residues mutated underlined and coloured in red.

P23 Mutagenesis	
P23 F103A	F: GGCTTAGTGTCGACGCCAATAATTGGAAAGACTGGGAAG
	R: CTTCCCAGTCTTTCCAATTATTGGCCGTCGACACTAAGCC
P23 W106A	F: GGCTTAGTGTCGACTTCAATAATGCGAAAGACTGGG
	R: CCCAGTCTTTCGCATTATTGAAGTCGACACTAAGCC
P23 F103/W106A	F: GGCTTAGTGTCGACGCCAATAATGCGAAAGACTGGG
	R: CCCAGTCTTTCGCATTATTGGCCGTCGACACTAAGCC
CS2 Mutagenesis	
Y330A	F: TTTGTCAAGAATGATTCGGCCGAGAAGGGGCCGGATTC
	R: GAATCCGGCCCCTTCTCGGCCCGAATCATTCTTGACAAA
Y342A	F: GTGGTGCACGTGGCCGTGAAGGAGAGCCG
	R: CGGCTCTCCTTCACGGCCACGTGCACCACCAC

2.1.2. Cell Culture and Transfection

HEK293 cells were grown in 1X DMEM (GIBCO), supplemented with 10% heat-inactivated fetal bovine serum (HI-FBS; GIBCO) and 1% penicillin/streptomycin (P/S; GIBCO), at 37°C with 5% CO₂. Cells were transfected using jetPrime Transfection Reagent (Polyplustransfection). HEK293 cells (200,000 in 2 mL of media) were transfected in suspension in a 6-well plate with a total of 1 μg of plasmid, 4 μL of transfection reagent and 200 μL of transfection buffer. 24-hours post-transfection, the cells were subcultured into a white 96-well plate for BRET measurement and a 12-well plate for western blot analysis (Section 2.2.3).

2.1.3. BRET Assay

Twenty-four hours post-subculturing, cells in the 96-well plate were washed twice with 90 μ L 1xHBSS (Gibco Hanks' Balanced Salt Solution no phenol red; Cat. #14175-095) per well then 90 μ L 1x HBSS was added to each well. DeepBlueC (DBC) substrate (5M coelenterazine 400a in ethanol, NanoLight Cat. #341) was diluted 100X in HBSS (50 μ M) and 10 μ L of the 50 μ M solution was added to each well for a final concentration of 5 μ M. The plate was shaken for 5 seconds at medium intensity then the luminescence was read at 410/80 nm and fluorescence read at 515/30 nm using a BioTek Synergy2 plate reader at ambient temperature (25-26°C). The BRET ratio was calculated as the ratio of the fluorescence (515/30 nm reading) over the luminescence (410/80 nm reading).

2.2. Regulation of GR Protein Levels by USP19 Overexpression

2.2.1. Plasmids and Site-Directed Mutagenesis

The plasmids listed in table 3 were co-transfected with HA-tagged GR. To mutate the nuclear receptor box (NR box) motif in USP19, site-directed mutagenesis (Agilent QuikChange II Site-Directed Mutagenesis) was performed with HPLC-purified oligonucleotides listed in table 4.

Table 3: List of plasmids co-transfected in COS-7 overexpression

Plasmid	Description	Amino Acid Residues
HA-GR-Flag	Expressing GR N-terminally tagged with HA and C-terminally tagged with Flag. Gift from Dr. Jacques Drouin at Institut de recherches cliniques de Montreal.	1-777
pcDNA3.1-6xHis-3xFlag- rUSP19Cyt	Expressing full-length cytoplasmic USP19 (On AddGene: Plasmid #155238)	1-1281
pcDNA3.1-6xHis-3xFlag- rUSP19ΔN1	N-terminal truncation of cytoplasmic USP19 lacking the CS1 domain	180-1281
pcDNA3.1-6xHis-3xFlag- rUSP19ΔN3	N-terminal truncation of cytoplasmic USP19 lacking both CS domains	545-1281
pcDNA3.1-6xHis-3xFlag- rUSP19\(\Delta\)CS2	Expressing cytoplasmic USP19 with CS2 domain deletion	1-295, 443-1281
pcDNA3.1-6xHis-3xFlag- rUSP19Cyt NR Box Mutant	Expressing full-length cytoplasmic USP19 mutated in the NR box (L898A, L901A, L902A)	1-1281 with L898A, L901A, L902A
pcDNA3.1-6xHis-3xFlag- rUSP19ΔCS2 NR Box Mutant	Expressing cytoplasmic USP19 with CS2 domain deletion and NR box mutated (L898A, L901A, L902A)	1-295, 443-1281 with L898A, L901A, L902A

Table 4: List of oligonucleotides used for site-directed mutagenesis of the nuclear receptor box (NR box) motif with the residues mutated underlined and coloured in red.

NR Box Mutagenesis Primers		
LXXAA	F: CGCCTCACTTATGCCCGTCTTGCTCAGGCAGCAGAAGGTTATGCCCGG	
	R: CCGGGCATAACCTTCTGCTGCCTGAGCAAGACGGGCATAAGTGAGGCG	
AXXAA	F: CGCCTCACTTATGCCCGTGCTGCTCAGGCAGCAGAAGGTTATGCCCGG	
	R: CCGGGCATAACCTTCTGCTGCCTGAGCAGCAGCACGGGCATAAGTGAGGCG	

2.2.2. Cell Culture and Transfection

COS7 cells were grown in 1X DMEM (GIBCO), supplemented with 10% heat-inactivated fetal bovine serum (HI-FBS; GIBCO) and 1% penicillin/streptomycin (P/S; GIBCO), at 37°C with 5% CO₂. Cells (100,000 cells in 1 mL of media) were transfected using jetPrime Transfection Reagent (Polyplus-transfection) in suspension in a 12-well plate with a total of 0.8 µg of plasmid, 1.6 µL transfection reagent and 75 µL transfection buffer. The media was changed 24-hours post-transfection and the cells harvested 48-hours post-transfection for western blotting by washing the cells twice with ice-cold 1X PBS and lysing with 150 µL RIPA buffer (50 mM Tris pH 8.0, 150 mM NaCl, 1 mM EDTA, 1% NP-40, 0.1% SDS, 1% sodium deoxycholate) supplemented with protease inhibitor (Roche).

2.2.3. Western Blot

After harvesting the cell lysates by scraping each well, the cell lysate collected was sheared using a 23G needle approximately 10 times and centrifuged at 17,000xg for 10 minutes at 4°C. The supernatant was carefully transferred to a new tube and stored at -80°C. The protein concentration was measured using a Micro BCA Protein Assay Kit (ThermoFisher Scientific). Cell lysates (12.5-15 μg protein) were loaded onto a 5-15% gradient SDS-PAGE gel. Proteins were transferred onto a 0.22 μm (for detection of p23 and CS2) or 0.45 μm (for detection of larger proteins) nitrocellulose (BioRad) membranes overnight at 125 mA (approximately 16-18 hours) and 400 mA for 1 hour the next day. The membrane was blocked with 5% non-fat milk in 1x TBS-T for one hour at room temperature. Membranes were probed with antibodies overnight at 4°C against USP19 (1:1000; Abcam Cat. #ab167059), Flag-M2 (1:1000; Sigma-Aldrich Cat. #F3165), Beta-Actin (1:10000, Sigma-Aldrich Cat. #A1978), GR (1:1000; Cell Signaling Technologies Cat. #3660), GAPDH (1:8000; ambion by Life TechnologiesTM Cat. #AM4300) and rLuc (1:1000, Millipore Sigma Cat. #MAB4410). Membranes were washed four times with 1x TBS-T for five

minutes then incubated with horse radish peroxidase (HRP)-conjugated to either anti-mouse, anti-rabbit or anti-rat IgG antibody (1:10000) for 1 hour in 2.5% BSA in 1x TBS-T at room temperature. ECL chemiluminescence substrate (BioRad) was used to detect the signal by incubating for five minutes at room temperature and quantified using a ChemiDocTM MP Imaging System (BioRad). Membranes were analyzed in ImageLab software (BioRad), normalizing against Beta-Actin (1:10000, Sigma-Aldrich Cat. #A1978) or GAPDH (1:8000; ambion by Life TechnologiesTM Cat. #AM4300) as a loading control. Membranes that needed to be re-blotted were stripped with RestoreTM PLUS Western Blot Stripping Buffer (Thermo Scientific) for 5-10 minutes then washed twice with 1X TBS-T for five minutes. The membrane was reblocked with 5% milk in 1x TBS-T for 15 to 30 minutes at room temperature and probed with primary and secondary antibodies in the same manner as before.

2.3. Nuclear Translocation Assay

2.3.1. Plasmids and Site-Directed Mutagenesis

Table 5: List of plasmids co-transfected in COS7 cells for the nuclear translocation assay

Plasmid	Description	Amino Acid Residues
pEGFP-GR	Expressing human GR N-terminally	
	tagged with eGFP. Purchased from	1-777
	AddGene (Plasmid #47504)	
pcDNA3.1-6xHis-3xFlag-	Expressing full-length cytoplasmic	1-1281
rUSP19Cyt	USP19 (On AddGene: Plasmid #155238)	
pcDNA3.1-6xHis-3xFlag-	N-terminal truncation of cytoplasmic	180-1281
rUSP19ΔN1	USP19 lacking the CS1 domain	
pcDNA3.1-6xHis-3xFlag-	N-terminal truncation of cytoplasmic	545-1281
rUSP19∆N3	USP19 lacking both CS domains	
pcDNA3.1-6xHis-3xFlag-	Expressing cytoplasmic USP19 with CS2	1-295, 443-1281
rUSP19ΔCS2	domain deletion	
pcDNA3.1-6xHis-3xFlag- rUSP19Cyt NR Box Mutant	Expressing full-length cytoplasmic	1-1281 with
	USP19 with mutated the NR box	L898A, L901A,
	(L898A, L901A, L902A)	L902A
pcDNA3.1-6xHis-3xFlag-	Expressing cytoplasmic USP19 with CS2	1-295, 443-1281
rUSP19∆CS2 NR Box	domain deletion and mutated NR box	with L898A,
Mutant	(L898A, L901A, L902A)	L901A, L902A

2.3.2. Cell Culture and Transfection

COS7 cells (50-60,000 cells in 0.5 mL media) were grown and transfected as described above (Section 2.2.2) in suspension in a 24-well plate containing 12 mm uncoated glass coverslips with a total of 0.5 μg of plasmid, 1 μL jetPrime transfection reagent and 50 μL jetPrime transfection buffer. The media was changed 24-hours post-transfection with 1x DMEM containing 10% charcoal-stripped FBS and 1% Penicillin/Streptomycin. The next day (48-hours post-transfection), the cells were treated with 100 nM dexamethasone (Dex) for four hours in 1x DMEM containing 10% charcoal-stripped FBS and 1% Penicillin/Streptomycin. Cells were fixed overnight at 4°C with 3.7% paraformaldehyde (PFA), by adding the PFA directly to the media-containing wells. The following day, the cells were washed twice for five minutes with 1x PBS then incubated with DAPI (1:5000) for 15 minutes at room temperature. Cells were washed twice for five minutes with 1x PBS then coverslips mounted with 5 μL ProlongTM Diamond Antifade mounting agent (InvitrogenTM).

2.3.3. Image Acquisition and Analysis

Whole coverslip images were acquired using the Zeiss AxioScan.Z1 slide imager with 10x objective in two channels: 405 (DAPI) and 488 (GFP). Single plain whole coverslips containing on average 30,000 cells were analyzed in QuPath software 0.3.0 using the built-in plugin 'Cell Detection' and custom-tailored parameters to detect the nuclei. The area of the cytoplasm was defined as the area 10-micron away from the edge of the nucleus. The integrated density was calculated as the raw pixel intensities divided by the area in microns. Non-transfected cells were excluded from the analysis by defining the cell GFP mean pixel intensity cut-off as 150, which was determined by examining a subset of non-transfected cells.

```
Script for batch processing:

setImageType('FLUORESCENCE');

createSelectAllObject(true);

selectAnnotations();

runPlugin('qupath.imagej.detect.cells.WatershedCellDetection', '{"detectionImage": "DAPI",

"requestedPixelSizeMicrons": 0.5, "backgroundRadiusMicrons": 8.0, "medianRadiusMicrons": 0.0,

"sigmaMicrons": 3.0, "minAreaMicrons": 20.0, "maxAreaMicrons": 400.0, "threshold": 100.0,

"watershedPostProcess": true, "cellExpansionMicrons": 10.0, "includeNuclei": true, "smoothBoundaries": true,

"makeMeasurements": true}');

getCellObjects().each{

nucleusAreaInPixels = it.getNucleusROI().getArea()
```

```
it.getMeasurementList().putMeasurement("Nucleus Pixel Area", nucleusAreaInPixels)
}
getCellObjects().each{
cellAreaInPixels = it.getROI().getArea()
it.getMeasurementList().putMeasurement("Cell Pixel Area", cellAreaInPixels)
}
getCellObjects().each{
cytoplasmAreaInPixels = it.getROI().getArea() - it.getNucleusROI().getArea()
it.getMeasurementList().putMeasurement("Cytoplasm Pixel Area", cytoplasmAreaInPixels)
}
```

2.3.4. Western Blotting

To verify the expression of the USP19 constructs overexpressed, cells were transfected without coverslips and harvested 48-hours post-transfection by washing the cells twice with ice-cold 1X PBS and lysing with 75 µL RIPA buffer (50 mM Tris pH 8.0, 150 mM NaCl, 1 mM EDTA, 1% NP-40, 0.1% SDS, 1% sodium deoxycholate) supplemented with protease inhibitor. Samples were analyzed by western blotting as described above (Section 2.2.3).

2.4. Statistical Analysis

Statistical analysis was carried out in GraphPad Prism 9 (GraphPad Software) or Excel 2020 (Microsoft Office). Ordinary one-way ANOVA were used to analyze data involving one independent variable (HA-tagged GR overexpression or GFP-GR nuclear translocation). Two-way ANOVA was used to analyze data with two or more independent variables, selecting for Tukey's or Dunnett's post-hoc multiple comparisons between columns and rows (BRET assay).

Chapter 3: Results

3.1. USP19 interacts indirectly with GR via HSP90

3.1.1. USP19 interacts with HSP90 and GR

Since HSP90 is involved in the maturation process of GR and USP19 and HSP90 have been shown to interact, we hypothesized USP19, HSP90 and GR may form a complex together. Previous immunoprecipitation studies in our laboratory showed that expressing Flag-USP19 coprecipitated with HSP90 and expressed HA-GR (Coyne et al., *manuscript in preparation*). Proximity ligation assays can generally detect two interacting proteins if they are within 40nm of each other²²⁸. Proximity ligation studies revealed that USP19 and HSP90, GR and HSP90, and USP19 and GR all interact (Coyne et al., *manuscript in preparation*). However, the signals were much decreased in the USP19 and GR study, consistent with an indirect interaction via HSP90.

To further examine the protein-protein interaction of USP19 with HSP90 and with GR, we established a bioluminescence resonance energy transfer (BRET) assay in collaboration with Dr. Yoon Namkung in the laboratory of Dr. Stephane Laporte. The BRET assay involves fusing *renilla* luciferase (rLuc) to one protein and *renilla* green fluorescent protein (hrGFP) to the other protein^{223,227}. If the two proteins interact such that the acceptor hrGFP is within 10nm of rLuc, then the luminescent energy from rLuc can be transferred to hrGFP and generate a fluorescent signal. To normalize for slightly different efficiencies of transfection of plasmids, the fluorescence can be divided by the luminescence, generating a BRET ratio. We tested whether rLuc-USP19 interacts with hrGFP-HSP90β and hrGFP-GR by co-transfecting increasing amounts of hrGFP-HSP90β, hrGFP-GR and hrGFP-control with a fixed amount of rLuc-USP19Cyt into HEK293 cells (Figure 3.1A-B).

We observed an increase and saturation in the BRET ratio with increasing amounts of hrGFP-HSP90β (later referred to as hrGFP-HSP90), suggesting USP19 and HSP90 interact through a specific binding site (Figure 3.1B). We also see an increase without saturation in the BRET ratio with increasing amounts of hrGFP-control, which only contains the hrGFP fluorophore and is not fused to any proteins. This increase in the BRET ratio shows the background non-specific, stochastic interaction of the rLuc-USP19Cyt donor and hrGFP acceptor fluorophores. Since the BRET ratio of hrGFP-HSP90 is significantly greater than the hrGFP-control between 0

to 400ng of plasmid (Figure 3.1B), this suggests that there is a specific interaction between USP19 and HSP90.

Interestingly, we also see an increase and possible saturation in the BRET ratio with increasing amounts of hrGFP-GR co-transfected with a fixed amount of rLuc-USP19Cyt (Figure 3.1B). However, the BRET ratio with hrGFP-GR is less than the BRET ratio observed with increasing amounts of hrGFP-control, raising the possibility that the BRET signal with hrGFP-GR may arise simply from the background observed with hrGFP. Altogether, these results confirm that USP19 interacts with HSP90 and that its interaction with GR is likely indirect, consistent with our laboratory's previous findings with the proximity ligation assay.

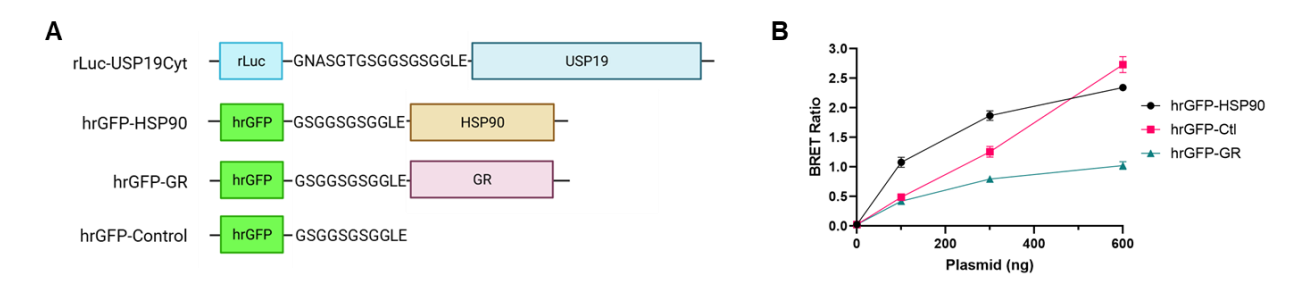


Figure 3.1: USP19 interacts directly with HSP90 and indirectly with GR. (A) Schematic of rLuc-USP19Cyt, hrGFP-HSP90, hrGFP-GR and hrGFP-control constructs. (B) Plotting the BRET ratio (fluorescence/luminescence) of rLuc-USP19Cyt with hrGFP-HSP90, hrGFP-GR or hrGFP-control shows their respective interactions. Shown are the means \pm SE (n = 4).

3.1.2. USP19 binds to the same region on HSP90 as p23

USP19 contains two N-terminal CS domains homologous to the CS domain in p23, a cochaperone of HSP90 known to promote GR maturation. This suggests that USP19 could be acting like p23. To evaluate this possibility, we tested if co-expression of p23 would compete the interaction of rLuc-USP19Cyt with hrGFP-HSP90. We co-transfected increasing amounts of p23-Flag (later referred to as p23) alongside fixed amounts of rLuc-USP19Cyt with hrGFP-HSP90 into HEK293 cells. We see a strong decrease in the BRET ratio of rLuc-USP19Cyt with hrGFP-HSP90 with increasing amounts of expressed p23 (Figure 3.2B). This ability of p23 to disrupt the interaction of USP19 with HSP90 suggests that USP19 and p23 bind to the same site on HSP90.

To test this further, we mutated two key residues in p23, F103 and W106, located at the interface of p23 and HSP90. Mutation of F103 or W106 to alanine has been shown to prevent or diminish p23 interaction with HSP90 respectively^{213,229} (Figure 3.2A). Indeed, the p23 F103A mutant, which completely loses the ability to bind to HSP90, did not compete the interaction of rLuc-USP19Cyt with hrGFP-HSP90 (Figure 3.2B-C). Interestingly, the p23 W106A mutant, which partially retains the ability to bind to HSP90, partially competes the interaction of rLuc-USP19Cyt with hrGFP-HSP90(Figure 3.2B-C). A p23 double mutant containing both F103A and W106A behaves in the same manner as the p23 F103A single mutant. To verify that the impaired competition of the p23 mutants was not due to poorer expression, the cell lysates were analyzed by western blotting and this revealed that the p23 mutants and wild-type proteins were well-expressed and showed similar expression (Figure 3.2D-E).

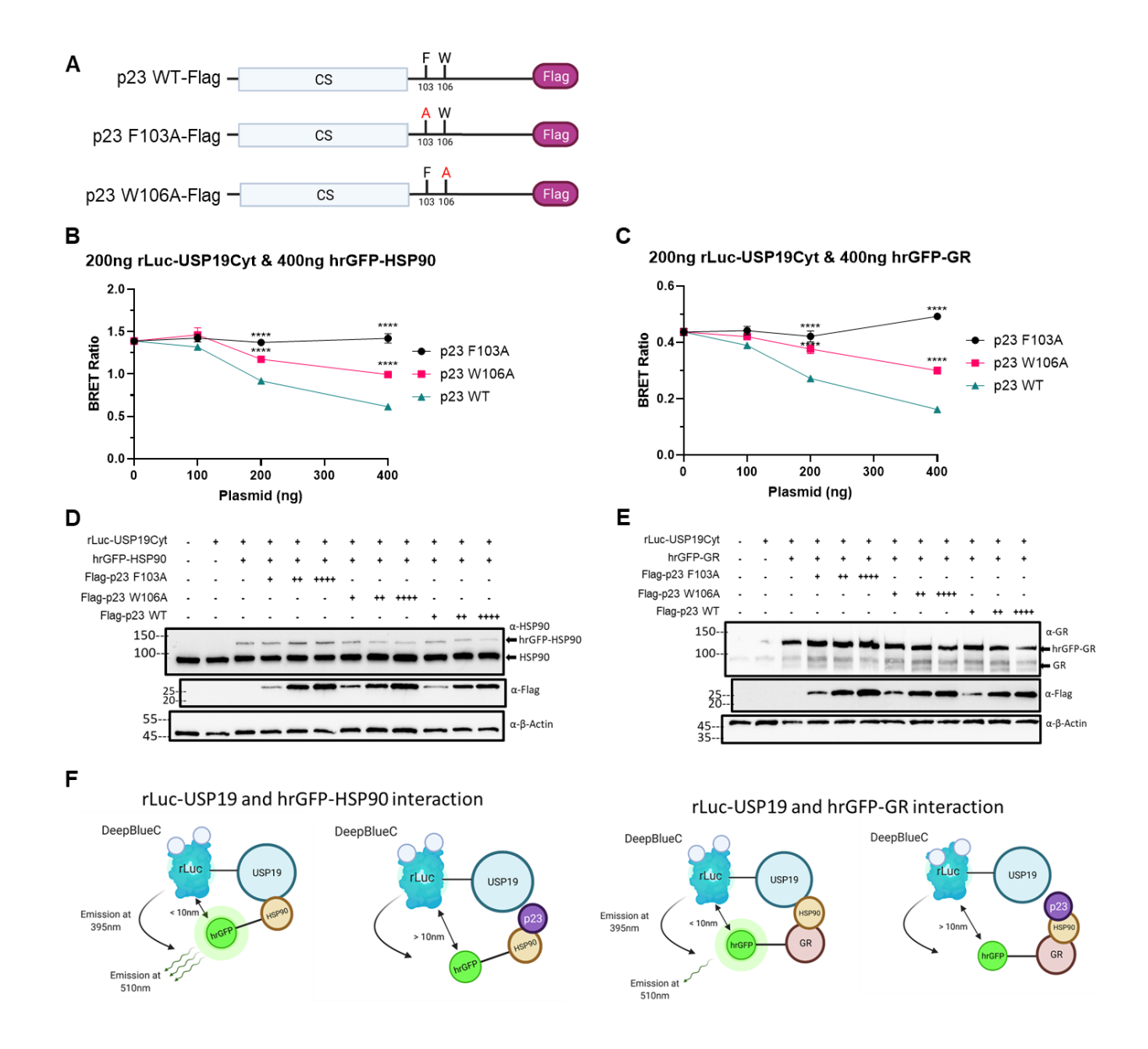


Figure 3.2: p23 competes the interaction of rLuc-USP19Cyt with hrGFP-HSP90. (A) Schematic of human p23 showing the key F103 and W106 residues. (B-C) The BRET ratio is obtained by dividing the fluorescence signal of hrGFP-HSP90 (B) or hrGFP-GR (C) by the luminescence upon coelenterazine 400a addition. (D-E) Western blot of 12.5 μ g of total cell lysate confirms the similar expression of p23 mutants and wild-type. (F) Schematic of disruption by p23 of USP19-HSP90 or USP19-GR interactions in the BRET assays. Shown are means \pm SE (n = 4). **** p < 0.0001 (Two-way ANOVA Tukey's multiple comparisons)

3.2. USP19 CS2 domain is required but insufficient for GR stabilization

3.2.1. CS2 binds to HSP90

Since USP19 binds to the same site on HSP90 as p23 and USP19 has two CS domains, we asked which of the CS domains specifically interacts with HSP90. We optimized the amount of rLuc-USP19Cyt and hrGFP-HSP90/GR plasmid used in the BRET assay, keeping the same acceptor-to-donor ratio of 1:2. We co-transfected plasmids expressing the individual CS domains, CS1 or CS2, and the full-length cytoplasmic USP19 (referred to as USP19) alongside the optimized amounts of BRET assay constructs into HEK293 cells (Figure 3.3A). We observe that USP19 and the CS2 domain strongly competes the interaction of USP19 with HSP90 (Figure 3.3B) and the proteins are similarity expressed (Figure 3.3D). We do not see competition with the CS1 domain, suggesting that specifically the CS2 domain of USP19 binds to HSP90. Additionally, we also observe that USP19 and the CS2 domain strongly competes the interaction of rLuc-USP19Cyt with hrGFP-GR, suggesting USP19 indirectly interacts with GR through binding of its CS2 domain to HSP90 (Figure 3.3 C, E). Overall, this suggests that the USP19 CS2 domain specifically binds to HSP90, which then interacts with GR (Figure 3.3F).

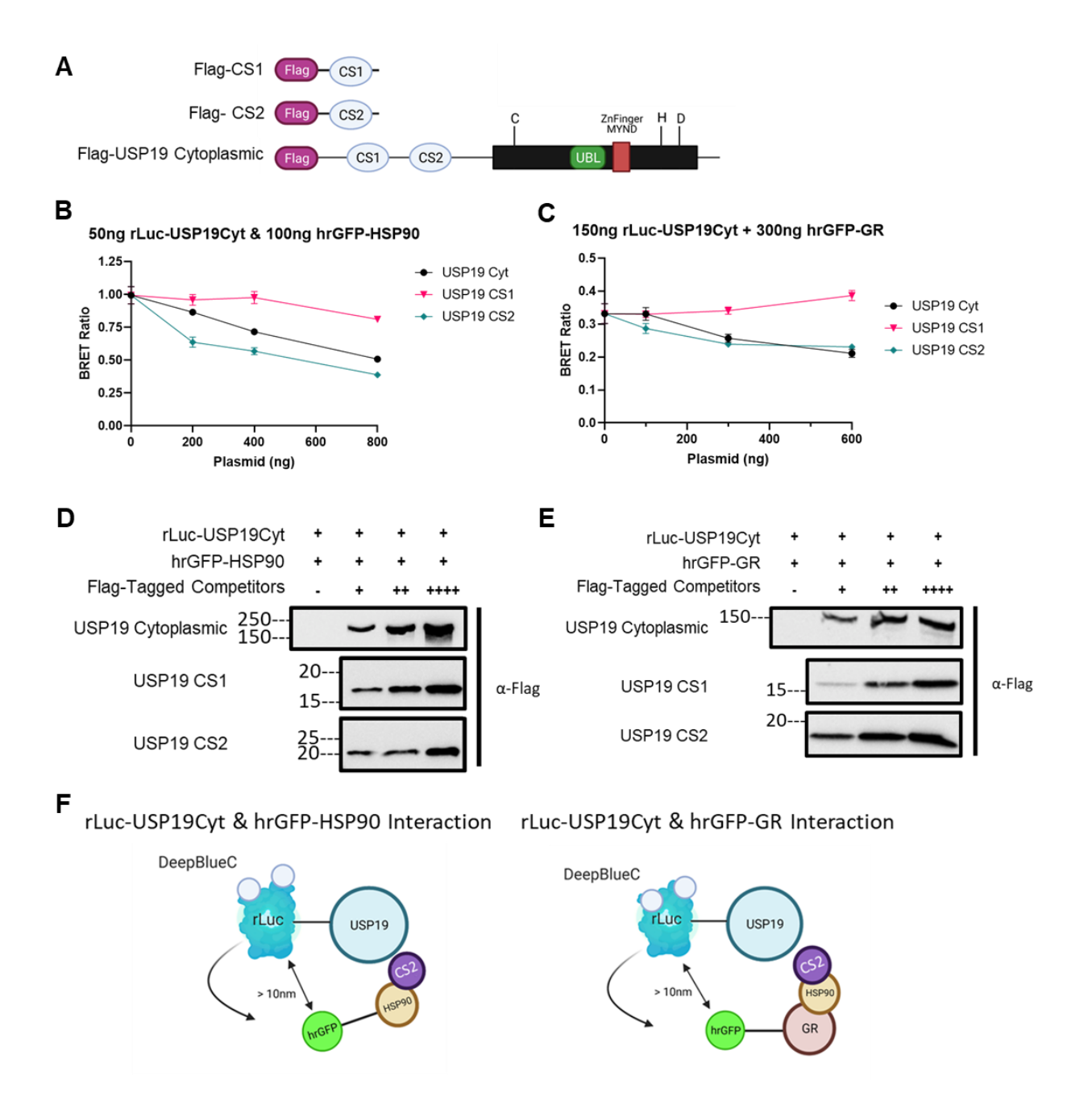


Figure 3.3: USP19 CS2 domain competes interaction of USP19 with HSP90. (A) Schematic of the constructs co-transfected with rLuc-USP19Cyt, hrGFP-HSP90 and hrGFP-GR into HEK293 cells. (B-C) We determined the BRET ratio by dividing the fluorescence by the luminescence upon substrate addition. Shown is the mean \pm SE (n = 4). (D-E) Western blot on the BRET assay cell lysates detecting the Flag-tagged CS1, CS2 and USP19 competitors in the USP19-HSP90 BRET assay (D) and USP19-GR BRET assay (E). (F) Illustration of the binding of CS2 in each BRET assay, showing the disruption between USP19 with HSP90 (Left) and with GR (Right).

3.2.2. CS2 mutants and deletion fail to abolish HSP90 binding

As previously noted, the CS domain of p23 and USP19 are homologous to one another. Our collaborator, Dr. Jason Young overlaid the structures of the CS domain of USP19 (PDB: 1WH0) on the structure of the complex of Sgt1, another CS domain-containing protein with HSP90 (PDB: 2JKI). The interaction of HSP90 N-terminal domain with Arabidopsis thaliana Sgt1-CS domain form a hydrophobic cleft and within this conserved cleft, Y157 and K221 are conserved in all species and F168 is well-conserved in plant and yeast²³⁰. Aligning the sequences of the CS2 domain with Sgt1-CS domain revealed three conserved residues with hydrophobic and basic properties, Y330, Y342 and R407. Mutating these residues to alanine has been reported to abolish binding to HSP90²³¹. To confirm that the CS2 domain is binding to HSP90, we performed sitedirected mutagenesis on Y330 and Y342 in the CS2 domain to test whether USP19 from binding to HSP90 is lost (Figure 3.4A). We observe decreased competition of the CS2 Y342A single mutant between USP19 with HSP90 (Figure 3.4B, D) and with GR (Figure 3.4C, E). Interestingly, we observe decreased competition of the CS2 Y330A/Y342A double mutant between USP19 with HSP90 only (Figure 3.4B, D) and not with GR (Figure 3.4C, E). However, the CS2 single and double mutants were less expressed compared to wild-type CS2 domain and so this may explain the incomplete disruption of the BRET signals (Figure 3.4D, E).

Since mutating two key residues in the CS2 domain decreased CS2 protein stability, yielding an inconclusive result, we compared the effects of expressing USP19Cyt or a form lacking the CS2 domain on the BRET ratio (Figure 3.5A). The full length USP19Cyt did compete the interaction of rLuc-USP19 and hrGFP-HSP90 as revealed by the decrease in the BRET ratio with increasing expression of the full length USP19Cyt. The mutant form lacking the CS2 domain showed a slightly impaired ability to decrease the BRET ratio, suggesting that the CS2 domain does play an important role, but not an exclusive role in binding to HSP90 (Figure 3.5B, D). A similar effect was seen when using hrGFP-GR in the assay (Figure 3.5C, E). The mutants and wild-type USP19 were similarly expressed (Figure 3.5D, E). The incomplete ability of the CS2 deleted form of USP19 to abolish the interaction between USP19 and HSP90 suggests there could be another domain in USP19 that also contribute to interacting with HSP90 and with GR.

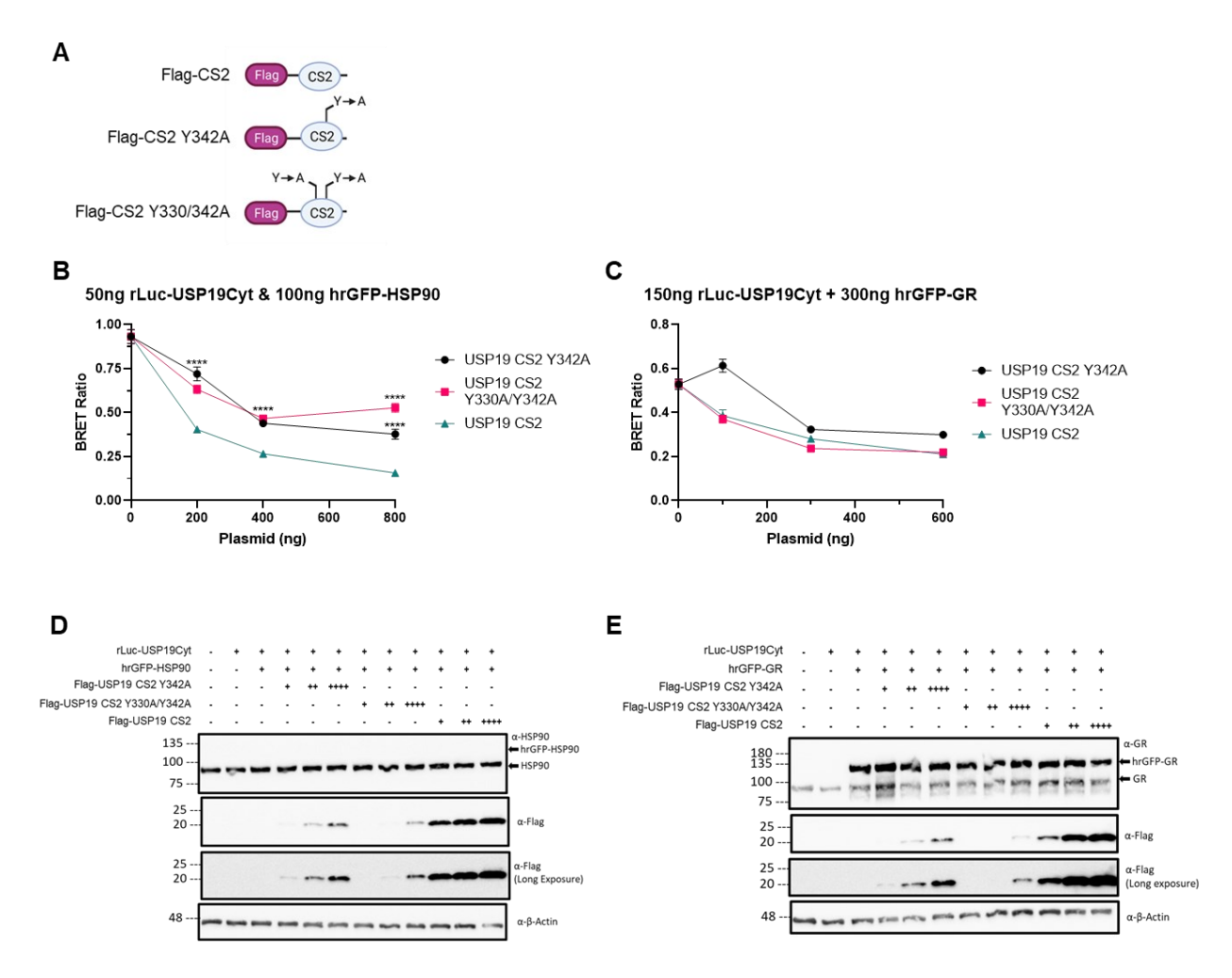


Figure 3.4 USP19 CS2 mutants still compete the interaction of USP19 with HSP90 and with GR. (A) Schematic of the constructs co-transfected with rLuc-USP19Cyt, hrGFP-HSP90 and hrGFP-GR into HEK293 cells. (B-C) We calculated the BRET ratio by dividing the fluorescence by the luminescence upon substrate addition. Shown is the mean \pm SE (n = 4). **** p < 0.001 (Two-way ANOVA Tukey's multiple comparisons). (D-E) Western blot on the BRET assay cell lysates to detect the Flag-tagged CS2 mutants and wildtype competitors in the USP19-HSP90 BRET assay (D) and USP19-GR BRET assay (E).

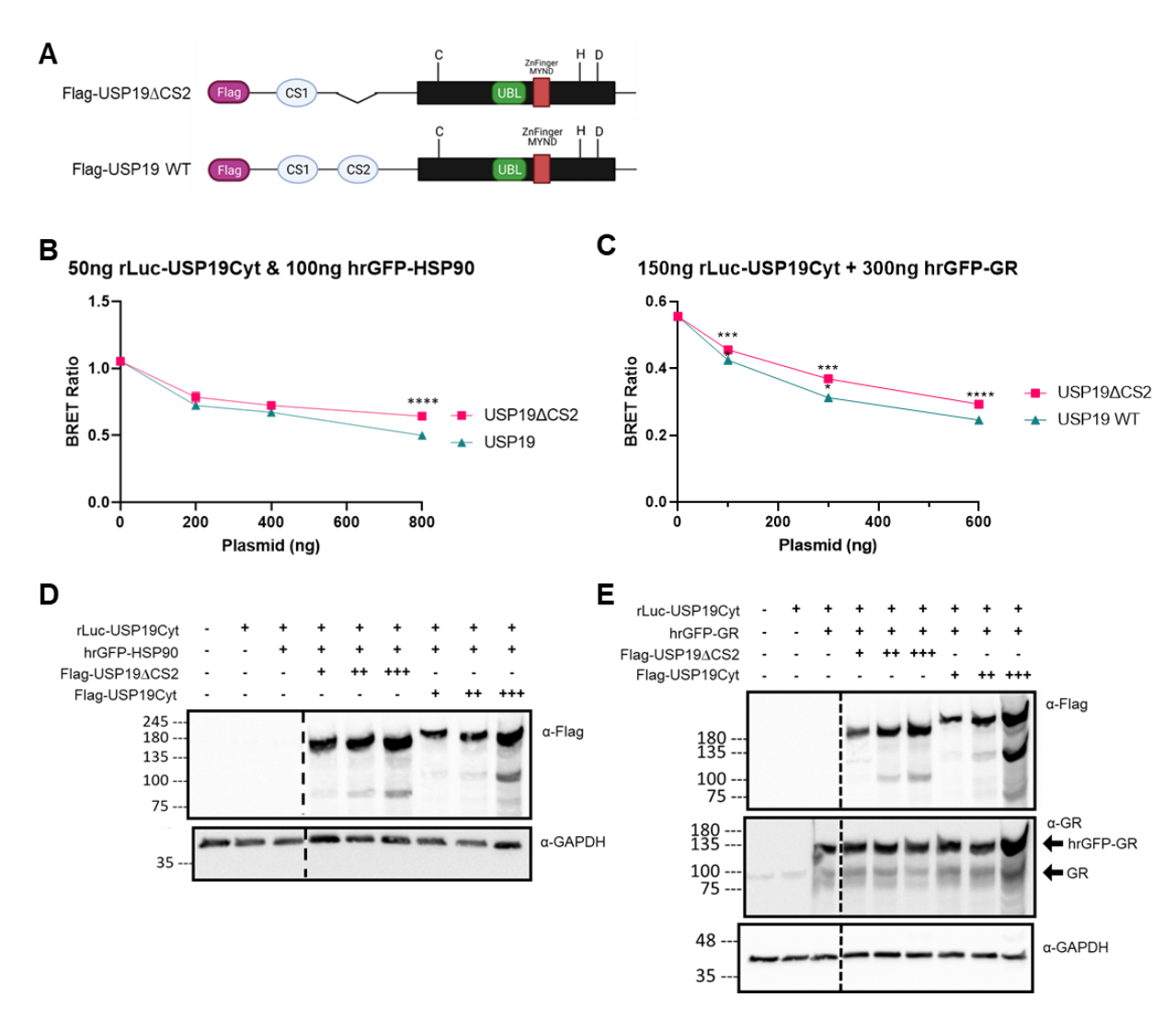


Figure 3.5: USP19 Δ CS2 still competes interaction of USP19 with HSP90 and with GR. (A) Schematic of the constructs co-transfected with rLuc-USP19Cyt, hrGFP-HSP90 and hrGFP-GR into HEK293 cells. (B-C) We calculated the BRET ratio by dividing the fluorescence by the luminescence upon substrate addition. Shown is the mean \pm SE (n = 4). **** p < 0.001 (Two-way ANOVA Tukey's multiple comparisons). (D-E) Western blot on the BRET assay cell lysates to detect the Flag-tagged CS2 mutants and wildtype competitors in the USP19-HSP90 BRET assay (D) and USP19-GR BRET assay (E).

3.2.3. The CS2 domain is required for GR stabilization

We have previously shown that knockout of USP19 reduces GR protein levels by 50% without affecting the mRNA levels in muscle¹⁸⁴. We have overexpressed USP19 in HEK293 cells and observe approximately two-fold increase in GR protein levels (Coyne et al., manuscript in preparation). This GR stabilization effect of USP19 is absent when a construct devoid of both CS domains is overexpressed, suggesting the CS domains are required for USP19 to stabilize GR (Coyne et al., manuscript in preparation). Since we observe that the CS2 domain of USP19 binds to HSP90 and not the CS1 domain, we tested if the CS2 domain is required for USP19 to stabilize GR. So, we overexpressed the cytoplasmic USP19 containing both CS domains and truncations of USP19 lacking the CS1 domain only (USP19ΔN1) or both CS domains (USP19ΔN3) alongside HA-tagged GR into COS7 cells (Figure 3.6A). We observed similar expression of Flag-tagged USP19, USP19ΔN1 and USP19ΔN3 (Figure 3.6B, C). We saw a two-fold increase in GR protein levels when USP19 was overexpressed, and the GR protein levels were still increased when the CS1 domain is absent (Figure 3.6B, D-E). This suggested that the CS1 domain is not required for the stabilization of GR by USP19. GR protein levels were no longer increased when both CS domains are absent (Figure 3.6B, D-E), suggesting the CS2 domain is required for USP19 to stabilize GR.

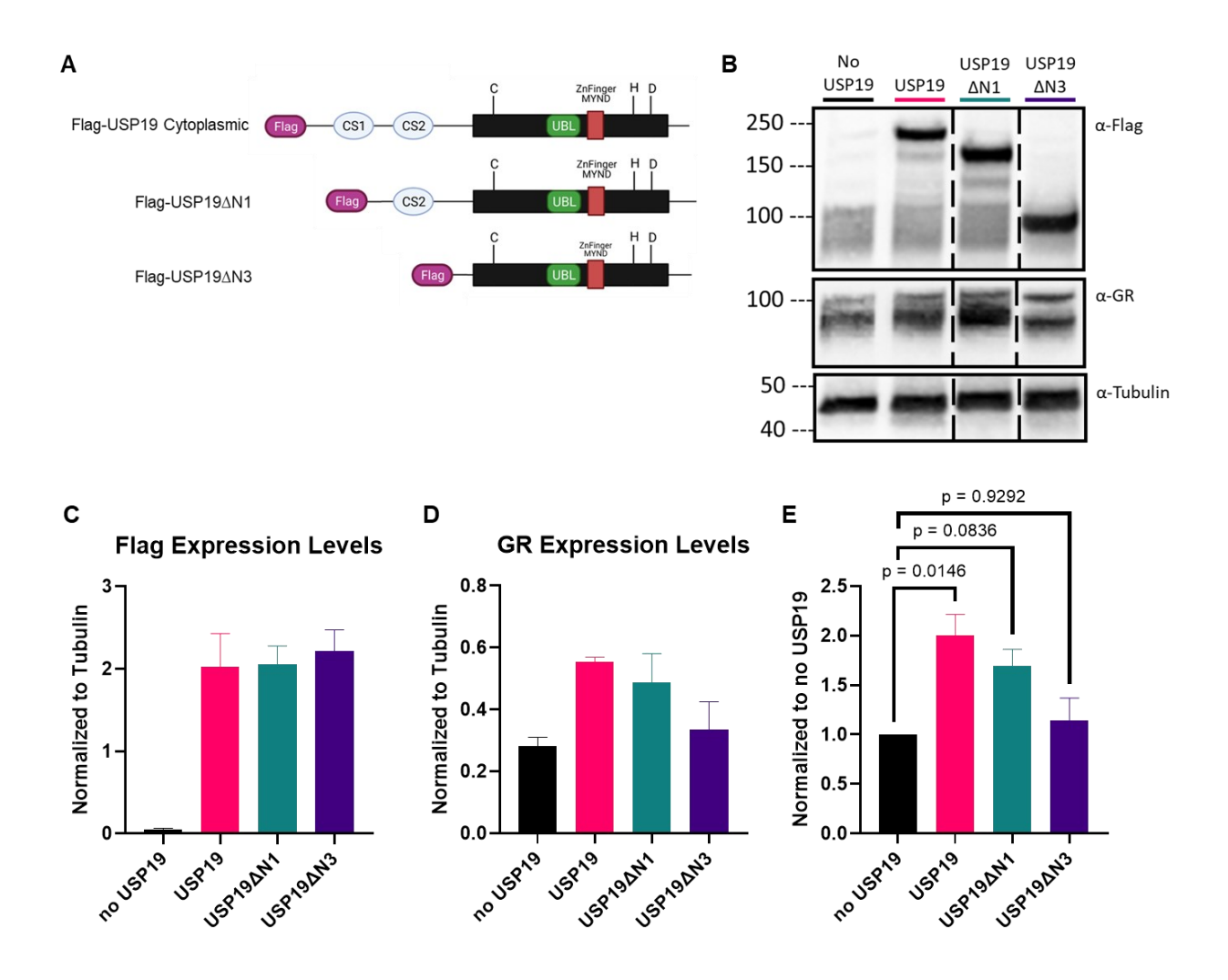


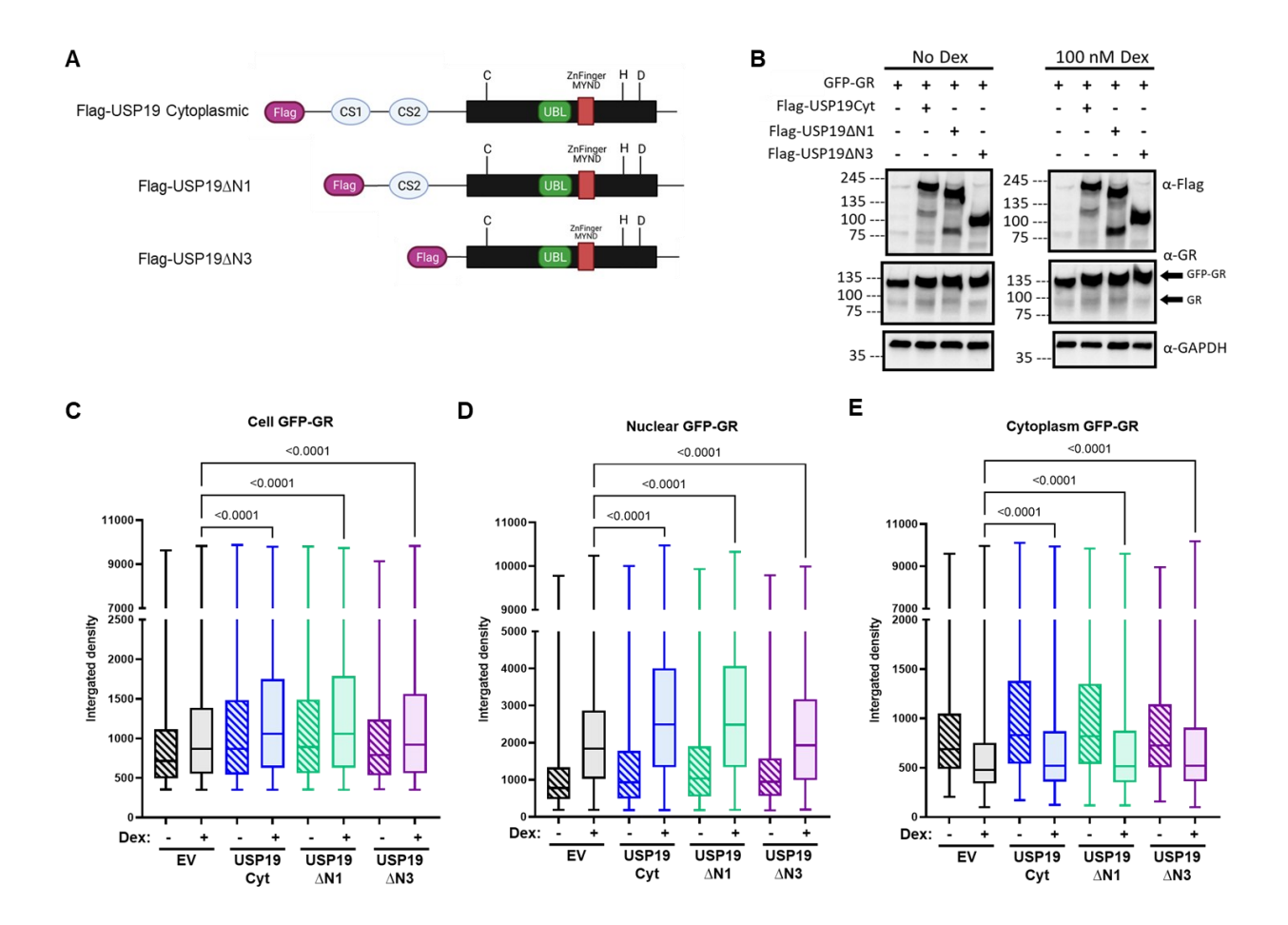
Figure 3.6: The CS1 domain is not required for USP19 stimulated increases in GR protein levels. (A) Schematic of the Flag-tagged constructs co-expressed with HA-tagged GR in COS7 cells. (B) Representative western blot of the total cell lysates showing the expression of the Flag-tagged constructs, HA-tagged GR and tubulin as a loading control. (C) Quantification of Flag-tagged protein levels normalized to tubulin. (D) Quantification of GR protein levels by normalizing to tubulin. (E) Fold-change in GR expression levels compared to no USP19 overexpressed. p-values indicated and obtained by ordinary one-way ANOVA with Tukey's multiple comparison (n = 3).

3.2.4. The CS2 domain is required for GR translocation

Since we observed that the CS2 domain is required for GR stabilization, we explored whether this increase GR represents mature GR. In the ligand-free state, GR is associated with many components such as immunophilins (e.g. Cyp40, FKBP51, FKBP52), HSP70 and its co-chaperone HOP and HSP90 and its co-chaperone p23. These components are involved in the GR maturation process which increases the ligand-binding affinity of GR such that upon ligand binding, it can translocate into the nucleus and regulate transcription.

To examine whether USP19 also enhances GR nuclear translocation, we designed a nuclear translocation assay by co-transfecting GFP-GR with various USP19 constructs into COS-7 cells (Figure 3.7A). We chose COS-7 cells for this assay as these cells have more cytoplasm and are flatter than HEK293 cells. We then measured the changes in localization of GFP-GR between the cytoplasm and nucleus (identified by DAPI) upon treatment of the cells with 100 nM dexamethasone (Dex) for four hours. In the translocation assay, we measured the integrated density which for the nucleus was the average GFP fluorescence in the nucleus multiplied by the pixel intensity and divided by the area of the nucleus in microns (defined by DAPI). We overexpressed GFP-GR and upon Dex treatment observed as expected an increase in nuclear GFP-GR and decrease in cytoplasm GFP-GR (Figure 3.7D-F). Co-expressing GFP-GR with USP19 increased nuclear translocation of GFP-GR with and without Dex treatment (Figure 3.7D-E, G). We also observed an increase in total cellular GFP-GR (Figure 3.7C) with and without Dex treatment consistent with what we observed above (Section 3.2.3).

We next tested whether the domains required for GR stabilization are also required for translocation. We co-expressed GFP-GR with USP19ΔN1 that lacks the CS1 domain only, and still observe an increase in nuclear GFP-GR like the wild-type USP19 (Figure 3.7D-E, H). USP19ΔN1 showed relatively similar expression (Figure 3.7B) and increase in cellular GFP-GR as wild-type USP19 (Figure 3.7C), further verifying that the CS1 domain is not required for GR stabilization. Interestingly, co-expressing USP19ΔN3 that lacks both CS domains no longer enhances nuclear GFP-GR, suggesting the CS2 domain of USP19 is required for GR nuclear translocation as it is for stabilization (Figure 3.7D-E, I).



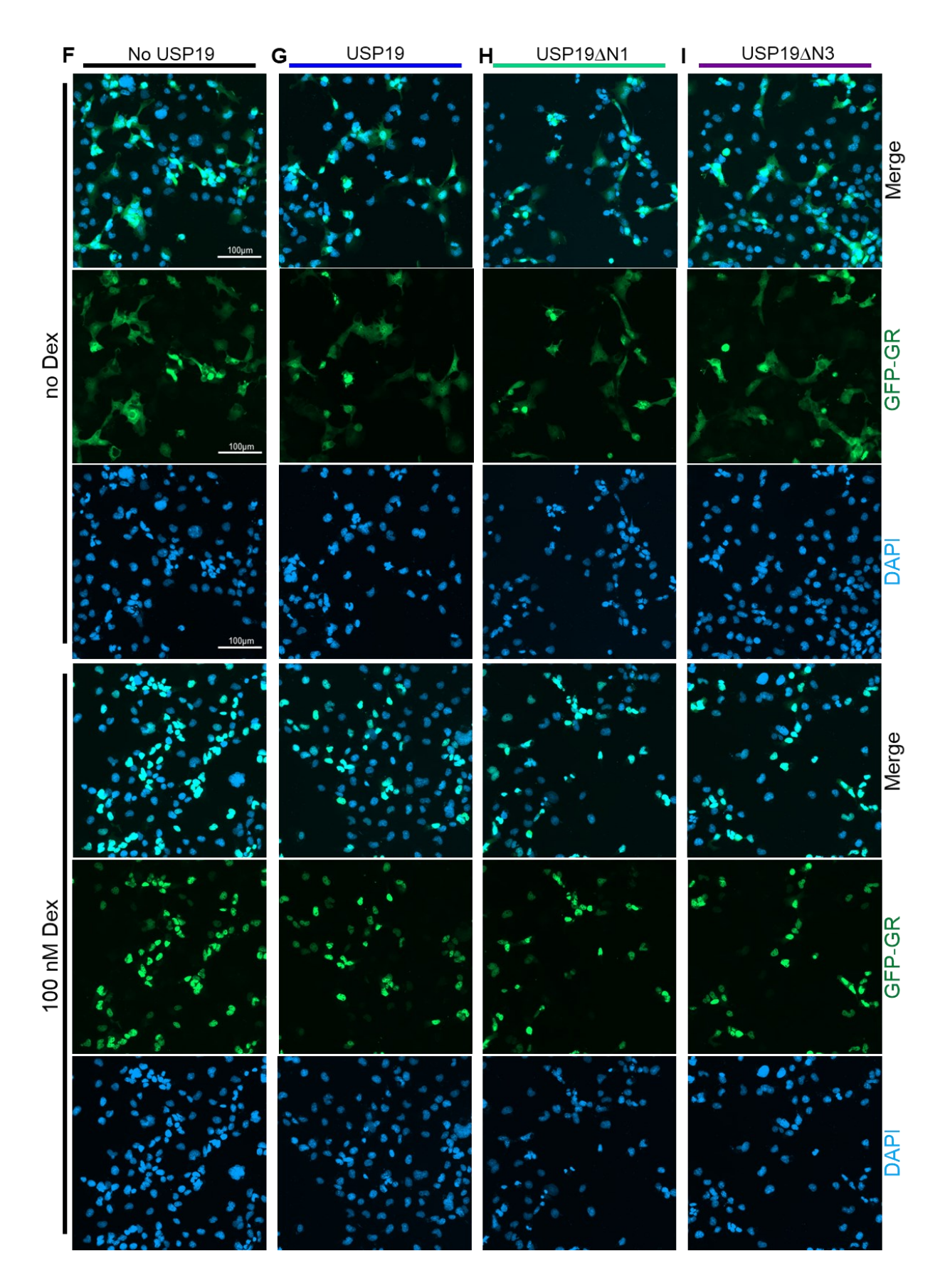


Figure 3.7: The CS1 domain is not required for USP19 stimulation of GFP-GR nuclear translocation. (A) Schematic of various Flag-tagged USP19 constructs co-transfected with GFP-GR in COS7 cells. (B) Western blot on total cell lysate showing the expression of Flag-tagged USP19 constructs, GFP-GR and loading control, GAPDH. (C) Quantification of the cellular GFP-GR (Cell GFP-GR) representing the total GFP-GR integrated density [(Average GFP * pixel intensity)_{nucleus} + (Average GFP * pixel intensity)_{cytoplasm}]/Total cell area. (D) Quantification of nuclear GFP-GR integrated density showing the increase in GFP-GR in the nucleus upon 100 nM Dex treatment for four hours. (E) Quantification of cytoplasmic GFP-GR showing the decrease in GFP-GR in the cytoplasm upon 100 nM Dex treatment for four hours (F-I) Representative images of GFP-GR co-transfected with empty vector (no USP19), USP19, USP19ΔN1 and USP19ΔN3 showing the decrease in cytoplasm GFP-GR and increase nuclear GFP-GR with 100nM Dex treatment. Shown in the box and whisker plot is the minimum, 25th percentile, median, 75th percentile and maximum signal from 30,000-90,000 cells - 2 independent experiments and p-values indicated (Ordinary one-way ANOVA and Tukey's multiple comparison).

3.3. USP19 catalytic domain contains a nuclear receptor box (NR box) motif

3.3.1. Identification of Nuclear Receptor Box (NR box) motif in USP19

The CS2 domain of USP19 binds to HSP90 at the same site as p23 and is required for the stabilization of GR. p23 is a highly conserved protein and one of its roles is to assist HSP90 with the maturation of nuclear receptors (NR) such as the glucocorticoid receptor (GR). The crystal structure of yeast p23/Sba1 has been solved for almost two decades revealing an unstructured C-terminal tail²³². Recent efforts to understand the mechanistic role of this C-terminal tail of p23 revealed novel structural elements²¹³. Specifically, there are two α-helices in the unstructured C-terminal tail of yeast p23/Sba1. One has a NR box motif (LXXLL) and the other has a motif (FXXMMN) found in nuclear co-activator 3 (NCoA3). Interestingly, the latter is conserved in all species but the NR box motif is only found in yeast p23/Sba1²¹². NR box motifs are commonly found in co-activators of nuclear receptors. Deletion of the NR box motif in yeast p23/Sba1 was found to reduce GR activity in a yeast-based assay²¹³. So, we asked if USP19 has any α-helices distal to the CS domains and whether they contain either of the motifs identified in p23 C-terminal tail.

We used Phyre2 to predict the secondary structure of USP19 as no complete crystal structure of USP19 exists. Interestingly, there was an α -helix distal to the CS domains in the catalytic domain with high secondary structure confidence and this α -helix contains a LXXLL NR box motif (Figure 3.8A). USP19 does not have the NCoA3 motif found in all species of p23. To verify the secondary structure prediction, we used another software, AlphaFold which uses artificial intelligence and machine learning to predict highly accurate secondary structures²³³. In the AlphaFold structure prediction, there was still an α -helix distal to the CS domains and it contained the NR box motif (Figure 3.8B). Using AlphaFold, we can visualize whether the α -helix is predicted to be exposed on the surface or buried inside, and it appeared to be somewhat exposed although the surrounding regions are not well predicted (Figure 3.8B). We aligned USP19 sequences from several closely and distantly related species and the NR box motif appears to be highly conserved (Figure 3.8C) within the catalytic domain of USP19 (Figure 3.8D).

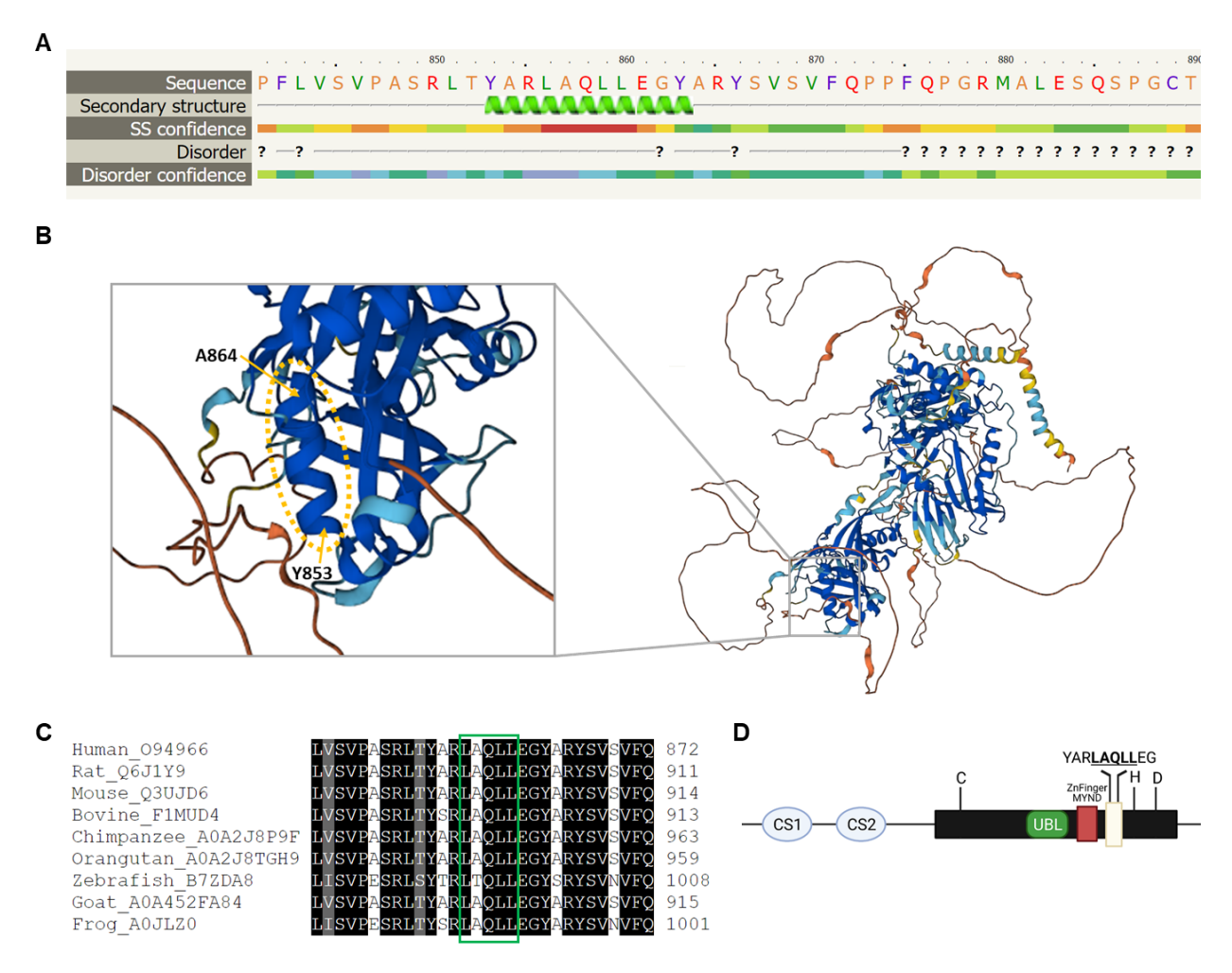


Figure 3.8: Identification of a nuclear receptor box (NR box) motif in the catalytic domain of USP19. (A) Phyre2 prediction on human USP19 (UniProt ID: O94966) revealing an α -helix with a NR box motif. (B) AlphaFold secondary structure prediction on human USP19 (UniProt ID: O94966) showing the location of the α -helix within the predicted structure of USP19. (C) Sequence alignment of USP19 using BLAST and Bioinformatics.org from eight different species showing conservation of the NR box motif, highlighted by the green rectangle. (D) Schematic of USP19 showing the location of the NR box motif within the catalytic domain.

3.3.2. Mutating the NR box or deletion of CS2 abolishes the ability of USP19 to stabilize GR

Since deleting the NR box in yeast p23/Sba1 reduced GR activity and USP19 has a similar NR box motif distal to the CS2 domain, we tested whether mutating the motif in USP19 would interfere with USP19's ability to promote GR stabilization and translocation. The three leucine residues in the NR box motif of co-activators interact with residues in the nuclear receptor activating helix 2 (AF-2) hydrophobic groove in GR²⁰⁶. We mutated all three leucine residues to alanine in the wild-type USP19 and USP19ΔCS2 constructs using site-directed mutagenesis (Figure 3.9A). We observed in our pilot experiments, that with the same amount of plasmid transfected, the NR box mutants are less expressed compared to wild-type USP19. We therefore optimized the amount of plasmids transfected in COS7 to give similar expression (unpublished data).

Previously, we saw that the overexpression of USP19 enhances HA-tagged GR stabilization by approximately two-fold (Figure 3.6E). We co-transfected varying amounts of Flagtagged USP19 wild-type and mutant plasmids with a fixed amount of HA-tagged GR into COS7 cells to permit comparison of conditions with similar levels of expression of USP19 wild-type and mutant forms (Figure 3.9A). We observed a dose-dependent increase in the expression of HA-tagged GR with increasing wild-type USP19 (Figure 3.9B-E). Interestingly, we saw a decrease in HA-tagged GR expression with increasing USP19 NR box mutant, USP19ΔCS2 and USP19ΔCS2 NR box mutant to similar levels as no USP19 (Figure 3.9B-E). The stabilization effect of HA-tagged GR by wild-type USP19 was abolished by the USP19ΔCS2 NR box mutant (Figure 3.9E). Overall, this suggested that both the NR box motif and the CS2 domain are required for USP19 to stabilize GR.

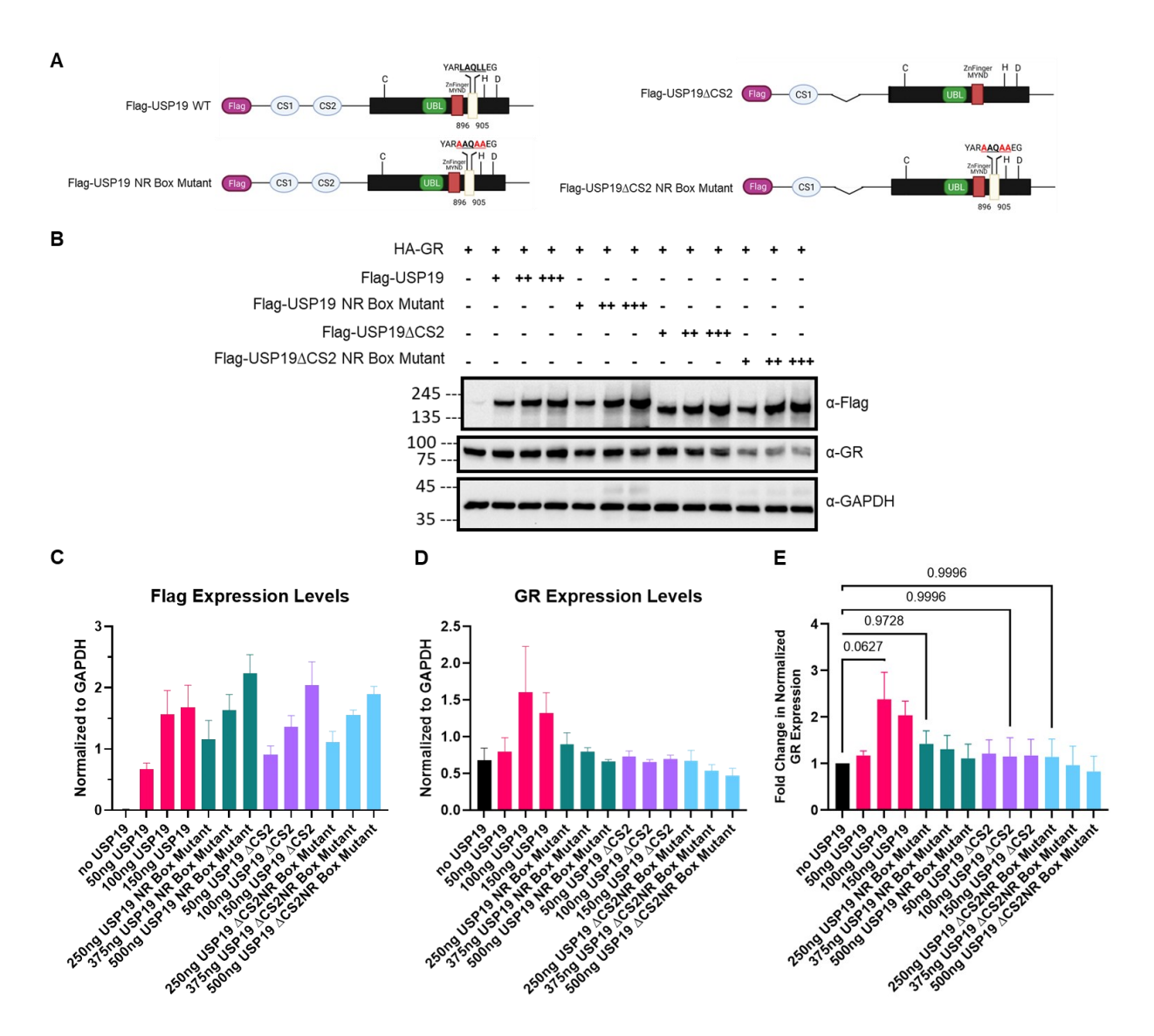
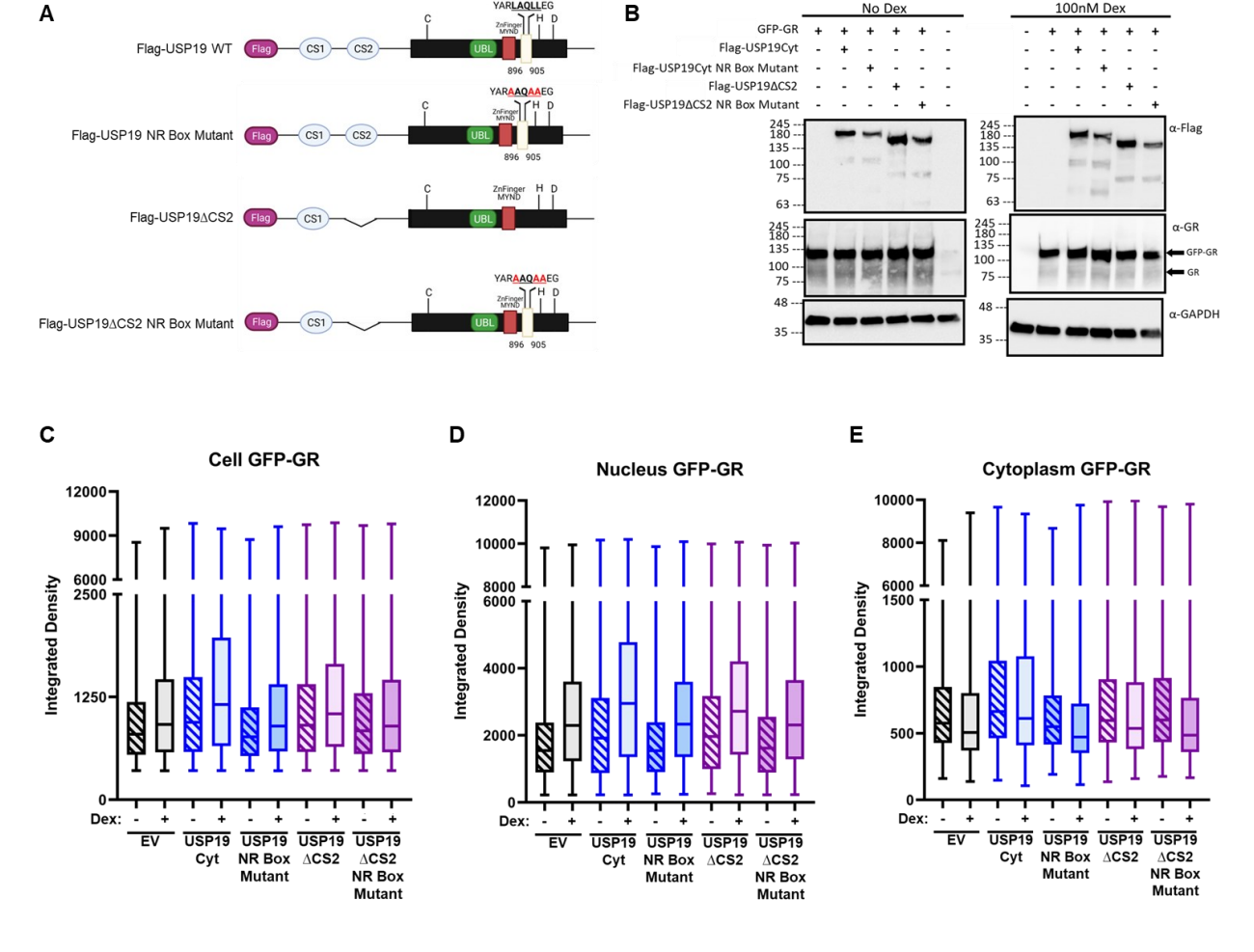


Figure 3.9: CS2 domain or intact NR box is required for USP19 stabilization of overexpressed HA-GR. (A) Schematic of the constructs co-transfected with HA-tagged GR in COS7 cells. (B) Representative Western Blot on the total cell lysates harvested 48-hours post-transfection with various USP19 constructs and HA-tagged GR. (C) Quantification of Flag-tagged USP19, USP19 NR box mutant, USP19 Δ CS2 and USP19 Δ CS2 NR box mutant expression levels normalized to loading control GAPDH. (D) Quantification of HA-tagged GR expression levels normalized to co-expression with empty vector (no USP19) showing the fold-change in GR expression. P-values (Ordinary one-way ANOVA Dunnett's multiple comparison) shown for comparison of conditions with similar Flag-USP19 expression. Mean \pm SEM (n = 3).

3.3.3. The NR box in USP19 is required for its ability to promote nuclear translocation of GR

We next asked whether the CS2 domain and NR box are also required for USP19's ability to enhance GFP-GR nuclear translocation (Figure 3.7E). We co-expressed USP19, USP19 NR box mutant, USP19 Δ CS2 and USP19 Δ CS2 NR box mutant with GFP-GR in COS7 cells and then measured nuclear GFP-GR upon Dex treatment (Figure 3.10A).

As we saw previously, Dex treatment induced GFP-GR translocation and this effect was further enhanced by expression of USP19 (Figure 3.10D, E, G). Deletion of the CS2 domain blunted (Figure 3.10D, E, I) and mutating the NR box abolished this effect of USP19 (Figure 3.10D, E, H). However, in this study, the NR box mutant was less expressed than wild-type USP19 (Figure 3.10B). The combined deletion of the CS2 domain and mutation of the NR box was well-expressed though (Figure 3.10B) and showed a stronger impairment of GFP-GR translocation than the deletion of CS2 alone (Figure 3.10D, E, J), suggesting that the NR box does indeed contribute a significant role in the ability of USP19 to promote GR translocation.



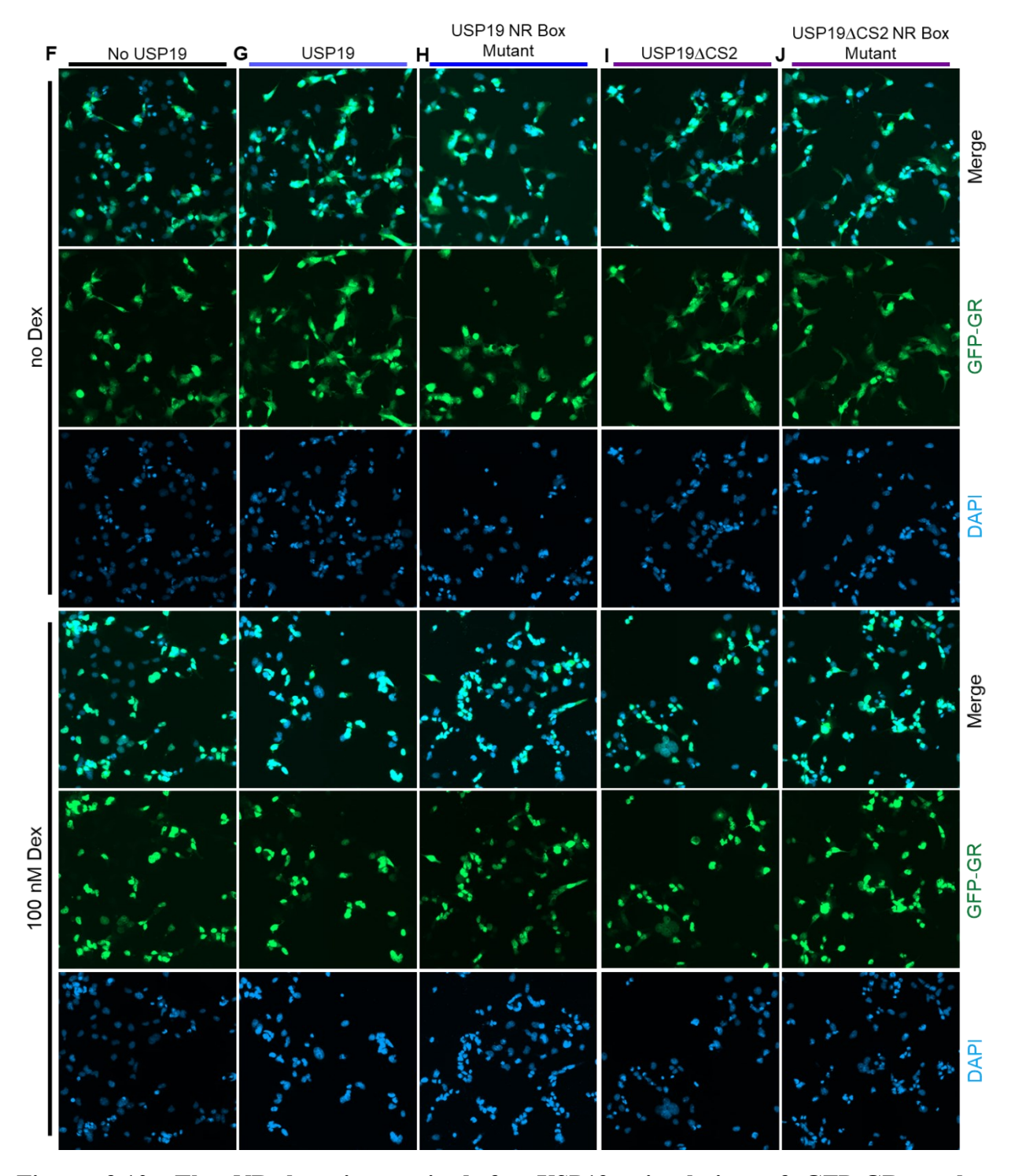


Figure 3.10: The NR box is required for USP19 stimulation of GFP-GR nuclear translocation. (A) Schematic of the various Flag-tagged USP19 constructs co-expressed with GFP-GR in COS7 cells. (B) Western blot on total cell lysate treated in the same manner as the coverslips, showing the decreased expression of the NR box mutants compared to USP19 wild-type and relatively similar expression of GFP-GR. (C) Quantification of cell GFP-GR which sums together the cytoplasm and nucleus GFP-GR integrated densities ((average GFP fluorescence x

pixel intensity)/area). (D) Quantification of nucleus GFP-GR showing the increase GFP-GR in the nucleus upon 100 nM Dex treatment for four hours. (E) Quantification of cytoplasm GFP-GR showing the decrease of GFP-GR in the cytoplasm upon 100 nM Dex treatment. (F-J) Representative images of GFP-GR co-transfected with empty vector (no USP19), USP19, USP19 NR box mutant, USP19ΔCS2 and USP19ΔCS2 NR box mutant showing the decrease in cytoplasm GFP-GR and increase in nuclear GFP-GR with 100 nM Dex treatment. Shown in the box and whisker plot is the minimum, 25th percentile, median, 75th percentile and maximum signals from 30,000-90,000 cells in 2 independent experiments.

Chapter 4: Discussion

Previous work in our laboratory demonstrated that USP19 promotes glucocorticoid signaling by increasing levels of GR¹⁸⁴. More recent unpublished work indicates that USP19 can be immunoprecipitated with GR, suggesting GR might be a substrate of USP19. However, these recent studies have also demonstrated that the catalytic activity is not required for the modulation of GR levels. In this thesis, I provide evidence indicating for the first time that USP19 acts as a novel co-chaperone of HSP90 to promote GR levels and function.

Previous work from other groups have utilized immunoprecipitation and GST pulldown assays to show that USP19 interacts with HSP90^{103,138,139}. More recently, Xue and colleagues have reported, using isothermal calorimetry and NMR, that this interaction is mediated between the CS2 domain of USP19 and the N-terminal domain of HSP90. In this thesis I have confirmed these findings using a novel BRET assay that monitors the interaction of USP19 with HSP90. The BRET assay is an *in vivo* assay that is sensitive that typically detects interactions between proteins that are less than 10 nm apart. Expressing increasing amounts of hrGFP-HSP90 and a constant amount of rLuc-USP19Cyt in this assay, we observed a progressively increasing BRET signal that plateaued, suggesting a specific and saturable interaction between USP19 and HSP90 (Figure 3.1). Performing a similar experiment with hrGFP-GR instead of hrGFP-HSP90 yielded a much smaller BRET signal that did not clearly saturate. The signal was also less than with the hrGFP-control. As these studies are in living cells and it is not possible to know the precise concentrations of the expressed proteins, the precise strength of the interactions cannot be quantified. It would also be interesting to test, as a negative control, the effect of the addition of dexamethasone which should bind o GR and result in GR translocation from HSP90 into the nucleus and therefore, a loss of the BRET signal. All together though, this data argues that this novel interaction between USP19 and GR that our lab recently detected by immunoprecipitation is indirect and mediated by HSP90. This conclusion could be further tested using a tripartite BRET assay in which either the luciferase donor or GFP acceptor fluorophore is split to create an assay with three components. USP19, HSP90 and GR would each be fused to one of the three components and a BRET signal would indicate a tripartite interaction between all three proteins. There is a commercially available split luciferase system known as NanoLuciferase (NanoLuc) Binary Technology (NanoBiT) which consists of a large subunit (LgBiT) and a small subunit (SmBiT)²³⁴. Each subunit is fused to either the N or C-terminus of the protein of interest and the protein-protein interaction reconstructs a functional NanoLuc, which upon furimazine substrate addition, emits light within the excitation spectrum of Venus or YFP fluorophores. We have started to generate the split luciferase constructs of USP19, HSP90 and GR but failed to reconstruct a functional NanoLuc with the positive control pair of HSP90 and GR, suggesting there is a technical problem.

We showed here for the first time that USP19 binds to the same site on HSP90 as p23, a co-chaperone of HSP90. We observed that the expression of p23 in the BRET assay competed with the interaction of rLuc-USP19Cyt with hrGFP-HSP90. Importantly, expressing F103A and/or W106A mutants of p23 abolished completely or partially respectively, the ability of p23 to disrupt the rLuc-USP19Cyt and hrGFP-HSP90 interaction in the BRET assay (Figure 3.2). Crystallographic analysis has revealed that p23 F103 and W106 both interact with a hydrophobic pocket in HSP90α middle domain (MD) (PDB: 7J7J)²³⁵. p23 F103 forms a hydrogen bond with HSP90 α Q405 whereas p23 W106 does not appear to form any hydrogen bonds with HSP90 α^{235} . However, p23 F103 hydrogen bond was not observed in the yeast HSP90-p23 (PDB: 2CG9) or in a human HSP90α-p23-GR crystal structures (PDB: 7KRJ)²¹². Regardless of whether p23 F103 makes a hydrogen bond with HSP90α or not, this finding provided insight on the function of USP19. This novel finding suggested that USP19, a CS domain containing DUB, may act like p23 and this is independent of the catalytic function of USP19. Numerous studies have showed that p23 functions to increase the ligand-binding capacity of GR by deaccelerating HSP90 ATP hydrolysis and this enhances the activation of GR²³⁶⁻²⁴¹. If USP19 does indeed act like p23 in the GR maturation cycle, then USP19 may also delay HSP90 ATP hydrolysis. This could be tested using an in vitro ATPase assay to examine changes in HSP90 ATP hydrolysis in the presence or absence of USP19.

The CS domain of p23 plays a critical role in binding to HSP90. We further used our BRET assay to test whether one or both USP19 CS domains are similarly involved. We confirmed the recent report that USP19 CS2 domain is required for binding to HSP90 (Figure 3.3)²³¹. In structural modelling of USP19 CS1 and CS2 domains (collaboration with Dr. Jason Young) based on the known structures of HSP90 co-chaperones p23 and Sgt1, we identified point residues in USP19 CS2 domain, Y330 and Y342 that likely contact HSP90 and indeed these residues were found to interact with HSP90 in the recently reported structure of the CS2 domain^{138,231}. We mutated these

residues to alanine and expressed them in the BRET assay, but did not see significant interference with the binding. However, the CS2 mutants were more poorly expressed than wild type, making it difficult to arrive at a conclusion (Figure 3.4). We deleted the CS2 domain and observed a statistically significant decrease in competition compared to wild-type USP19 but not a complete abolishment (Figure 3.5). Possible explanations for these observations are that 1) there are additional domains in USP19 that also contribute to binding to HSP90, 2) there could be additional proteins bound to USP19 resulting in competition, and 3) the CS2 deletion results in misfolding of the remainder of the protein and therefore inability to compete. To further explore this, we could use a GST-pulldown assay with GST-tagged CS2 to pulldown HSP90 from cell lysate and subsequently mutate CS2 to examine whether HSP90 is still pulled down.

In this thesis, we have also provided insight into the functional consequences of USP19 binding to HSP90. We confirmed unpublished data in our laboratory that USP19 stabilizes GR (Coyne et al., *manuscript in preparation*) and made the new discovery that USP19 also promotes GR cytoplasm-to-nucleus translocation. We deleted the CS1 domain in USP19 and still observed GR stabilization and nuclear translocation, suggesting the CS1 domain is not needed for the ability of USP19 to regulate GR (Figure 3.6, 3.7). Subsequent deletion of the CS2 domain reduced the ability of USP19 to stabilize GR and promote translocation, suggesting that the CS2 domain and its interaction with HSP90 are required (Figure 3.6, 3.7). This is consistent with the recent findings of Xue and colleagues who recently concluded that USP19 has an autoinhibitory conformation in which the CS2 domain binds intramolecularly to the catalytic domain and this autoinhibition is relieved upon CS2 binding to HSP90²³¹. However, we observed that overexpressing the CS2 domain itself did not stabilize GR, suggesting the CS2 domain is insufficient for the ability of USP19 to modulate GR. This raises the question of whether other regions of USP19 are also required to modulate GR and what functions these other domains may have.

With respect to this possibility, we identified a nuclear receptor box (NR box) motif in USP19 catalytic domain (Figure 3.8). NR box motifs are commonly found in nuclear receptor co-activators such as SRC-2/GRIP-1/TIF-2. These co-activators recruit additional proteins, acetylate histones, and unwind chromatin, allowing for NR binding to response elements on the DNA and thereby transcriptional activation²⁰⁵. The NR box is found within an α -helix and interacts with the AF-2 helix in the GR ligand binding domain which is exposed upon ligand binding. The

identification of such a motif in an α-helix within the USP19 catalytic domain, suggests a novel function of USP19 that has not been studied. In fact, to our knowledge, there are very few studies published that explore the function of a DUB in the context of nuclear receptors such as GR. Interestingly, USP2 and USP7 also have NR box motifs in their catalytic domain and ubiquitin-like domain (HUBL3), respectively. The presence of the NR box motif in USP19 raises a question about whether USP19 may act like a co-activator of GR. Indeed, we have previously observed that KO of USP19 reduces the transcription of GR target genes in skeletal muscle¹⁸⁴. USP19 has also been previously reported to interact with HDAC1 and surprisingly, HDAC1 has been reported to be a co-activator of GR rather than a co-repressor, suggesting the possibility that USP19 may recruit HDAC1 to assist with GR activation ^{122,242,243}.

We have started addressing the function of the NR box motif in USP19. In doing so, we have made the novel observation that mutating the motif reduces the ability of USP19 to stabilize and promote ligand-stimulated GR translocation to the nucleus. This was observed in the presence and absence of the CS2 domain, suggesting the function of the NR box in USP19 is independent of the function of the CS2 domain (Figure 3.9, 3.10). As mentioned earlier, Saccharomyces cerevisiae p23/Sba1 unstructured C-terminal tail contains an α-helix with a NR box motif and has been suggested to transiently interact with the client binding site in HSP90 MD/CTD to properly position the CS domain on the HSP90 N-terminal domain²¹³. USP19 has both the CS domains and the NR box motif, and our data suggests that both are required for its ability to modulate GR like p23/Sba1. Whether the CS2 domain and the NR box together are sufficient for the ability of USP19 to modulate GR remains unclear. To address this, we are currently generating a fusion protein consisting of the CS2 domain, some linkage sequence and the α-helix containing the NR box and will test if it can increase GR levels and promote its nuclear translocation. In addition, we could use molecular modelling software such as PyMol and apply it to the AlphaFold predicted structure of human USP19 and the known structures of HSP90 and GR ligand binding domain. Using modelling software, we may uncover whether the predicted structure of USP19 might fit into the complex of HSP90 and GR. Additionally, we may reveal whether the positioning of the CS2 domain and the NR box of USP19 aligns with the regions on HSP90 and/or GR to which the p23 CS domain and NR box of p23/Sba1 bind. In this regard, it is noteworthy that the deletion of a portion of the USP19 catalytic domain that contains the NR box motif has been reported to reduce its binding to HSP90^{103,213}. We have conducted pilot experiments testing whether the USP19 NR

box directly interacts with HSP90 or GR using our BRET assay and obtained inconclusive results. We could use immunoprecipitation or a GST pulldown assay with GST-tagged USP19 catalytic domain to pulldown HSP90 or GR from cell lysate and subsequently mutate the NR box to determine whether this abolishes or decreases the interactions.

The CS2 domain plus the NR box motif may not be sufficient for modulating GR function because the cytoplasmic isoform of USP19 also contains a MEEVD motif at the C-terminus that is identical to the motif found in HSP90. MEEVD motifs binds tetratricopeptide repeat (TPR) domain-containing proteins such as immunophilins, FKBP51/FKBP5 and FKBP52/FKBP4. These immunophilins are associated with the maturation process of GR, specifically in the cytoplasm-tonucleus translocation^{244,245}. There are several studies indicating that HSP90, p23 and FKBP52 remain associated with ligand-bound GR while being actively transported on dynein through the nuclear pore complex into the nucleus and then dissociates^{209,246–248}. Intriguingly, USP19 has been observed to interact with FKBP52/FKBP4 through an interactome study²⁴⁹. Additionally, we have observed that deletion of the MEEVD motif in USP19 reduces its ability to promote GR nuclear translocation (Nathalie Bedard, unpublished data). One possibility is that the deletion of the USP19 MEEVD motif prevents FKBP52 from binding to the heterocomplex and impairs the active transport, resulting in reduced GR translocation. Another possibility is that USP19 binds and deubiquitinates FKBP52/FKBP4, resulting in more FKBP52 available to actively transport GR into the nucleus. Interestingly CyP-40/CyPD/PPID is another immunophilin that has been reported to compete with FKBP52 for HSP90 binding and is also involved in nuclear transport^{250–252}. We have some preliminary data from a protein microarray experiment showing that both CyP-40/CyPD/PPID and FKBP51/FKBP5 on the array are more ubiquitinated following incubation of the microarray with USP19 KO C2C12 cell extracts than with WT C2C12 extracts. However, FKBP52/FKBP4 was not present on the protein microarray (unpublished data). These observations suggest that PPID, FKBP5 and FKBP4 are substrates of USP19, possibilities that could be explored in the future.

Overall, in this thesis, we have made significant progress in elucidating the mechanisms by which USP19 regulates GR. We previously showed that USP19 is upregulated in skeletal muscle upon catabolic stimuli and essential for the increased GR level and signaling and subsequent muscle wasting under these conditions. Here, we revealed through deletion and

mutagenesis studies that both the CS2 domain and the NR box are required for the ability of USP19 to stabilize GR and promote its translocation to the nucleus. Targeting the CS2 domain of USP19 with a small molecule may prevent the direct association of USP19 with HSP90 and indirectly with GR. This specific disruption of USP19 binding with HSP90 may yield protection against muscle wasting and avoid off-target effects of less specific targeting that might affect all functions of USP19. Since the interaction of USP19 CS2 domain with HSP90 has also been implicated to be important for USP19's ability to deubiquitinate and stabilize polyQ-expanded huntingtin (Htt) and ataxin-3 (Atx3), such a specific inhibitor may also be beneficial for Huntingtin's disease and spinocerebellar ataxia type-3 (SCA3)^{138,231}. Similarly, we could target the region containing the NR box in the USP19 catalytic domain with a small molecule which may prevent USP19 from stabilizing GR without impairing the interaction of USP19 with HSP90. This may be a more specific tactic to prevent GC-induced muscle wasting. In conclusion, in this thesis, we have identified two sites in USP19 that could be targeted with small molecules to reduce GC-induced muscle wasting, which could improve patient quality of life and survival in the many diseases that are complicated by muscle wasting dependent on the presence of glucocorticoid signaling.

Chapter 5: Conclusion

In this thesis, we explored the mechanism of action of USP19 in glucocorticoid-induced muscle atrophy. Our previous work suggested that USP19 increases GR level and function by acting on it indirectly via binding to HSP90. We tested whether the CS domains of USP19 binds to HSP90 similarly to the p23 CS domains. We showed for the first time that USP19 directly interacts with HSP90, indirectly with GR and binds to the same site on HSP90 as p23 using a bioluminescence resonance energy transfer (BRET) assay. We asked whether one or both USP19 CS domains interact with HSP90 and identified that the CS2 domain of USP19 binds to HSP90 similar with previously published studies. Overexpressing USP19 increases GR expression levels and nuclear translocation. This effect is retained when the CS1 domain is deleted but not when both CS domains were deleted, suggesting that the CS2 domain is required. When we overexpressed the CS2 domain alone, we did not observe an increase in GR expression levels or nuclear translocation upon Dex treatment, suggesting that the CS2 domain is required but insufficient. In addition, when we mutated or deleted the CS2 domain in USP19, we were unable to abolish completely its interaction with HSP90. We therefore explored whether there could be another domain in USP19 that interacts with HSP90 and/or GR and identified a nuclear receptor box (NR box) motif that is commonly found in co-activators of nuclear receptors. We mutated the NR box in USP19 and the mutant also failed to increase GR expression levels and nuclear translocation. Overall, our results suggested that both the CS2 domain and nuclear receptor box motif are required for the ability of USP19 to modulate GR. These results identified two potential sites in USP19 that could be targeted with small molecules to prevent the ability of USP19 to modulate GR and thereby reduce or prevent the burden of GC-induced muscle atrophy.

References

- 1. Frontera, W. R. & Ochala, J. Skeletal Muscle: A Brief Review of Structure and Function. *Calcif. Tissue Int.* **96**, 183–195 (2015).
- 2. Sartori, R., Romanello, V. & Sandri, M. Mechanisms of muscle atrophy and hypertrophy: implications in health and disease. *Nat. Commun.* **12,** 330 (2021).
- 3. Baskin, K. K., Winders, B. R. & Olson, E. N. Muscle as a "Mediator" of Systemic Metabolism. *Cell Metab.* **21**, 237–248 (2015).
- 4. Sandri, M. Autophagy in skeletal muscle. *FEBS Lett.* **584**, 1411–1416 (2010).
- 5. Cretoiu, D., Pavelescu, L., Duica, F., Radu, M., Suciu, N. & Cretoiu, S. M. in *Muscle Atrophy* (ed. Xiao, J.) 23–46 (Springer, 2018). doi:10.1007/978-981-13-1435-3 2
- 6. Bentzinger, C. F., Wang, Y. X. & Rudnicki, M. A. Building Muscle: Molecular Regulation of Myogenesis. *Cold Spring Harb. Perspect. Biol.* **4,** a008342 (2012).
- 7. Huxley, H. E. Electron microscope studies of the organisation of the filaments in striated muscle. *Biochim. Biophys. Acta* **12**, 387–394 (1953).
- 8. Grigorenko, B. L., Rogov, A. V., Topol, I. A., Burt, S. K., Martinez, H. M. & Nemukhin, A. V. Mechanism of the myosin catalyzed hydrolysis of ATP as rationalized by molecular modeling. *Proc. Natl. Acad. Sci. U. S. A.* **104**, 7057–7061 (2007).
- 9. Rahman, F. A. & Quadrilatero, J. Mitochondrial network remodeling: an important feature of myogenesis and skeletal muscle regeneration. *Cell. Mol. Life Sci.* **78**, 4653–4675 (2021).
- 10. Tisdale, M. J. Cachexia in cancer patients. Nat. Rev. Cancer 2, 862–871 (2002).
- Bodine, S. C., Latres, E., Baumhueter, S., Lai, V. K.-M., Nunez, L., Clarke, B. A., Poueymirou, W. T., Panaro, F. J., Na, E., Dharmarajan, K., Pan, Z.-Q., Valenzuela, D. M., DeChiara, T. M., Stitt, T. N., Yancopoulos, G. D. & Glass, D. J. Identification of Ubiquitin Ligases Required for Skeletal Muscle Atrophy. Science 294, 1704–1708 (2001).
- 12. Carnio, S., LoVerso, F., Baraibar, M. A., Longa, E., Khan, M. M., Maffei, M., Reischl, M., Canepari, M., Loefler, S., Kern, H., Blaauw, B., Friguet, B., Bottinelli, R., Rudolf, R. & Sandri, M. Autophagy impairment in muscle induces neuromuscular junction degeneration and precocious aging. Cell Rep. 8, 1509–1521 (2014).
- 13. Bonetto, A., Aydogdu, T., Jin, X., Zhang, Z., Zhan, R., Puzis, L., Koniaris, L. G. & Zimmers, T. A. JAK/STAT3 pathway inhibition blocks skeletal muscle wasting downstream of IL-6 and in experimental cancer cachexia. Am. J. Physiol. Endocrinol. Metab. 303, E410-421 (2012).
- 14. Magomedova, L. & Cummins, C. L. in Metab. Control (ed. Herzig, S.) 73–93 (Springer International Publishing, 2016). doi:10.1007/164 2015 1
- 15. Vainshtein, A. & Sandri, M. Signaling Pathways That Control Muscle Mass. Int. J. Mol. Sci. 21, E4759 (2020).
- 16. Schakman, O., Kalista, S., Barbé, C., Loumaye, A. & Thissen, J. P. Glucocorticoid-induced skeletal muscle atrophy. Int. J. Biochem. Cell Biol. 45, 2163–2172 (2013).
- 17. Medina, R., Wing, S. S., Haas, A. & Goldberg, A. L. Activation of the ubiquitin-ATP-dependent proteolytic system in skeletal muscle during fasting and denervation atrophy. *Biomed. Biochim. Acta* **50**, 347–356 (1991).
- 18. Medina, R., Wing, S. S. & Goldberg, A. L. Increase in levels of polyubiquitin and proteasome mRNA in skeletal muscle during starvation and denervation atrophy. *Biochem. J.* **307**, 631–637 (1995).

- 19. Wing, S. S., Haas, A. L. & Goldberg, A. L. Increase in ubiquitin-protein conjugates concomitant with the increase in proteolysis in rat skeletal muscle during starvation and atrophy denervation. *Biochem. J.* **307** (**Pt 3**), 639–645 (1995).
- 20. Kedar, V., McDonough, H., Arya, R., Li, H.-H., Rockman, H. A. & Patterson, C. Musclespecific RING finger 1 is a bona fide ubiquitin ligase that degrades cardiac troponin I. *Proc. Natl. Acad. Sci. U. S. A.* **101**, 18135–18140 (2004).
- 21. Paul, P. K., Bhatnagar, S., Mishra, V., Srivastava, S., Darnay, B. G., Choi, Y. & Kumar, A. The E3 Ubiquitin Ligase TRAF6 Intercedes in Starvation-Induced Skeletal Muscle Atrophy through Multiple Mechanisms. *Mol. Cell. Biol.* **32**, 1248–1259 (2012).
- 22. Sartori, R., Schirwis, E., Blaauw, B., Bortolanza, S., Zhao, J., Enzo, E., Stantzou, A., Mouisel, E., Toniolo, L., Ferry, A., Stricker, S., Goldberg, A. L., Dupont, S., Piccolo, S., Amthor, H. & Sandri, M. BMP signaling controls muscle mass. *Nat. Genet.* **45**, 1309–1318 (2013).
- 23. Milan, G., Romanello, V., Pescatore, F., Armani, A., Paik, J.-H., Frasson, L., Seydel, A., Zhao, J., Abraham, R., Goldberg, A. L., Blaauw, B., DePinho, R. A. & Sandri, M. Regulation of autophagy and the ubiquitin–proteasome system by the FoxO transcriptional network during muscle atrophy. *Nat. Commun.* **6**, 6670 (2015).
- 24. Goldberg, A. L., Cascio, P., Saric, T. & Rock, K. L. The importance of the proteasome and subsequent proteolytic steps in the generation of antigenic peptides. *Mol. Immunol.* **39**, 147–164 (2002).
- 25. Bachiller, S., Alonso-Bellido, I. M., Real, L. M., Pérez-Villegas, E. M., Venero, J. L., Deierborg, T., Armengol, J. Á. & Ruiz, R. The Ubiquitin Proteasome System in Neuromuscular Disorders: Moving Beyond Movement. *Int. J. Mol. Sci.* **21**, 6429 (2020).
- 26. Hershko, A. & Ciechanover, A. The ubiquitin system. *Annu. Rev. Biochem.* **67**, 425–479 (1998).
- 27. Wang, Y. & Wang, F. Post-Translational Modifications of Deubiquitinating Enzymes: Expanding the Ubiquitin Code. *Front. Pharmacol.* **12**, (2021).
- 28. Lee, I. & Schindelin, H. Structural Insights into E1-Catalyzed Ubiquitin Activation and Transfer to Conjugating Enzymes. *Cell* **134**, 268–278 (2008).
- 29. Haas, A. L. & Rose, I. A. The mechanism of ubiquitin activating enzyme. A kinetic and equilibrium analysis. *J. Biol. Chem.* **257**, 10329–10337 (1982).
- 30. Olsen, S. K. & Lima, C. D. Structure of a Ubiquitin E1-E2 Complex: Insights to E1-E2 Thioester Transfer. *Mol. Cell* **49**, 884–896 (2013).
- 31. Buetow, L. & Huang, D. T. Structural insights into the catalysis and regulation of E3 ubiquitin ligases. *Nat. Rev. Mol. Cell Biol.* **17**, 626–642 (2016).
- 32. Finley, D., Ciechanover, A. & Varshavsky, A. Thermolability of ubiquitin-activating enzyme from the mammalian cell cycle mutant ts85. *Cell* **37**, 43–55 (1984).
- 33. Michelle, C., Vourc'h, P., Mignon, L. & Andres, C. R. What Was the Set of Ubiquitin and Ubiquitin-Like Conjugating Enzymes in the Eukaryote Common Ancestor? *J. Mol. Evol.* **68**, 616–628 (2009).
- 34. Ye, Y. & Rape, M. Building ubiquitin chains: E2 enzymes at work. *Nat. Rev. Mol. Cell Biol.* **10,** 755–764 (2009).
- 35. Lin, Y., Hwang, W. C. & Basavappa, R. Structural and Functional Analysis of the Human Mitotic-specific Ubiquitin-conjugating Enzyme, UbcH10*. *J. Biol. Chem.* **277**, 21913–21921 (2002).

- 36. Özkan, E., Yu, H. & Deisenhofer, J. Mechanistic insight into the allosteric activation of a ubiquitin-conjugating enzyme by RING-type ubiquitin ligases. *Proc. Natl. Acad. Sci. U. S. A.* **102**, 18890–18895 (2005).
- 37. Das, R., Mariano, J., Tsai, Y. C., Kalathur, R. C., Kostova, Z., Li, J., Tarasov, S. G., McFeeters, R. L., Altieri, A. S., Ji, X., Byrd, R. A. & Weissman, A. M. Allosteric Activation of E2-RING Finger-Mediated Ubiquitylation by a Structurally Defined Specific E2-Binding Region of gp78. *Mol. Cell* 34, 674–685 (2009).
- 38. Jin, J., Li, X., Gygi, S. P. & Harper, J. W. Dual E1 activation systems for ubiquitin differentially regulate E2 enzyme charging. *Nature* **447**, 1135–1138 (2007).
- 39. Li, W., Bengtson, M. H., Ulbrich, A., Matsuda, A., Reddy, V. A., Orth, A., Chanda, S. K., Batalov, S. & Joazeiro, C. A. P. Genome-Wide and Functional Annotation of Human E3 Ubiquitin Ligases Identifies MULAN, a Mitochondrial E3 that Regulates the Organelle's Dynamics and Signaling. *PLoS ONE* **3**, e1487 (2008).
- 40. Deshaies, R. J. & Joazeiro, C. A. P. RING domain E3 ubiquitin ligases. *Annu. Rev. Biochem.* **78**, 399–434 (2009).
- 41. Ohi, M. D., Vander Kooi, C. W., Rosenberg, J. A., Chazin, W. J. & Gould, K. L. Structural insights into the U-box, a domain associated with multi-ubiquitination. *Nat. Struct. Biol.* **10**, 250–255 (2003).
- 42. Rotin, D. & Kumar, S. Physiological functions of the HECT family of ubiquitin ligases. *Nat. Rev. Mol. Cell Biol.* **10,** 398–409 (2009).
- 43. Huang, L., Kinnucan, E., Wang, G., Beaudenon, S., Howley, P. M., Huibregtse, J. M. & Pavletich, N. P. Structure of an E6AP-UbcH7 complex: insights into ubiquitination by the E2-E3 enzyme cascade. *Science* **286**, 1321–1326 (1999).
- 44. Wenzel, D. M., Lissounov, A., Brzovic, P. S. & Klevit, R. E. UBCH7 reactivity profile reveals parkin and HHARI to be RING/HECT hybrids. *Nature* **474**, 105–108 (2011).
- 45. Ulrich, H. D. & Walden, H. Ubiquitin signalling in DNA replication and repair. *Nat. Rev. Mol. Cell Biol.* **11**, 479–489 (2010).
- 46. Chau, V., Tobias, J. W., Bachmair, A., Marriott, D., Ecker, D. J., Gonda, D. K. & Varshavsky, A. A Multiubiquitin Chain Is Confined to Specific Lysine in a Targeted Short-Lived Protein. *Science* **243**, 1576–1583 (1989).
- 47. Komander, D. & Rape, M. The Ubiquitin Code. Annu. Rev. Biochem. 81, 203–229 (2012).
- 48. Park, C.-W. & Ryu, K.-Y. Cellular ubiquitin pool dynamics and homeostasis. *BMB Rep.* 47, 475–482 (2014).
- 49. Clague, M. J., Heride, C. & Urbé, S. The demographics of the ubiquitin system. *Trends Cell Biol.* **25**, 417–426 (2015).
- 50. Sahu, I. & Glickman, M. H. Proteasome in action: substrate degradation by the 26S proteasome. *Biochem. Soc. Trans.* **49**, 629–644 (2021).
- 51. Stone, M., Hartmann-Petersen, R., Seeger, M., Bech-Otschir, D., Wallace, M. & Gordon, C. Uch2/Uch37 is the major deubiquitinating enzyme associated with the 26S proteasome in fission yeast. *J. Mol. Biol.* **344**, 697–706 (2004).
- 52. Park, K. C., Woo, S. K., Yoo, Y. J., Wyndham, A. M., Baker, R. T. & Chung, C. H. Purification and characterization of UBP6, a new ubiquitin-specific protease in Saccharomyces cerevisiae. *Arch. Biochem. Biophys.* **347**, 78–84 (1997).
- 53. Kisselev, A. F., Akopian, T. N., Castillo, V. & Goldberg, A. L. Proteasome Active Sites Allosterically Regulate Each Other, Suggesting a Cyclical Bite-Chew Mechanism for Protein Breakdown. *Mol. Cell* 4, 395–402 (1999).

- 54. Dong, Y., Zhang, S., Wu, Z., Li, X., Wang, W. L., Zhu, Y., Stoilova-McPhie, S., Lu, Y., Finley, D. & Mao, Y. Cryo-EM structures and dynamics of substrate-engaged human 26S proteasome. *Nature* **565**, 49–55 (2019).
- 55. de la Peña, A. H., Goodall, E. A., Gates, S. N., Lander, G. C. & Martin, A. Substrate-engaged 26S proteasome structures reveal mechanisms for ATP-hydrolysis-driven translocation. *Science* **362**, eaav0725 (2018).
- 56. Emmerich, N. P., Nussbaum, A. K., Stevanovic, S., Priemer, M., Toes, R. E., Rammensee, H. G. & Schild, H. The human 26 S and 20 S proteasomes generate overlapping but different sets of peptide fragments from a model protein substrate. *J. Biol. Chem.* **275**, 21140–21148 (2000).
- 57. Harrigan, J. A., Jacq, X., Martin, N. M. & Jackson, S. P. Deubiquitylating enzymes and drug discovery: emerging opportunities. *Nat. Rev. Drug Discov.* **17**, 57–78 (2018).
- 58. Nijman, S. M. B., Luna-Vargas, M. P. A., Velds, A., Brummelkamp, T. R., Dirac, A. M. G., Sixma, T. K. & Bernards, R. A Genomic and Functional Inventory of Deubiquitinating Enzymes. *Cell* **123**, 773–786 (2005).
- 59. Clague, M. J., Urbé, S. & Komander, D. Breaking the chains: deubiquitylating enzyme specificity begets function. *Nat. Rev. Mol. Cell Biol.* **20**, 338–352 (2019).
- 60. Amerik, A. Y. & Hochstrasser, M. Mechanism and function of deubiquitinating enzymes. *Biochim. Biophys. Acta BBA Mol. Cell Res.* **1695**, 189–207 (2004).
- 61. Johnston, S. C., Riddle, S. M., Cohen, R. E. & Hill, C. P. Structural basis for the specificity of ubiquitin C-terminal hydrolases. *EMBO J.* **18**, 3877–3887 (1999).
- 62. Hu, M., Li, P., Li, M., Li, W., Yao, T., Wu, J.-W., Gu, W., Cohen, R. E. & Shi, Y. Crystal Structure of a UBP-Family Deubiquitinating Enzyme in Isolation and in Complex with Ubiquitin Aldehyde. *Cell* 111, 1041–1054 (2002).
- 63. Ye, Y., Scheel, H., Hofmann, K. & Komander, D. Dissection of USP catalytic domains reveals five common insertion points. *Mol. Biosyst.* **5,** 1797–1808 (2009).
- 64. Makarova, K. S., Aravind, L. & Koonin, E. V. A novel superfamily of predicted cysteine proteases from eukaryotes, viruses and Chlamydia pneumoniae. *Trends Biochem. Sci.* **25**, 50–52 (2000).
- 65. Balakirev, M. Y., Tcherniuk, S. O., Jaquinod, M. & Chroboczek, J. Otubains: a new family of cysteine proteases in the ubiquitin pathway. *EMBO Rep.* **4**, 517–522 (2003).
- 66. Nanao, M. H., Tcherniuk, S. O., Chroboczek, J., Dideberg, O., Dessen, A. & Balakirev, M. Y. Crystal structure of human otubain 2. *EMBO Rep.* **5**, 783–788 (2004).
- 67. Beyaert, R., Heyninck, K. & Van Huffel, S. A20 and A20-binding proteins as cellular inhibitors of nuclear factor-κB-dependent gene expression and apoptosis. *Biochem. Pharmacol.* **60**, 1143–1151 (2000).
- 68. Scheel, H., Tomiuk, S. & Hofmann, K. Elucidation of ataxin-3 and ataxin-7 function by integrative bioinformatics. *Hum. Mol. Genet.* **12**, 2845–2852 (2003).
- 69. Burnett, B., Li, F. & Pittman, R. N. The polyglutamine neurodegenerative protein ataxin-3 binds polyubiquitylated proteins and has ubiquitin protease activity. *Hum. Mol. Genet.* **12**, 3195–3205 (2003).
- 70. Zhu, M., Shao, F., Innes, R. W., Dixon, J. E. & Xu, Z. The crystal structure of Pseudomonas avirulence protein AvrPphB: a papain-like fold with a distinct substrate-binding site. *Proc. Natl. Acad. Sci. U. S. A.* **101**, 302–307 (2004).
- 71. Nicastro, G., Menon, R. P., Masino, L., Knowles, P. P., McDonald, N. Q. & Pastore, A. The solution structure of the Josephin domain of ataxin-3: Structural determinants for molecular recognition. *Proc. Natl. Acad. Sci. U. S. A.* **102**, 10493–10498 (2005).

- 72. Abdul Rehman, S. A., Kristariyanto, Y. A., Choi, S.-Y., Nkosi, P. J., Weidlich, S., Labib, K., Hofmann, K. & Kulathu, Y. MINDY-1 Is a Member of an Evolutionarily Conserved and Structurally Distinct New Family of Deubiquitinating Enzymes. *Mol. Cell* **63**, 146–155 (2016).
- 73. Mevissen, T. E. T. & Komander, D. Mechanisms of Deubiquitinase Specificity and Regulation. *Annu. Rev. Biochem.* **86,** 159–192 (2017).
- 74. Kwasna, D., Abdul Rehman, S. A., Natarajan, J., Matthews, S., Madden, R., De Cesare, V., Weidlich, S., Virdee, S., Ahel, I., Gibbs-Seymour, I. & Kulathu, Y. Discovery and Characterization of ZUFSP/ZUP1, a Distinct Deubiquitinase Class Important for Genome Stability. *Mol. Cell* 70, 150-164.e6 (2018).
- 75. Hermanns, T., Pichlo, C., Woiwode, I., Klopffleisch, K., Witting, K. F., Ovaa, H., Baumann, U. & Hofmann, K. A family of unconventional deubiquitinases with modular chain specificity determinants. *Nat. Commun.* **9,** 799 (2018).
- 76. Haahr, P., Borgermann, N., Guo, X., Typas, D., Achuthankutty, D., Hoffmann, S., Shearer, R., Sixma, T. K. & Mailand, N. ZUFSP Deubiquitylates K63-Linked Polyubiquitin Chains to Promote Genome Stability. *Mol. Cell* **70**, 165-174.e6 (2018).
- 77. Hewings, D. S., Heideker, J., Ma, T. P., AhYoung, A. P., El Oualid, F., Amore, A., Costakes, G. T., Kirchhofer, D., Brasher, B., Pillow, T., Popovych, N., Maurer, T., Schwerdtfeger, C., Forrest, W. F., Yu, K., Flygare, J., Bogyo, M. & Wertz, I. E. Reactive-site-centric chemoproteomics identifies a distinct class of deubiquitinase enzymes. *Nat. Commun.* 9, 1162 (2018).
- 78. Ambroggio, X. I., Rees, D. C. & Deshaies, R. J. JAMM: A Metalloprotease-Like Zinc Site in the Proteasome and Signalosome. *PLoS Biol.* **2**, e2 (2004).
- 79. Cope, G. A., Suh, G. S. B., Aravind, L., Schwarz, S. E., Zipursky, S. L., Koonin, E. V. & Deshaies, R. J. Role of Predicted Metalloprotease Motif of Jab1/Csn5 in Cleavage of Nedd8 from Cul1. *Science* **298**, 608–611 (2002).
- 80. Yao, T. & Cohen, R. E. A cryptic protease couples deubiquitination and degradation by the proteasome. *Nature* **419**, 403–407 (2002).
- 81. Shrestha, R. K., Ronau, J. A., Davies, C. W., Guenette, R. G., Strieter, E. R., Paul, L. N. & Das, C. Insights into the Mechanism of Deubiquitination by JAMM Deubiquitinases from Cocrystal Structures of the Enzyme with the Substrate and Product. *Biochemistry* **53**, 3199–3217 (2014).
- 82. Davies, C. W., Paul, L. N., Kim, M.-I. & Das, C. Structural and Thermodynamic Comparison of the Catalytic Domain of AMSH and AMSH-LP: Nearly Identical Fold but Different Stability. *J. Mol. Biol.* **413**, 416–429 (2011).
- 83. Verma, R., Aravind, L., Oania, R., McDonald, W. H., Yates, J. R., Koonin, E. V. & Deshaies, R. J. Role of Rpn11 Metalloprotease in Deubiquitination and Degradation by the 26S Proteasome. *Science* **298**, 611–615 (2002).
- 84. Wing, S. S. Deubiquitinases in skeletal muscle atrophy. *Int. J. Biochem. Cell Biol.* **45,** 2130–2135 (2013).
- 85. Wada, K. & Kamitani, T. UnpEL/Usp4 is ubiquitinated by Ro52 and deubiquitinated by itself. *Biochem. Biophys. Res. Commun.* **342**, 253–258 (2006).
- 86. Wada, K., Tanji, K. & Kamitani, T. Oncogenic protein UnpEL/Usp4 deubiquitinates Ro52 by its isopeptidase activity. *Biochem. Biophys. Res. Commun.* **339**, 731–736 (2006).
- 87. Zhang, L., Zhou, F., Drabsch, Y., Gao, R., Snaar-Jagalska, B. E., Mickanin, C., Huang, H., Sheppard, K.-A., Porter, J. A., Lu, C. X. & ten Dijke, P. USP4 is regulated by AKT

- phosphorylation and directly deubiquitylates TGF-β type I receptor. *Nat. Cell Biol.* **14,** 717–726 (2012).
- 88. Lecker, S. H., Jagoe, R. T., Gilbert, A., Gomes, M., Baracos, V., Bailey, J., Price, S. R., Mitch, W. E. & Goldberg, A. L. Multiple types of skeletal muscle atrophy involve a common program of changes in gene expression. *FASEB J.* **18**, 39–51 (2004).
- 89. Park, K. C., Kim, J. H., Choi, E.-J., Min, S. W., Rhee, S., Baek, S. H., Chung, S. S., Bang, O., Park, D., Chiba, T., Tanaka, K. & Chung, C. H. Antagonistic regulation of myogenesis by two deubiquitinating enzymes, UBP45 and UBP69. *Proc. Natl. Acad. Sci. U. S. A.* **99**, 9733–9738 (2002).
- 90. Bedard, N., Yang, Y., Gregory, M., Cyr, D. G., Suzuki, J., Yu, X., Chian, R.-C., Hermo, L., O'Flaherty, C., Smith, C. E., Clarke, H. J. & Wing, S. S. Mice Lacking the USP2 Deubiquitinating Enzyme Have Severe Male Subfertility Associated with Defects in Fertilization and Sperm Motility 1. *Biol. Reprod.* 85, 594–604 (2011).
- 91. Wertz, I. E., O'Rourke, K. M., Zhou, H., Eby, M., Aravind, L., Seshagiri, S., Wu, P., Wiesmann, C., Baker, R., Boone, D. L., Ma, A., Koonin, E. V. & Dixit, V. M. De-ubiquitination and ubiquitin ligase domains of A20 downregulate NF-κB signalling. *Nature* **430**, 694–699 (2004).
- 92. Charan, R. A., Hanson, R. & Clemens, P. R. Deubiquitinating enzyme A20 negatively regulates NF-κB signaling in skeletal muscle in mdx mice. *FASEB J.* **26**, 587–595 (2012).
- 93. Combaret, L., Adegoke, O. A. J., Bedard, N., Baracos, V., Attaix, D. & Wing, S. S. USP19 is a ubiquitin-specific protease regulated in rat skeletal muscle during catabolic states. *Am. J. Physiol.-Endocrinol. Metab.* **288**, E693–E700 (2005).
- 94. Mei, Y., Hahn, A. A., Hu, S. & Yang, X. The USP19 Deubiquitinase Regulates the Stability of c-IAP1 and c-IAP2*. *J. Biol. Chem.* **286**, 35380–35387 (2011).
- 95. Wing, S. S. Deubiquitinating enzymes in skeletal muscle atrophy—An essential role for USP19. *Int. J. Biochem. Cell Biol.* **79**, 462–468 (2016).
- 96. Hassink, G. C., Zhao, B., Sompallae, R., Altun, M., Gastaldello, S., Zinin, N. V., Masucci, M. G. & Lindsten, K. The ER-resident ubiquitin-specific protease 19 participates in the UPR and rescues ERAD substrates. *EMBO Rep.* **10**, 755–761 (2009).
- 97. Shirasu, K., Lahaye, T., Tan, M.-W., Zhou, F., Azevedo, C. & Schulze-Lefert, P. A Novel Class of Eukaryotic Zinc-Binding Proteins Is Required for Disease Resistance Signaling in Barley and Development in C. elegans. *Cell* **99**, 355–366 (1999).
- 98. Kitagawa, K., Skowyra, D., Elledge, S. J., Harper, J. W. & Hieter, P. SGT1 Encodes an Essential Component of the Yeast Kinetochore Assembly Pathway and a Novel Subunit of the SCF Ubiquitin Ligase Complex. *Mol. Cell* **4**, 21–33 (1999).
- 99. Garcia-Ranea, J. a, Mirey, G., Camonis, J. & Valencia, A. p23 and HSP20/α-crystallin proteins define a conserved sequence domain present in other eukaryotic protein families. *FEBS Lett.* **529**, 162–167 (2002).
- 100. Lee, Y.-T., Jacob, J., Michowski, W., Nowotny, M., Kuznicki, J. & Chazin, W. J. Human Sgt1 Binds HSP90 through the CHORD-Sgt1 Domain and Not the Tetratricopeptide Repeat Domain*. *J. Biol. Chem.* **279**, 16511–16517 (2004).
- 101. Xue, W., Zhang, S.-X., He, W.-T., Hong, J.-Y., Jiang, L.-L. & Hu, H.-Y. Domain interactions reveal auto-inhibition of the deubiquitinating enzyme USP19 and its activation by HSP90 in modulation of huntingtin aggregation. *Biochem. J.* doi:10.1042/BCJ20200536

- 102. Weaver, A. J., Sullivan, W. P., Felts, S. J., Owen, B. A. L. & Toft, D. O. Crystal Structure and Activity of Human p23, a Heat Shock Protein 90 Co-chaperone*. *J. Biol. Chem.* 275, 23045–23052 (2000).
- 103. Lee, J.-G., Kim, W., Gygi, S. & Ye, Y. Characterization of the Deubiquitinating Activity of USP19 and Its Role in Endoplasmic Reticulum-associated Degradation. *J. Biol. Chem.* **289**, 3510–3517 (2014).
- 104. Xu, Y., Cui, L., Dibello, A., Wang, L., Lee, J., Saidi, L., Lee, J.-G. & Ye, Y. DNAJC5 facilitates USP19-dependent unconventional secretion of misfolded cytosolic proteins. *Cell Discov.* 4, 1–18 (2018).
- 105. Faesen, A. C., Luna-Vargas, M. P. A. & Sixma, T. K. The role of UBL domains in ubiquitin-specific proteases. *Biochem. Soc. Trans.* **40**, 539–545 (2012).
- 106. Gross, C. T. & McGinnis, W. DEAF-1, a novel protein that binds an essential region in a Deformed response element. *EMBO J.* **15**, 1961–1970 (1996).
- 107. Lutterbach, B., Westendorf, J. J., Linggi, B., Patten, A., Moniwa, M., Davie, J. R., Huynh, K. D., Bardwell, V. J., Lavinsky, R. M., Rosenfeld, M. G., Glass, C., Seto, E. & Hiebert, S. W. ETO, a Target of t(8;21) in Acute Leukemia, Interacts with the N-CoR and mSin3 Corepressors. *Mol. Cell. Biol.* 18, 7176–7184 (1998).
- 108. Zhang, Q., Wang, Z., Hou, F., Harding, R., Huang, X., Dong, A., Walker, J. R. & Tong, Y. The substrate binding domains of human SIAH E3 ubiquitin ligases are now crystal clear. *Biochim. Biophys. Acta BBA Gen. Subj.* **1861**, 3095–3105 (2017).
- 109. House, C. M., Möller, A. & Bowtell, D. D. L. Siah Proteins: Novel Drug Targets in the Ras and Hypoxia Pathways. *Cancer Res.* **69**, 8835–8838 (2009).
- 110. Velasco, K., Zhao, B., Callegari, S., Altun, M., Liu, H., Hassink, G., Masucci, M. G. & Lindsten, K. An N-terminal SIAH-interacting motif regulates the stability of the ubiquitin specific protease (USP)-19. *Biochem. Biophys. Res. Commun.* 433, 390–395 (2013).
- 111. House, C. M., Hancock, N. C., Möller, A., Cromer, B. A., Fedorov, V., Bowtell, D. D. L., Parker, M. W. & Polekhina, G. Elucidation of the substrate binding site of Siah ubiquitin ligase. *Struct. Lond. Engl. 1993* **14**, 695–701 (2006).
- 112. Vijay-Kumar, S., Bugg, C. E. & Cook, W. J. Structure of ubiquitin refined at 1.8Åresolution. *J. Mol. Biol.* **194**, 531–544 (1987).
- 113. Sundaram, P., Pang, Z., Miao, M., Yu, L. & Wing, S. S. USP19-deubiquitinating enzyme regulates levels of major myofibrillar proteins in L6 muscle cells. *Am. J. Physiol.-Endocrinol. Metab.* **297**, E1283–E1290 (2009).
- 114. Wiles, B., Miao, M., Coyne, E., Larose, L., Cybulsky, A. V. & Wing, S. S. USP19 deubiquitinating enzyme inhibits muscle cell differentiation by suppressing unfolded-protein response signaling. *Mol. Biol. Cell* **26**, 913–923 (2015).
- 115. Bohnert, K. R., McMillan, J. D. & Kumar, A. Emerging roles of ER stress and unfolded protein response pathways in skeletal muscle health and disease. *J. Cell. Physiol.* **233**, 67–78 (2018).
- 116. Alter, J. & Bengal, E. Stress-Induced C/EBP Homology Protein (CHOP) Represses MyoD Transcription to Delay Myoblast Differentiation. *PLoS ONE* **6**, e29498 (2011).
- 117. Bédard, N., Jammoul, S., Moore, T., Wykes, L., Hallauer, P. L., Hastings, K. E. M., Stretch, C., Baracos, V., Chevalier, S., Plourde, M., Coyne, E. & Wing, S. S. Inactivation of the ubiquitin-specific protease 19 deubiquitinating enzyme protects against muscle wasting. *FASEB J.* **29**, 3889–3898 (2015).

- 118. Ogawa, M., Kariya, Y., Kitakaze, T., Yamaji, R., Harada, N., Sakamoto, T., Hosotani, K., Nakano, Y. & Inui, H. The preventive effect of β-carotene on denervation-induced soleus muscle atrophy in mice. *Br. J. Nutr.* **109**, 1349–1358 (2013).
- 119. Liu, Q., Xu, W.-G., Luo, Y., Han, F.-F., Yao, X.-H., Yang, T.-Y., Zhang, Y., Pi, W.-F. & Guo, X.-J. Cigarette smoke-induced skeletal muscle atrophy is associated with up-regulation of USP-19 via p38 and ERK MAPKs. *J. Cell. Biochem.* **112**, 2307–2316 (2011).
- 120. Lu, Y., Adegoke, O. A. J., Nepveu, A., Nakayama, K. I., Bedard, N., Cheng, D., Peng, J. & Wing, S. S. USP19 Deubiquitinating Enzyme Supports Cell Proliferation by Stabilizing KPC1, a Ubiquitin Ligase for p27Kip1. *Mol. Cell. Biol.* **29**, 547–558 (2009).
- 121. Lu, Y., Bedard, N., Chevalier, S. & Wing, S. S. Identification of Distinctive Patterns of USP19-Mediated Growth Regulation in Normal and Malignant Cells. *PLOS ONE* **6**, e15936 (2011).
- 122. Wu, M., Tu, H., Chang, Y., Tan, B., Wang, G., Zhou, J., Wang, L., Mu, R. & Zhang, W. USP19 deubiquitinates HDAC1/2 to regulate DNA damage repair and control chromosomal stability. *Oncotarget* **8**, 2197–2208 (2016).
- 123. Braakman, I. & Hebert, D. N. Protein Folding in the Endoplasmic Reticulum. *Cold Spring Harb. Perspect. Biol.* **5**, a013201 (2013).
- 124. Olzmann, J. A., Kopito, R. R. & Christianson, J. C. The Mammalian Endoplasmic Reticulum-Associated Degradation System. *Cold Spring Harb. Perspect. Biol.* **5**, a013185 (2013).
- 125. Hwang, J. & Qi, L. Quality Control in the Endoplasmic Reticulum: Crosstalk between ERAD and UPR pathways. *Trends Biochem. Sci.* **43**, 593–605 (2018).
- 126. Colla, E. Linking the Endoplasmic Reticulum to Parkinson's Disease and Alpha-Synucleinopathy. *Front. Neurosci.* **13**, (2019).
- 127. Welihinda, A. A., Tirasophon, W. & Kaufman, R. J. The cellular response to protein misfolding in the endoplasmic reticulum. *Gene Expr.* **7**, 293–300 (1999).
- 128. Walter, P. & Ron, D. The Unfolded Protein Response: From Stress Pathway to Homeostatic Regulation. *Science* **334**, 1081–1086 (2011).
- 129. Hetz, C., Zhang, K. & Kaufman, R. J. Mechanisms, regulation and functions of the unfolded protein response. *Nat. Rev. Mol. Cell Biol.* **21**, 421–438 (2020).
- 130. Harding, H. P., Zhang, Y. & Ron, D. Protein translation and folding are coupled by an endoplasmic-reticulum-resident kinase. *Nature* **397**, 271–274 (1999).
- 131. Nakamura, N., Harada, K., Kato, M. & Hirose, S. Ubiquitin-specific protease 19 regulates the stability of the E3 ubiquitin ligase MARCH6. *Exp. Cell Res.* **328**, 207–216 (2014).
- 132. Ventii, K. H. & Wilkinson, K. D. Protein Partners of Deubiquitinating Enzymes. *Biochem. J.* **414**, 161–175 (2008).
- 133. Volkmar, N., Fenech, E. & Christianson, J. C. New MAPS for misfolded proteins. *Nat. Cell Biol.* **18,** 724–726 (2016).
- 134. Wolff, S., Weissman, J. S. & Dillin, A. Differential Scales of Protein Quality Control. *Cell* **157**, 52–64 (2014).
- 135. Lee, J.-G., Takahama, S., Zhang, G., Tomarev, S. I. & Ye, Y. Unconventional secretion of misfolded proteins promotes adaptation to proteasome dysfunction in mammalian cells. *Nat. Cell Biol.* **18**, 765–776 (2016).
- 136. Ye, Y. Regulation of protein homeostasis by unconventional protein secretion in mammalian cells. *Semin. Cell Dev. Biol.* **83,** 29–35 (2018).
- 137. Bieri, G., Gitler, A. D. & Brahic, M. Internalization, axonal transport and release of fibrillar forms of alphasynuclein. *Neurobiol. Dis.* **109**, 219–225 (2018).

- 138. He, W.-T., Zheng, X.-M., Zhang, Y.-H., Gao, Y.-G., Song, A.-X., van der Goot, F. G. & Hu, H.-Y. Cytoplasmic Ubiquitin-Specific Protease 19 (USP19) Modulates Aggregation of Polyglutamine-Expanded Ataxin-3 and Huntingtin through the HSP90 Chaperone. *PLoS ONE* 11, e0147515 (2016).
- 139. He, W.-T., Xue, W., Gao, Y.-G., Hong, J.-Y., Yue, H.-W., Jiang, L.-L. & Hu, H.-Y. HSP90 recognizes the N-terminus of huntingtin involved in regulation of huntingtin aggregation by USP19. *Sci. Rep.* **7**, (2017).
- 140. Kaelin, W. G. & Ratcliffe, P. J. Oxygen Sensing by Metazoans: The Central Role of the HIF Hydroxylase Pathway. *Mol. Cell* **30**, 393–402 (2008).
- 141. Papandreou, I., Cairns, R. A., Fontana, L., Lim, A. L. & Denko, N. C. HIF-1 mediates adaptation to hypoxia by actively downregulating mitochondrial oxygen consumption. *Cell Metab.* **3**, 187–197 (2006).
- 142. Kim, H., Scimia, M. C., Wilkinson, D., Trelles, R. D., Wood, M. R., Bowtell, D., Dillin, A., Mercola, M. & Ronai, Z. A. Fine-Tuning of Drp1/Fis1 Availability by AKAP121/Siah2 Regulates Mitochondrial Adaptation to Hypoxia. *Mol. Cell* 44, 532–544 (2011).
- 143. Altun, M., Zhao, B., Velasco, K., Liu, H., Hassink, G., Paschke, J., Pereira, T. & Lindsten, K. Ubiquitin-specific Protease 19 (USP19) Regulates Hypoxia-inducible Factor 1α (HIF-1α) during Hypoxia*. *J. Biol. Chem.* **287**, 1962–1969 (2012).
- 144. Yang, X., Wang, Z., Kai, J., Wang, F., Jia, Y., Wang, S., Tan, S., Shen, X., Chen, A., Shao, J., Zhang, F., Zhang, Z. & Zheng, S. Curcumol attenuates liver sinusoidal endothelial cell angiogenesis via regulating Glis-PROX1-HIF-1α in liver fibrosis. *Cell Prolif.* **53**, e12762 (2020).
- 145. Wu, W., Lin, C., Wu, K., Jiang, L., Wang, X., Li, W., Zhuang, H., Zhang, X., Chen, H., Li, S., Yang, Y., Lu, Y., Wang, J., Zhu, R., Zhang, L., Sui, S., Tan, N., Zhao, B., Zhang, J., Li, L. & Feng, D. FUNDC1 regulates mitochondrial dynamics at the ER–mitochondrial contact site under hypoxic conditions. *EMBO J.* **35**, 1368–1384 (2016).
- 146. Liu, L., Feng, D., Chen, G., Chen, M., Zheng, Q., Song, P., Ma, Q., Zhu, C., Wang, R., Qi, W., Huang, L., Xue, P., Li, B., Wang, X., Jin, H., Wang, J., Yang, F., Liu, P., Zhu, Y., Sui, S. & Chen, Q. Mitochondrial outer-membrane protein FUNDC1 mediates hypoxia-induced mitophagy in mammalian cells. *Nat. Cell Biol.* 14, 177–185 (2012).
- 147. Chai, P., Cheng, Y., Hou, C., Yin, L., Zhang, D., Hu, Y., Chen, Q., Zheng, P., Teng, J. & Chen, J. USP19 promotes hypoxia-induced mitochondrial division via FUNDC1 at Exmitochondria contact sites. *J. Cell Biol.* **220**, e202010006 (2021).
- 148. Zarnegar, B. J., Wang, Y., Mahoney, D. J., Dempsey, P. W., Cheung, H. H., He, J., Shiba, T., Yang, X., Yeh, W., Mak, T. W., Korneluk, R. G. & Cheng, G. Noncanonical NF-κB activation requires coordinated assembly of a regulatory complex of the adaptors cIAP1, cIAP2, TRAF2 and TRAF3 and the kinase NIK. *Nat. Immunol.* 9, 1371–1378 (2008).
- 149. Sun, S.-C. The non-canonical NF-κB pathway in immunity and inflammation. *Nat. Rev. Immunol.* **17**, 545–558 (2017).
- 150. Vallabhapurapu, S. & Karin, M. Regulation and function of NF-kappaB transcription factors in the immune system. *Annu. Rev. Immunol.* **27**, 693–733 (2009).
- 151. Wu, X., Lei, C., Xia, T., Zhong, X., Yang, Q. & Shu, H.-B. Regulation of TRIF-mediated innate immune response by K27-linked polyubiquitination and deubiquitination. *Nat. Commun.* **10,** 4115 (2019).
- 152. Gu, Z., Shi, W., Zhang, L., Hu, Z. & Xu, C. USP19 suppresses cellular type I interferon signaling by targeting TRAF3 for deubiquitination. *Future Microbiol.* **12,** 767–779 (2017).

- 153. Lei, C.-Q., Wu, X., Zhong, X., Jiang, L., Zhong, B. & Shu, H.-B. USP19 Inhibits TNF-α– and IL-1β–Triggered NF-κB Activation by Deubiquitinating TAK1. *J. Immunol.* **203**, 259–268 (2019).
- 154. Hanahan, D. Hallmarks of Cancer: New Dimensions. Cancer Discov. 12, 31–46 (2022).
- 155. Zhong, Z., Yu, J., Virshup, D. M. & Madan, B. Wnts and the hallmarks of cancer. *Cancer Metastasis Rev.* **39**, 625–645 (2020).
- 156. Joiner, D. M., Ke, J., Zhong, Z., Xu, H. E. & Williams, B. O. LRP5 and LRP6 in development and disease. *Trends Endocrinol. Metab.* **24**, 31–39 (2013).
- 157. Perrody, E., Abrami, L., Feldman, M., Kunz, B., Urbé, S. & van der Goot, F. G. Ubiquitin-dependent folding of the Wnt signaling coreceptor LRP6. *eLife* **5**, e19083
- 158. Rossi, F. A., Enriqué Steinberg, J. H., Calvo Roitberg, E. H., Joshi, M. U., Pandey, A., Abba, M. C., Dufrusine, B., Buglioni, S., De Laurenzi, V., Sala, G., Lattanzio, R., Espinosa, J. M. & Rossi, M. USP19 modulates cancer cell migration and invasion and acts as a novel prognostic marker in patients with early breast cancer. *Oncogenesis* 10, 28 (2021).
- 159. Shahriyari, L., Abdel-Rahman, M. & Cebulla, C. BAP1 expression is prognostic in breast and uveal melanoma but not colon cancer and is highly positively correlated with RBM15B and USP19. *PLoS ONE* **14**, e0211507 (2019).
- 160. Hu, W., Su, Y., Fei, X., Wang, X., Zhang, G., Su, C., Du, T., Yang, T., Wang, G., Tang, Z. & Zhang, J. Ubiquitin specific peptidase 19 is a prognostic biomarker and affect the proliferation and migration of clear cell renal cell carcinoma. *Oncol. Rep.* 43, 1964–1974 (2020).
- 161. Kang, H., Choi, M. C., Kim, S., Jeong, J.-Y., Kwon, A.-Y., Kim, T.-H., Kim, G., Joo, W. D., Park, H., Lee, C., Song, S. H., Jung, S. G., Hwang, S. & An, H. J. USP19 and RPL23 as Candidate Prognostic Markers for Advanced-Stage High-Grade Serous Ovarian Carcinoma. *Cancers* 13, 3976 (2021).
- 162. Gierisch, M. E., Pedot, G., Walser, F., Lopez-Garcia, L. A., Jaaks, P., Niggli, F. K. & Schäfer, B. W. USP19 deubiquitinates EWS-FLI1 to regulate Ewing sarcoma growth. *Sci. Rep.* **9**, 951 (2019).
- 163. Zhu, Y., Gu, L., Lin, X., Zhou, X., Lu, B., Liu, C., Lei, C., Zhou, F., Zhao, Q., Prochownik, E. V. & Li, Y. USP19 exacerbates lipogenesis and colorectal carcinogenesis by stabilizing ME1. *Cell Rep.* 37, 110174 (2021).
- 164. Zhu, Y., Gu, L., Lin, X., Zhou, X., Lu, B., Liu, C., Li, Y., Prochownik, E. V., Karin, M., Wang, F. & Li, Y. P53 deficiency affects cholesterol esterification to exacerbate hepatocarcinogenesis. *Hepatology* n/a,
- 165. Dong, Z., Guo, S., Wang, Y., Zhang, J., Luo, H., Zheng, G., Yang, D., Zhang, T., Yan, L., Song, L., Liu, K., Sun, Z., Meng, X., Zheng, Z., Zhang, J. & Zhao, Y. USP19 Enhances MMP2/MMP9-Mediated Tumorigenesis in Gastric Cancer. *OncoTargets Ther.* **13**, 8495–8510 (2020).
- 166. Miao, R., Lu, Y., He, X., Liu, X., Chen, Z. & Wang, J. Ubiquitin-specific protease 19 blunts pathological cardiac hypertrophy via inhibition of the TAK1-dependent pathway. *J. Cell. Mol. Med.* **24**, 10946–10957 (2020).
- 167. Yang, F., Xue, L., Han, Z., Xu, F., Cao, S., Dai, S., Liu, B., Yuan, Q., Wang, Z., Guo, P. & Chen, Y. Vaspin alleviates myocardial ischaemia/reperfusion injury via activating autophagic flux and restoring lysosomal function. *Biochem. Biophys. Res. Commun.* **503**, 501–507 (2018).
- 168. Olivas-Aguirre, F. J., Rodrigo-García, J., Martínez-Ruiz, N. D. R., Cárdenas-Robles, A. I., Mendoza-Díaz, S. O., Álvarez-Parrilla, E., González-Aguilar, G. A., de la Rosa, L. A., Ramos-

- Jiménez, A. & Wall-Medrano, A. Cyanidin-3-O-glucoside: Physical-Chemistry, Foodomics and Health Effects. *Mol. Basel Switz.* **21,** E1264 (2016).
- 169. Shan, X., Lv, Z.-Y., Yin, M.-J., Chen, J., Wang, J. & Wu, Q.-N. The Protective Effect of Cyanidin-3-Glucoside on Myocardial Ischemia-Reperfusion Injury through Ferroptosis. *Oxid. Med. Cell. Longev.* **2021**, 8880141 (2021).
- 170. Pastor, R. F., Restani, P., Di Lorenzo, C., Orgiu, F., Teissedre, P.-L., Stockley, C., Ruf, J. C., Quini, C. I., Garcìa Tejedor, N., Gargantini, R., Aruani, C., Prieto, S., Murgo, M., Videla, R., Penissi, A. & Iermoli, R. H. Resveratrol, human health and winemaking perspectives. *Crit. Rev. Food Sci. Nutr.* **59**, 1237–1255 (2019).
- 171. Li, T., Tan, Y., Ouyang, S., He, J. & Liu, L. Resveratrol protects against myocardial ischemia-reperfusion injury via attenuating ferroptosis. *Gene* **808**, 145968 (2022).
- 172. Nazio, F., Strappazzon, F., Antonioli, M., Bielli, P., Cianfanelli, V., Bordi, M., Gretzmeier, C., Dengjel, J., Piacentini, M., Fimia, G. M. & Cecconi, F. mTOR inhibits autophagy by controlling ULK1 ubiquitylation, self-association and function through AMBRA1 and TRAF6. *Nat. Cell Biol.* **15**, 406–416 (2013).
- 173. Choi, A. M. K., Ryter, S. W. & Levine, B. Autophagy in human health and disease. *N. Engl. J. Med.* **368**, 651–662 (2013).
- 174. Cui, J., Jin, S. & Wang, R.-F. The BECN1-USP19 axis plays a role in the crosstalk between autophagy and antiviral immune responses. *Autophagy* **12**, 1210–1211 (2016).
- 175. Jin, S., Tian, S., Chen, Y., Zhang, C., Xie, W., Xia, X., Cui, J. & Wang, R. USP19 modulates autophagy and antiviral immune responses by deubiquitinating Beclin-1. *EMBO J.* **35**, 866–880 (2016).
- 176. Liu, T., Wang, L., Liang, P., Wang, X., Liu, Y., Cai, J., She, Y., Wang, D., Wang, Z., Guo, Z., Bates, S., Xia, X., Huang, J. & Cui, J. USP19 suppresses inflammation and promotes M2-like macrophage polarization by manipulating NLRP3 function via autophagy. *Cell. Mol. Immunol.* **18**, 2431–2442 (2021).
- 177. Zhao, X., Di, Q., Yu, J., Quan, J., Xiao, Y., Zhu, H., Li, H., Ling, J. & Chen, W. USP19 (ubiquitin specific peptidase 19) promotes TBK1 (TANK-binding kinase 1) degradation via chaperone-mediated autophagy. *Autophagy* **0**, 1–18 (2021).
- 178. Sever, R. & Glass, C. K. Signaling by Nuclear Receptors. *Cold Spring Harb. Perspect. Biol.* **5,** a016709 (2013).
- 179. Ogawa, M., Yamaji, R., Higashimura, Y., Harada, N., Ashida, H., Nakano, Y. & Inui, H. 17β-Estradiol Represses Myogenic Differentiation by Increasing Ubiquitin-specific Peptidase 19 through Estrogen Receptor α*. *J. Biol. Chem.* **286**, 41455–41465 (2011).
- 180. Ogawa, M., Kitakaze, T., Harada, N. & Yamaji, R. Female-specific regulation of skeletal muscle mass by USP19 in young mice. *J. Endocrinol.* **225**, 135–145 (2015).
- 181. Wiik, A., Ekman, M., Johansson, O., Jansson, E. & Esbjörnsson, M. Expression of both oestrogen receptor alpha and beta in human skeletal muscle tissue. *Histochem. Cell Biol.* **131**, 181–189 (2009).
- 182. Ogawa, M., Kitano, T., Kawata, N., Sugihira, T., Kitakaze, T., Harada, N. & Yamaji, R. Daidzein down-regulates ubiquitin-specific protease 19 expression through estrogen receptor β and increases skeletal muscle mass in young female mice. *J. Nutr. Biochem.* **49**, 63–70 (2017).
- 183. Boscaro, C., Carotti, M., Albiero, M., Trenti, A., Fadini, G. P., Trevisi, L., Sandonà, D., Cignarella, A. & Bolego, C. Non-genomic mechanisms in the estrogen regulation of glycolytic protein levels in endothelial cells. *FASEB J.* **34**, 12768–12784 (2020).

- 184. Coyne, E. S., Bedard, N., Wykes, L., Stretch, C., Jammoul, S., Li, S., Zhang, K., Sladek, R. S., Bathe, O. F., Jagoe, R. T., Posner, B. I. & Wing, S. S. Knockout of USP19 Deubiquitinating Enzyme Prevents Muscle Wasting by Modulating Insulin and Glucocorticoid Signaling. *Endocrinology* **159**, 2966–2977 (2018).
- 185. Coyne, E. S., Bédard, N., Gong, Y. J., Faraj, M., Tchernof, A. & Wing, S. S. The deubiquitinating enzyme USP19 modulates adipogenesis and potentiates high-fat-diet-induced obesity and glucose intolerance in mice. *Diabetologia* **62**, 136–146 (2019).
- 186. Kadmiel, M. & Cidlowski, J. A. Glucocorticoid receptor signaling in health and disease. *Trends Pharmacol. Sci.* **34**, 518–530 (2013).
- 187. Germain, P., Staels, B., Dacquet, C., Spedding, M. & Laudet, V. Overview of nomenclature of nuclear receptors. *Pharmacol. Rev.* **58**, 685–704 (2006).
- 188. Mangelsdorf, D. J., Thummel, C., Beato, M., Herrlich, P., Schütz, G., Umesono, K., Blumberg, B., Kastner, P., Mark, M., Chambon, P. & Evans, R. M. The nuclear receptor superfamily: The second decade. *Cell* 83, 835–839 (1995).
- 189. Smith, S. M. & Vale, W. W. The role of the hypothalamic-pituitary-adrenal axis in neuroendocrine responses to stress. *Dialogues Clin. Neurosci.* **8**, 383–395 (2006).
- 190. Chen, T.-C., Kuo, T., Dandan, M., Lee, R. A., Chang, M., Villivalam, S. D., Liao, S.-C., Costello, D., Shankaran, M., Mohammed, H., Kang, S., Hellerstein, M. K. & Wang, J.-C. The role of striated muscle Pik3r1 in glucose and protein metabolism following chronic glucocorticoid exposure. *J. Biol. Chem.* **296**, 100395 (2021).
- 191. Goldberg, A. L., Tischler, M., DeMartino, G. & Griffin, G. Hormonal regulation of protein degradation and synthesis in skeletal muscle. *Fed. Proc.* **39**, 31–36 (1980).
- 192. Hanaoka, B. Y., Peterson, C. A., Horbinski, C. & Crofford, L. J. Implications of glucocorticoid therapy in idiopathic inflammatory myopathies. *Nat. Rev. Rheumatol.* **8**, 448–457 (2012).
- 193. Frost, R. A. & Lang, C. H. Regulation of insulin-like growth factor-I in skeletal muscle and muscle cells. *Minerva Endocrinol.* **28**, 53–73 (2003).
- 194. Yoshida, T. & Delafontaine, P. Mechanisms of IGF-1-Mediated Regulation of Skeletal Muscle Hypertrophy and Atrophy. *Cells* **9**, 1970 (2020).
- 195. Gayan-Ramirez, G., Vanderhoydonc, F., Verhoeven, G. & Decramer, M. Acute Treatment with Corticosteroids Decreases IGF-1 and IGF-2 Expression in the Rat Diaphragm and Gastrocnemius. *Am. J. Respir. Crit. Care Med.* **159**, 283–289 (1999).
- 196. Kuo, T., Harris, C. A. & Wang, J.-C. Metabolic functions of glucocorticoid receptor in skeletal muscle. *Mol. Cell. Endocrinol.* **380**, 79–88 (2013).
- 197. Wang, H., Kubica, N., Ellisen, L. W., Jefferson, L. S. & Kimball, S. R. Dexamethasone Represses Signaling through the Mammalian Target of Rapamycin in Muscle Cells by Enhancing Expression of REDD1*. *J. Biol. Chem.* **281**, 39128–39134 (2006).
- 198. Ma, K., Mallidis, C., Bhasin, S., Mahabadi, V., Artaza, J., Gonzalez-Cadavid, N., Arias, J. & Salehian, B. Glucocorticoid-induced skeletal muscle atrophy is associated with upregulation of myostatin gene expression. *Am. J. Physiol. Endocrinol. Metab.* **285**, E363-371 (2003).
- 199. Sandri, M., Sandri, C., Gilbert, A., Skurk, C., Calabria, E., Picard, A., Walsh, K., Schiaffino, S., Lecker, S. H. & Goldberg, A. L. Foxo Transcription Factors Induce the Atrophy-Related Ubiquitin Ligase Atrogin-1 and Cause Skeletal Muscle Atrophy. *Cell* 117, 399–412 (2004).
- 200. Frank, F., Ortlund, E. A. & Liu, X. Structural insights into glucocorticoid receptor function. *Biochem. Soc. Trans.* **49**, 2333–2343 (2021).

- 201. Baumann, H., Paulsen, K., Kovács, H., Berglund, H., Wright, A. P., Gustafsson, J. A. & Härd, T. Refined solution structure of the glucocorticoid receptor DNA-binding domain. *Biochemistry* **32**, 13463–13471 (1993).
- 202. Härd, T., Kellenbach, E., Boelens, R., Maler, B. A., Dahlman, K., Freedman, L. P., Carlstedt-Duke, J., Yamamoto, K. R., Gustafsson, J. A. & Kaptein, R. Solution structure of the glucocorticoid receptor DNA-binding domain. *Science* 249, 157–160 (1990).
- 203. Paakinaho, V., Johnson, T. A., Presman, D. M. & Hager, G. L. Glucocorticoid receptor quaternary structure drives chromatin occupancy and transcriptional outcome. *Genome Res.* **29**, 1223–1234 (2019).
- 204. Bledsoe, R. K., Montana, V. G., Stanley, T. B., Delves, C. J., Apolito, C. J., McKee, D. D., Consler, T. G., Parks, D. J., Stewart, E. L., Willson, T. M., Lambert, M. H., Moore, J. T., Pearce, K. H. & Xu, H. E. Crystal Structure of the Glucocorticoid Receptor Ligand Binding Domain Reveals a Novel Mode of Receptor Dimerization and Coactivator Recognition. *Cell* 110, 93–105 (2002).
- 205. Savkur, R. S. & Burris, T. P. The coactivator LXXLL nuclear receptor recognition motif. *J. Pept. Res.* **63**, 207–212 (2004).
- 206. Heery, D. M., Kalkhoven, E., Hoare, S. & Parker, M. G. A signature motif in transcriptional co-activators mediates binding to nuclear receptors. *Nature* **387**, 733–736 (1997).
- 207. Leo, C. & Chen, J. D. The SRC family of nuclear receptor coactivators. *Gene* **245**, 1–11 (2000).
- 208. Sommerfeld, A., Krones-Herzig, A. & Herzig, S. Transcriptional co-factors and hepatic energy metabolism. *Mol. Cell. Endocrinol.* **332**, 21–31 (2011).
- 209. Vandevyver, S., Dejager, L. & Libert, C. On the Trail of the Glucocorticoid Receptor: Into the Nucleus and Back. *Traffic* **13**, 364–374 (2012).
- 210. Vandevyver, S., Dejager, L. & Libert, C. Comprehensive overview of the structure and regulation of the glucocorticoid receptor. *Endocr. Rev.* **35**, 671–693 (2014).
- 211. Picard, D., Khursheed, B., Garabedian, M. J., Fortin, M. G., Lindquist, S. & Yamamoto, K. R. Reduced levels of hsp90 compromise steroid receptor action in vivo. *Nature* **348**, 166–168 (1990).
- 212. Noddings, C. M., Wang, R. Y.-R., Johnson, J. L. & Agard, D. A. Structure of Hsp90–p23–GR reveals the Hsp90 client-remodelling mechanism. *Nature* **601**, 465–469 (2022).
- 213. Biebl, M. M., Lopez, A., Rehn, A., Freiburger, L., Lawatscheck, J., Blank, B., Sattler, M. & Buchner, J. Structural elements in the flexible tail of the co-chaperone p23 coordinate client binding and progression of the Hsp90 chaperone cycle. *Nat. Commun.* 12, 828 (2021).
- 214. Weikum, E. R., Knuesel, M. T., Ortlund, E. A. & Yamamoto, K. R. Glucocorticoid receptor control of transcription: precision and plasticity via allostery. *Nat. Rev. Mol. Cell Biol.* **18**, 159–174 (2017).
- 215. Sinclair, D., Fillman, S. G., Webster, M. J. & Weickert, C. S. Dysregulation of glucocorticoid receptor co-factors FKBP5, BAG1 and PTGES3 in prefrontal cortex in psychotic illness. *Sci. Rep.* **3**, 3539 (2013).
- 216. Timmermans, S., Souffriau, J. & Libert, C. A General Introduction to Glucocorticoid Biology. *Front. Immunol.* **10**, (2019).
- 217. Anker, S. D., Ponikowski, P. P., Clark, A. L., Leyva, F., Rauchhaus, M., Kemp, M., Teixeira, M. M., Hellewell, P. G., Hooper, J., Poole-Wilson, P. A. & Coats, A. J. Cytokines and neurohormones relating to body composition alterations in the wasting syndrome of chronic heart failure. *Eur. Heart J.* 20, 683–693 (1999).

- 218. Sapolsky, R., Rivier, C., Yamamoto, G., Plotsky, P. & Vale, W. Interleukin-1 Stimulates the Secretion of Hypothalamic Corticotropin-Releasing Factor. *Science* **238**, 522–524 (1987).
- 219. Schäcke, H., Döcke, W. D. & Asadullah, K. Mechanisms involved in the side effects of glucocorticoids. *Pharmacol. Ther.* **96**, 23–43 (2002).
- 220. Ma, K., Mallidis, C., Bhasin, S., Mahabadi, V., Artaza, J., Gonzalez-Cadavid, N., Arias, J. & Salehian, B. Glucocorticoid-induced skeletal muscle atrophy is associated with upregulation of myostatin gene expression. *Am. J. Physiol. Endocrinol. Metab.* **285**, E363-371 (2003).
- 221. Haber, R. S. & Weinstein, S. P. Role of glucose transporters in glucocorticoid-induced insulin resistance. GLUT4 isoform in rat skeletal muscle is not decreased by dexamethasone. *Diabetes* **41**, 728–735 (1992).
- 222. Pfleger, K. D. G. & Eidne, K. A. Illuminating insights into protein-protein interactions using bioluminescence resonance energy transfer (BRET). *Nat. Methods* **3**, 165–174 (2006).
- 223. Namkung, Y., Le Gouill, C., Lukashova, V., Kobayashi, H., Hogue, M., Khoury, E., Song, M., Bouvier, M. & Laporte, S. A. Monitoring G protein-coupled receptor and β-arrestin trafficking in live cells using enhanced bystander BRET. *Nat. Commun.* 7, 12178 (2016).
- 224. Mercier, J.-F., Salahpour, A., Angers, S., Breit, A. & Bouvier, M. Quantitative Assessment of β1- and β2-Adrenergic Receptor Homo- and Heterodimerization by Bioluminescence Resonance Energy Transfer*. *J. Biol. Chem.* 277, 44925–44931 (2002).
- 225. Xu, Y., Piston, D. W. & Johnson, C. H. A bioluminescence resonance energy transfer (BRET) system: Application to interacting circadian clock proteins. *Proc. Natl. Acad. Sci. U. S. A.* **96**, 151–156 (1999).
- 226. Hamdan, F. F., Percherancier, Y., Breton, B. & Bouvier, M. Monitoring Protein-Protein Interactions in Living Cells by Bioluminescence Resonance Energy Transfer (BRET). *Curr. Protoc. Neurosci.* **34**, 5.23.1-5.23.20 (2006).
- 227. Ward, W. W. & Cormier, M. J. An energy transfer protein in coelenterate bioluminescence. Characterization of the Renilla green-fluorescent protein. *J. Biol. Chem.* **254**, 781–788 (1979).
- 228. Fredriksson, S., Gullberg, M., Jarvius, J., Olsson, C., Pietras, K., Gústafsdóttir, S. M., Östman, A. & Landegren, U. Protein detection using proximity-dependent DNA ligation assays. *Nat. Biotechnol.* **20**, 473–477 (2002).
- 229. Wochnik, G. M., Young, J. C., Schmidt, U., Holsboer, F., Hartl, F. U. & Rein, T. Inhibition of GR-mediated transcription by p23 requires interaction with Hsp90. *FEBS Lett.* **560**, 35–38 (2004).
- 230. Zhang, M., Botër, M., Li, K., Kadota, Y., Panaretou, B., Prodromou, C., Shirasu, K. & Pearl, L. H. Structural and functional coupling of Hsp90- and Sgt1-centred multi-protein complexes. *EMBO J.* 27, 2789–2798 (2008).
- 231. Xue, W., Zhang, S.-X., He, W.-T., Hong, J.-Y., Jiang, L.-L. & Hu, H.-Y. Domain interactions reveal auto-inhibition of the deubiquitinating enzyme USP19 and its activation by HSP90 in the modulation of huntingtin aggregation. *Biochem. J.* 477, 4295–4312 (2020).
- 232. Ali, M. M. U., Roe, S. M., Vaughan, C., Meyer, P., Panaretou, B., Piper, P. W., Prodromou, C. & Pearl, L. H. Crystal structure of an Hsp90-nucleotide-p23/Sba1 closed chaperone complex. *Nature* **440**, 1013–1017 (2006).
- 233. Jumper, J., Evans, R., Pritzel, A., Green, T., Figurnov, M., Ronneberger, O., Tunyasuvunakool, K., Bates, R., Žídek, A., Potapenko, A., Bridgland, A., Meyer, C., Kohl, S. A. A., Ballard, A. J., Cowie, A., Romera-Paredes, B., Nikolov, S., Jain, R., Adler, J., Back, T., Petersen, S., Reiman, D., Clancy, E., Zielinski, M., Steinegger, M., Pacholska, M., Berghammer, T., Bodenstein, S., Silver, D., Vinyals, O., Senior, A. W., Kavukcuoglu, K.,

- Kohli, P. & Hassabis, D. Highly accurate protein structure prediction with AlphaFold. *Nature* **596**, 583–589 (2021).
- 234. Dixon, A. S., Schwinn, M. K., Hall, M. P., Zimmerman, K., Otto, P., Lubben, T. H., Butler, B. L., Binkowski, B. F., Machleidt, T., Kirkland, T. A., Wood, M. G., Eggers, C. T., Encell, L. P. & Wood, K. V. NanoLuc Complementation Reporter Optimized for Accurate Measurement of Protein Interactions in Cells. ACS Chem. Biol. 11, 400–408 (2016).
- 235. Lee, K., Thwin, A. C., Nadel, C. M., Tse, E., Gates, S. N., Gestwicki, J. E. & Southworth, D. R. The structure of an Hsp90-immunophilin complex reveals cochaperone recognition of the client maturation state. *Mol. Cell* **81**, 3496-3508.e5 (2021).
- 236. Sullivan, W., Stensgard, B., Caucutt, G., Bartha, B., McMahon, N., Alnemri, E. S., Litwack, G. & Toft, D. Nucleotides and Two Functional States of hsp90*. *J. Biol. Chem.* **272**, 8007–8012 (1997).
- 237. Young, J. C. & Hartl, F. U. Polypeptide release by Hsp90 involves ATP hydrolysis and is enhanced by the co-chaperone p23. *EMBO J.* **19**, 5930–5940 (2000).
- 238. Hutchison, K. A., Stancato, L. F., Owens-Grillo, J. K., Johnson, J. L., Krishna, P., Toft, D. O. & Pratt, W. B. The 23-kDa Acidic Protein in Reticulocyte Lysate Is the Weakly Bound Component of the hsp Foldosome That Is Required for Assembly of the Glucocorticoid Receptor into a Functional Heterocomplex with hsp90 (*). *J. Biol. Chem.* **270**, 18841–18847 (1995).
- 239. McLaughlin, S. H., Sobott, F., Yao, Z., Zhang, W., Nielsen, P. R., Grossmann, J. G., Laue, E. D., Robinson, C. V. & Jackson, S. E. The Co-chaperone p23 Arrests the Hsp90 ATPase Cycle to Trap Client Proteins. *J. Mol. Biol.* **356**, 746–758 (2006).
- 240. Oxelmark, E., Roth, J. M., Brooks, P. C., Braunstein, S. E., Schneider, R. J. & Garabedian, M. J. The Cochaperone p23 Differentially Regulates Estrogen Receptor Target Genes and Promotes Tumor Cell Adhesion and Invasion. *Mol. Cell. Biol.* **26**, 5205–5213 (2006).
- 241. Stavreva, D. A., Müller, W. G., Hager, G. L., Smith, C. L. & McNally, J. G. Rapid glucocorticoid receptor exchange at a promoter is coupled to transcription and regulated by chaperones and proteasomes. *Mol. Cell. Biol.* 24, 2682–2697 (2004).
- 242. Qiu, Y., Stavreva, D. A., Luo, Y., Indrawan, A., Chang, M. & Hager, G. L. Dynamic Interaction of HDAC1 with a Glucocorticoid Receptor-regulated Gene Is Modulated by the Activity State of the Promoter*. *J. Biol. Chem.* 286, 7641–7647 (2011).
- 243. Qiu, Y., Zhao, Y., Becker, M., John, S., Parekh, B. S., Huang, S., Hendarwanto, A., Martinez, E. D., Chen, Y., Lu, H., Adkins, N. L., Stavreva, D. A., Wiench, M., Georgel, P. T., Schiltz, R. L. & Hager, G. L. HDAC1 Acetylation Is Linked to Progressive Modulation of Steroid Receptor-Induced Gene Transcription. *Mol. Cell* 22, 669–679 (2006).
- 244. Pratt, W. B., Silverstein, A. M. & Galigniana, M. D. A Model for the Cytoplasmic Trafficking of Signalling Proteins Involving the hsp90-Binding Immunophilins and p50cdc37. *Cell. Signal.* **11,** 839–851 (1999).
- 245. Smith, D. F. & Toft, D. O. Minireview: The Intersection of Steroid Receptors with Molecular Chaperones: Observations and Questions. *Mol. Endocrinol.* **22**, 2229–2240 (2008).
- 246. Echeverría, P. C., Mazaira, G., Erlejman, A., Gomez-Sanchez, C., Pilipuk, G. P. & Galigniana, M. D. Nuclear Import of the Glucocorticoid Receptor-hsp90 Complex through the Nuclear Pore Complex Is Mediated by Its Interaction with Nup62 and Importin β. *Mol. Cell. Biol.* **29**, 4788–4797 (2009).
- 247. Galigniana, M. D., Radanyi, C., Renoir, J.-M., Housley, P. R. & Pratt, W. B. Evidence That the Peptidylprolyl Isomerase Domain of the hsp90-binding Immunophilin FKBP52 Is Involved

- in Both Dynein Interaction and Glucocorticoid Receptor Movement to the Nucleus*. *J. Biol. Chem.* **276**, 14884–14889 (2001).
- 248. Pratt, W. B. & Toft, D. O. Steroid Receptor Interactions with Heat Shock Protein and Immunophilin Chaperones*. *Endocr. Rev.* **18**, 306–360 (1997).
- 249. Taipale, M., Tucker, G., Peng, J., Krykbaeva, I., Lin, Z.-Y., Larsen, B., Choi, H., Berger, B., Gingras, A.-C. & Lindquist, S. A quantitative chaperone interaction network reveals the architecture of cellular protein homeostasis pathways. *Cell* **158**, 434–448 (2014).
- 250. Pratt, W. B., Galigniana, M. D., Harrell, J. M. & DeFranco, D. B. Role of hsp90 and the hsp90-binding immunophilins in signalling protein movement. *Cell. Signal.* **16,** 857–872 (2004).
- 251. Ratajczak, T. & Carrello, A. Cyclophilin 40 (CyP-40), Mapping of Its hsp90 Binding Domain and Evidence That FKBP52 Competes with CyP-40 for hsp90 Binding (*). *J. Biol. Chem.* **271**, 2961–2965 (1996).
- 252. Owens-Grillo, J. K., Hoffmann, K., Hutchison, K. A., Yem, A. W., Deibel, M. R., Handschumacher, R. E. & Pratt, W. B. The Cyclosporin A-binding Immunophilin CyP-40 and the FK506-binding Immunophilin hsp56 Bind to a Common Site on hsp90 and Exist in Independent Cytosolic Heterocomplexes with the Untransformed Glucocorticoid Receptor (*). *J. Biol. Chem.* 270, 20479–20484 (1995).